

**This PDF was created from the British Library's microfilm copy of the original thesis. As such the images are greyscale and no colour was captured.**

**Due to the scanning process, an area greater than the page area is recorded and extraneous details can be captured.**

**This is the best available copy**

D 53686 / 85

Attention is drawn to the fact that the copyright of this thesis rests with its author.

This copy of the thesis has been supplied on condition that anyone who consults it is understood to recognise that its copyright rests with its author and that no quotation from the thesis and no information derived from it may be published without the author's prior written consent.

III

151

D53686/85

BOYLE, W.J.O.

151

CITY OF LONDON POLY.

THE APPLICATION OF LOW DOSE SIMS  
TO SURFACE STUDIES ON COMPOUND SEMICONDUCTORS

A thesis submitted in partial fulfillment of CNA  
Regulations for the award of the Degree of Doctor of  
Philosophy

by

WILLIAM JOHN OGILVIE BOYLE BSc.

Department of Physics, City of London Polytechnic

In collaboration with RSRE (Malvern)

SEPTEMBER 1984

#### ABSTRACT

In this thesis secondary ion mass spectrometry is assessed as a surface analysis technique for compound semiconductor surfaces.

Two types of surface analysis problems are addressed - the use of SIMS to monitor cleaning of GaAs substrates in UHV for MBE growth and adsorption studies - and the use of SIMS in studying low coverage oxygen adsorption on MBE grown (111)PbTe and (100)GaAs surfaces.

As a monitoring technique for surface preparation, SIMS shows the presence of oxygen on (100)GaAs at coverages below the detection limit of AES. The detection of both intact and fragmented sulphate radicals conclusively demonstrates the sensitivity of SIMS to molecular cluster ions from contamination on the surface. This sensitivity proved a useful tool for determining the likely sources of contamination.

The sensitivity of the (111)PbTe surface to surface damage produced by ion bombardment, prevented a conclusive analysis of oxygen adsorption on this surface. Correlations are observed, however, between changes in the electrical conductivity of the PbTe which are induced by ion bombardment and the SIMS signals from this surface. These correlations suggest that oxygen interacts chiefly with Pb, as proposed by current models based on electrical assessment alone.

Differences are observed in the oxygen adsorption behaviour on (100)GaAs which are dependant on both the surface type, Ga-stabilised or As-rich, and on the excitation state of the oxygen. The results are not fully conclusive because of difficulties in estimating surface coverages and in acquiring sufficient data using the configuration of the present SIMS apparatus.

<u>CONTENTS</u>		Page
<u>Chapter 1</u>		
GENERAL INTRODUCTION		1
<u>Chapter 2</u>		
THEORETICAL AND EMPIRICAL BACKGROUND		7
2.1	Introduction	8
2.2	Surface excitation	8
2.3	Sputtering	9
2.4	Bombardment induced damage	11
2.5	Ionisation and neutralisation	12
2.6	Conclusions	18
<u>Chapter 3</u>		
EXPERIMENTAL APPARATUS AND TECHNIQUES		20
3.1	UHV systems	21
3.2	Gas-handling systems	24
3.3	SIMS	25
3.4	Ion sputter cleaning gun	42
3.5	Sample heating and MBE growth	43
<u>Chapter 4</u>		
A SIMS STUDY OF OXYGEN RETENTION ON PbTe FILMS GROWN BY MBE ON MICA SUBSTRATES		46
4.1	Introduction	47
4.2	Experimental	51
4.3	Results	56
4.4	Conclusions	78
	Appendix	81
<u>Chapter 5</u>		
A SIMS ASSESSMENT OF (100)GaAs SURFACE PREPARATION FOR MBE AND ADSORPTION STUDIES		85
5.1	Introduction	86
5.2	Experimental	88
5.3	Results	92
5.4	Conclusions	113
<u>Chapter 6</u>		
A PRELIMINARY STUDY OF LOW COVERAGE OXYGEN ADSORPTION ON MBE GROWN (100)GaAs		115
6.1	Introduction	116
6.2	Experimental	119
6.3	Results	121
6.4	Conclusions	136
<u>Chapter 7</u>		
CONCLUSIONS		138
<u>References</u>		144

#### ACKNOWLEDGEMENTS

My sincere thanks to Dr. Evan Parker for his helpful discussions and continuous encouragement. I also thank my parents, brothers and sisters and Ingrid for their encouragement, and I especially thank Anne.

I am also indebted to Dr. Mark Dowsett, Dr. Richard King, Dr. Beverly Meggitt, Dr. John Grange, Dr. Richard Kubiak, P. Driscoll, W. Hugglestone and everyone else during my studentship at John Cass for their encouragement, assistance and comments during the work for this thesis.



CHAPTER 1

GENERAL INTRODUCTION

This thesis provides a preliminary assessment of the use of the surface analysis technique, 'low dose' Secondary Ion Mass Spectrometry (SIMS) (G. Blaise 1978, K. Wittmaack 1977), in characterisation of compound semiconductor surfaces. There is currently a growing need for the high sensitivity which SIMS can often provide in analysing films grown by molecular beam epitaxy (A.Y. Cho, J.R. Arther 1975) and in investigations of oxide formation on such surfaces.

In SIMS analysis, surfaces under investigation are bombarded with a primary ion flux of sufficient energy to sputter atomic and molecular species from the surface monolayer(s). Species which are sputtered as ions are then energy and mass analysed, to determine characteristics of the surface.

One of the main advantages of SIMS is that sensitivity is typically sufficient to obtain mass spectra of interest, while detecting surface concentrations of  $10^{-6}$  monolayers in some cases, before appreciable surface damage is produced by the primary ion beam. SIMS used in this mode is often called 'static' (A. Benninghoven 1975) or, more recently, 'low damage' SIMS (K. Wittmaack 1979). Relying on mass spectrometry, the technique has the advantages of hydrogen and isotopic detection. Since ion bombardment of specific samples gives characteristic +ve and -ve spectra, 'fingerprint' techniques are also available to the user (G. Blaise 1978, K. Wittmaack 1977). The technique is widely employed today in bulk analysis by sputter depth profiling, analytical

assay of thin films and the surface monolayer, and in adsorbate studies.

The main disadvantage of SIMS, is that secondary ion emission probabilities vary over several orders of magnitude, depending on primary ion species and energy, and the substrate chemistry in the region of the emitted species (G. Blaise 1978, K. Wittmaack 1977, 1979). Sputter yields, secondary ion emission probabilities and the mechanisms which control emission can rarely be predicted with accuracy because there is presently a severe lag between experimental 'low dose' SIMS and a theoretical basis of the technique.

Quantitative analysis of SIMS data is therefore seldom possible. More recently, however, experimental studies by Dawson (P.H. Dawson and Wing-Cheung Tam 1979) and Yu (M.L. Yu 1979), have shown that for elemental surfaces, 'low dose' SIMS can provide very detailed qualitative information about the physics and chemistry of adsorption, provided the technique is exploited to the full.

In the area which this thesis addresses - the SIMS analysis of compound targets - sputtering and ionisation processes are much less understood. This is chiefly because the number of variables controlling sputtering and ion emission increases sharply with the increasing number of constituent species. This has serious consequences for the application of SIMS to compound targets, for although similar sensitivity can be expected in analysis of elemental and compound

targets, the data arising from compound targets will be much more complex. This will not only affect quantitative estimation, but it will also severely affect the qualitative analytical powers of the technique. The question arises of whether SIMS can be used to advantage in surface analysis of compound semi-conductor surfaces.

This question of viability is addressed in the thesis by applying SIMS and assessing its performance in three studies which use the technique to investigate three current problems in the surface physics of compound semi-conductors. These studies are outlined below.

The first study, presented in Chapter 4, addresses a problem in oxygen interaction with MBE grown (111)PbTe for which work at the City of London Polytechnic has indicated, a conclusive result could be expected with SIMS analysis. Electrical measurements had previously shown the presence of a donor defect associated with intentional Pb doping, which obeyed diffusion limited kinetics during low pressure, approximately  $10^{-6}$  Torr exposures. (S.R. McGlashan, E.H.C. Parker and R.M. King 1979). This effect was thought to be due to oxygen interacting with a mobile Pb intersitial defect. Using a diffusion model, the effect was predicted to saturate in the region of a tenth of a monolayer oxygen coverage, well within detection limits of AES and other common techniques. Attempts to use AES to find an association between oxygen and lead have, however, been inconclusive. Electrical analysis has shown that AES analysis, produces

targets, the data arising from compound targets will be much more complex. This will not only affect quantitative estimation, but it will also severely affect the qualitative analytical powers of the technique. The question arises of whether SIMS can be used to advantage in surface analysis of compound semi-conductor surfaces.

This question of viability is addressed in the thesis by applying SIMS and assessing its performance in three studies which use the technique to investigate three current problems in the surface physics of compound semi-conductors. These studies are outlined below.

The first study, presented in Chapter 4, addresses a problem in oxygen interaction with MBE grown (111)PbTe for which work at the City of London Polytechnic has indicated, a conclusive result could be expected with SIMS analysis. Electrical measurements had previously shown the presence of a donor defect associated with intentional Pb doping, which obeyed diffusion limited kinetics during low pressure, approximately  $10^{-6}$  Torr exposures. (S.R. McGlashan, E.H.C. Parker and R.M. King 1979). This effect was thought to be due to oxygen interacting with a mobile Pb intersitial defect. Using a diffusion model, the effect was predicted to saturate in the region of a tenth of a monolayer oxygen coverage, well within detection limits of AES and other common techniques. Attempts to use AES to find an association between oxygen and lead have, however, been inconclusive. Electrical analysis has shown that AES analysis, produces

extensive compositional changes. It is possible that oxygen desorbs in the analysis area before detection with AES. It was hoped that surface modifications would be much less with 'low dose' SIMS and, if oxygen was in fact bonded to lead atoms, this would be immediately apparent in the behaviour of oxygen and lead related SIMS signals. The present study also employs 'in-situ' measurement of electrical properties of the PbTe. These measurements are extremely sensitive to modifications to the film and they provide useful additional information with which to assess the SIMS analysis.

In the study in Chapter 5, SIMS is used to determine the effectiveness of treatments which are normally employed for preparing (100)GaAs single crystal surfaces prior to molecular beam epitaxy. This is a common role for surface analysis, usually fulfilled by combinations of techniques like AES (C.C Chang, B. Shartz, and S.P. Murarka 1977) and/or the electron diffraction techniques LEED, MEED and RHEED. SIMS provides the possibility of studying contamination and unintentional gaseous adsorbates at surface concentrations which are well below detection limits of these other more commonly used techniques. The ability of SIMS to detect hydrocarbons and other molecular species can also help to provide clues to contaminant source(s).

The study in Chapter 6 is a preliminary investigation with 'low dose' SIMS, which attempts to determine the influences of surface structure and the excitation state of oxygen on

extensive compositional changes. It is possible that oxygen desorbs in the analysis area before detection with AES. It was hoped that surface modifications would be much less with 'low dose' SIMS and, if oxygen was in fact bonded to lead atoms, this would be immediately apparent in the behaviour of oxygen and lead related SIMS signals. The present study also employs 'in-situ' measurement of electrical properties of the PbTe. These measurements are extremely sensitive to modifications to the film and they provide useful additional information with which to assess the SIMS analysis.

In the study in Chapter 5, SIMS is used to determine the effectiveness of treatments which are normally employed for preparing (100)GaAs single crystal surfaces prior to molecular beam epitaxy. This is a common role for surface analysis, usually fulfilled by combinations of techniques like AES (C.C Chang, B. Shartz, and S.P. Murarka 1977) and/or the electron diffraction techniques LEED, MEED and RHEED. SIMS provides the possibility of studying contamination and unintentional gaseous adsorbates at surface concentrations which are well below detection limits of these other more commonly used techniques. The ability of SIMS to detect hydrocarbons and other molecular species can also help to provide clues to contaminant source(s).

The study in Chapter 6 is a preliminary investigation with 'low dose' SIMS, which attempts to determine the influences of surface structure and the excitation state of oxygen on

the oxygen adsorption behaviour of (100) GaAs. This study has similar objectives to the one on PbTe in Chapter 4, i.e. to determine whether oxygen is preferentially associated with one or other of the substrate species, in this case Ga or As atoms.

The theoretical and empirical background of SIMS analysis is discussed in Chapter 2. In Chapter 3, the experimental apparatus, its calibration and experimental practice are detailed. The conclusions derived from the studies in this thesis are presented in Chapter 7.



CHAPTER 2

THEORETICAL AND EMPIRICAL BACKGROUND

## 2.1 INTRODUCTION

This chapter reviews the theoretical and empirical basis of SIMS. The aspects of this basis which are related to the analysis of compound layers and adsorbates are emphasised.

The processes involved in secondary ion production in SIMS can be roughly categorised into three parts: 1) the excitation of the surface by the primary ion beam; 2) sputtering of species from the surface; and 3) ionisation and escape from neutralisation of sputtered species.

## 2.2 Surface Excitation

In SIMS analysis, excitation of the surface is brought about by the impact of heavy ions (mostly inert gas ions  $O_2^+$  or  $Cs^+$ ) with energies typically between 500eV and 10KeV. In this regime the primary ion energy is dissipated almost exclusively amongst several generations of recoiling target atoms, set in motion by a series of quasi-elastic collisions called a collision cascade (P. Sigmund, 1969). Energy dissipation in the collision cascade will be relatively independent of substrate structure and composition since collisions can be considered random and dominated by nuclear interactions.

In general, the target surface intersects the cascade, and energy and momentum are transferred to the surface atoms. Surface atoms with enough momentum in the direction outwards from the surface to overcome the surface binding energy, will be ejected i.e. sputtered. Because the energy spectrum of recoil atoms peaks at very low energies, (M.W. Thomson 1968), sputtered

particles originate only from the topmost monolayer of the surface. This results in a correspondingly small information depth for SIMS and other techniques relying on sputter excitation.

### 2.3 Sputtering

Sputtering from one component, amorphous and polycrystalline targets by ion bombardment can be described fairly well by Sigmund's multiple collision theory (P. Sigmund, 1969). The total sputter yield (S), i.e. the average number of target atoms emitted per incoming projectile may be written as:

$$S = KxF \qquad \text{Equation 2.1}$$

K is a material constant which depends on target properties, (K is inversely proportional to surface binding energy).

F is proportional to the nuclear energy deposited at the surface by the collision cascade. At the energy levels with which we are concerned (<1KeV), F is proportional to  $T_m$ , (where  $T_m$  is the maximum energy that can be transferred between projectile and target atoms.)

For more complex surfaces (anisotropic or compound surfaces), determination of mean escape depths, sputter yield and energetic state of sputtered species is non-trivial. This is especially true for the compound semiconductors and adsorbate layers.

Ion induced desorption (or sputtering) of adsorbates constitutes a particular case of interest in this thesis. Exposure to ion bombardment can be characterised by at least three

effects: 1) emission of adsorbed species into the vacuum (desorption); 2) disintegration of molecular species (damage); and 3) uptake in the bulk (recoil implantation, and bombardment induced surface and bulk diffusion).

The effect of each of the above processes on the surface density of the adsorbate can be described by interaction cross-sections which reflect the probabilities of each process. For a randomly distributed adsorbate with surface density of  $N(\bar{x})$ , the cross-sections ( $\rho_j$ ) can be related to the accumulated ion bombardment dose ( $\bar{x}$ ), (ions -  $\text{cm}^{-2}$ ) and the surface density of adsorbate by:

$$\frac{dN(\bar{x})}{d\bar{x}} = -\sum_j \rho_j \times N(\bar{x}) \quad \text{Equation 2.2}$$

Solution of this equation shows that the surface density of the adsorbate will decrease exponentially. Such exponential decay in surface coverage has been observed by several groups of workers and examples of this form a major part of experimental data in Chapter 4 of this thesis.

It has been shown that the sputter yield of adsorbates is different from that of the substrate material, particularly at low energies (Winters and Sigmund, 1974). Accordingly, they state that it is likely that direct collisions of projectiles with adsorbates are largely responsible for desorption. Desorption cross-sections exhibit a peak around  $60^\circ$ . This is similar to the peak in sputter yield for cascade sputtering.

#### 2.4 Bombardment induced damage

Bombardment induced damage can be classified into two types: damage occurring in the lifetime of a collision cascade which can cause surface disorder before a sputtering event occurs; and permanent damage in the surface region which accumulates with projectile dose. We should be aware of the first type in 'low dose' SIMS analysis as this is a possible source of mis-information in relating secondary ions in spectra to surface species. A particular example of this is the possibility of recombination of sputtered species above the surface, termed a 'recombination cluster'. (N. Winograd, D.E. Harrison and B.J. Garrison 1978). The second type of damage can determine depth resolution in depth profile studies. It also sets limits for the maximum dose that can be permitted in 'low dose' SIMS.

A maximum dose can be determined fairly readily. Allowing a maximum permitted probability of 0.1 for an ion striking a previously bombarded area, and assuming a damage radius per impact ion of approximately 70Å for 1.0KeV Ar<sup>+</sup> ions (M.G. Dowsett, 1979), the maximum dose per analysis will be  $1.5 \times 10^{13}$  (ions - cm<sup>-2</sup>). The present SIMS instrument requires a total bombardment dose of approximately  $5 \times 10^{13}$  (ions - cm<sup>-2</sup>) to record spectra of sufficient sensitivity. It can be seen that with such a dose, damage effects cannot be completely neglected.

## 2.5 Ionisation and neutralisation

### 2.5.1 Theoretical background

The total number of secondary ions leaving the surface per incident ion for a particular species (the secondary ion emission probability) can vary over several orders of magnitude depending on local surface chemistry (K. Wittmaack 1977). Probabilities are particularly sensitive to partial coverage of electro-positive and electro-negative species, even when these are present only at low coverages.

It is evident from the empirical history of SIMS that mechanisms of secondary ion production and related ion impact phenomena (photon and electron emission) depend very much on the type of substrate, and the type of impact ion. Ion emission is a complex affair that may well involve more than one mechanism, each dominant over a particular energy range. This complexity is particularly true for compounds and adsorbate layers.

The processes for secondary ion emission can be divided for convenience into 'metal' and 'chemical' categories. Metallic processes are the only possible processes available for ion emission from pure or dilute metal alloys under inert gas bombardment. Secondary ion emission from metals has mostly been treated with quantum mechanical models (G. Blaise 1973, M. Cini 1976, P. Joyce 1973, H.D. Hagstrum 1975, J.M. Schroer et al. 1973, Z. Sroubek 1974). These models consider how atoms in various states of excitation lose or gain charge, to the vacuum, or by interaction with the conduction band.

Chemical processes are concerned with more local influences, i.e. the species chemical environment. Such processes are considered responsible for ion emission, from ionic adsorbed reactive gas layers, and samples under reactive ion bombardment. Chemical models are of more interest in the present cases of analysing compound-semiconductor and oxide surfaces, where bonding is polar-covalent.

Most of the previous work with SIMS is concerned with metal oxide surfaces. The first systematic measurements of secondary ion yields were performed by Beske (1967), who noticed that a correlation existed between the positive ion yields of elements in a sample and their respective ionisation potentials. Such correlations have been found in many studies since then, particularly from oxide layers or surfaces bombarded with oxygen. A strong dependence has also been found for negative ion emission on electron affinity under caesium bombardment, but a functional relationship is less evident.

Many approaches to quantifying secondary ion emission have been based on assumptions that the degree of ionisation is thermal in character. Both the non-equilibrium Dobretson equation (Z. Jurela 1973) and the Saha-Eggert equation (Z. Jurela 1973, C.A. Anderson 1975) have been applied with equilibrium constants and temperature treated as fitting parameters in statistical fits (F.G. Rudenaur and W. Steigar 1976). Anderson (1975) postulated the existence of a dense plasma in local thermal equilibrium (LTE) immediately above the irradiated region.

There is little experimental support for the LTE model apart from an exponential dependence of ion yield on ionisation potential. There are many reasons for rejecting the validity of the model. Amongst these are the following: 1) oxygen is assumed to increase electronic work function - this is not experimentally observed (G. Blaise and G Slodziam 1973); 2) the model predicts that the ionisation probability is inversely proportional to electron density - on the contrary, electron flux from argon-bombarded oxidised silicon is a factor of 4-6 times higher than for a clean surface (P. Gaworski, K.H. Kebs and M. Mai 1974); 3) temperature variations by more than a factor of two, and Ne variations of four orders of magnitude have been observed by D.A. Smith et.al. (1978) - this is not as would be expected if local equilibrium had been attained.

As an alternative explanation of yield enhancement, Blaise (1976) has specified a model, based on the ionic character of metal-oxygen bonds, M-O (the bond breaking model). By considering how the potential energy diagram of the M-O system changes as a function of interatomic distance, he showed that as a metal and oxygen atom pair become separated, a large variety of states become available for dissociation into the fundamental state M and O, and excited states M\* and O. The lowest lying ionisation state is M<sup>+</sup> + O, in which case the energy required for ionisation amounts to:

$$E_i - EA(O) = E_i - 1.46\text{eV} \quad \text{Equation 2.3}$$



$E_i$  and  $EA(O)$  are the ionisation potential and electron affinity of the metal and oxygen atoms respectively. It can be seen from the equation, that the effect of oxygen can be considered, in part, to be a lowering of the effective ionisation energy.

In 'low damage' SIMS analysis we are interested in two factors: how secondary ions found in mass spectra relate to the composition of their source and; the significance of changes in these signals induced by external effects, i.e. heating, gas exposure, etc. Most of the above theoretical studies are of limited use in providing a basis in this area because, 1) they are concerned with specific ion emission processes from specific surface types and 2) in the case of thermodynamic models, they are concerned with the overall emission, with little recourse to the underlying physical processes. This means that analysis of 'low damage' SIMS data relies mainly on an empirical approach. The rest of this chapter is concerned with providing such a background for the experimental work presented in the thesis.

### 2.5.2 Empirical background

#### Secondary ion emission from clean, single crystal surfaces

A principal concern in 'low damage' SIMS is how secondary ion signals of emitted 'clusters' relate to their source (or origin) on the surface. Many examples have been reported, particularly from materials with ionic bonding. Amongst these are: the detection of cluster ions  $(KF)_n K^+$  from potassium fluoride with up to  $n = 12$  (E.Honda et al. 1978); the detection of

'cluster' ions from ZnS and CaF<sub>2</sub> which are representative of surface structure (R. Buhl and A. Priesinger, 1975) and; successful determination of the surface structure on UHV cleaved mica from detected 'cluster' ions (M.G. Dowsett 1978). Such results are generally consistent with a 'bond breaking model'.

#### Secondary ion emission from adsorbate layers

Analysis of single crystal alkali halide has shown secondary ion clusters of sorbate, substrate and sorbate-substrate species comprising of very large groups of ions which are unlikely to have resulted from re-combination (J. Estel et al. 1976).

This example gives strong supportive evidence that 'cluster ions' are related to substrate/sorbate structure and chemistry.

In the past, low coverage oxygen adsorption has mostly been studied on metals. The first experiments were performed by Benninghoven (1975). The results of such experiments were interpreted by an oversimplified 'oxidation' model which did not take into account the fact that the various stages of oxygen adsorption are usually complex. Nevertheless, analysis of SIMS results still rests on the idea that characteristic changes in ion yield reflect different stages of oxidation.

SIMS has shown quite impressive results with regard to low coverage adsorption on metals, provided that certain precautions are taken. Principal amongst these precautions is that primary ion energy should be kept to a minimum in order to preserve weakly bonded adsorption states.

Yu (1978) has studied oxygen adsorption on (100)W in some detail and has shown that the sensitivity to change in oxide phase decreases with increasing primary ion energy. Change in the oxide phase is characterised by change in the slope of the response of the  $O^-$  signal to oxygen exposure. Yu suggests that this decrease in sensitivity is caused by first order damage, where energy deposited by the primary ion creates electronic excitations at the surface. These excitations perturb the initial electronic configuration and thus smear the bonding information.

Wittmaack (1979) suggests that the effects of primary ion energy are due to the differences in sputter mechanisms between adsorbate and substrate atoms. He cites studies on Tungsten and Molybdenum by Benninghoven and Dawson respectively. Apart from showing strong dependence of secondary ion yields on primary ion energy, these works also reveal that widths of secondary ion energy distributions increase with increasing primary ion energy. It is suggested that a direct relationship may exist between energy distribution width and adsorbate bond strength.

Wittmaack (1979) also provides an interesting analysis of Dawson's study of oxygen adsorption and subsequent sputter removal from Mo (P.H. Dawson 1977). During sputter removal the  $MoO^+$  signal decreases exponentially, (as is characteristic of sputtering from a finite monolayer source with constant secondary ion emission probability). Using the intensity of this signal as an independent variable (related to relative coverage), he has made a direct comparison of the behaviour of positive ion signals during oxygen exposure with that

of positive ions during sputter removal of the adsorbed oxygen. The behaviour of the signal intensities during oxygen exposure and sputter removal of the adsorbed oxygen are found to be identical to within 10% over two orders of magnitude for the  $\text{MoO}^+$  signal. This result suggest the following: the intensity of this signal is directly related to the surface coverage of oxygen; sputter removal of relatively thick adsorption layers causes repopulation of adsorption states which are characteristic of low coverage.

Yu (1978) has reported that the intensity of  $\text{WO}_2^-$  is low, up to an exposure of 2.0 Langmuirs. From statistical arguments it is evident that for less than a monolayer surface coverage, the intensity of molecular ions with two oxygen atoms will be low. This is provided that oxygen is distributed at random. The result therefore suggests that this exposure (2.0 Langmuirs) corresponds to a coverage where O-O bonding starts to take effect. Detection of the  $\text{WO}_2^+$  on the other hand, only occurs after completion of the first monolayer. This suggests that incorporation of oxygen, possibly in ionic bonding, is necessary for emission of the positive oxygen-carrying molecular ions.

### 2.6 Conclusions

The semiconductors studied in this thesis (GaAs, PbTe) can be expected to have more similarities, in terms of ion emission, to the alkali halides than to the clean metal surfaces discussed in this chapter. Bonding in compound semiconductors is always, to some extent, polar-covalent, i.e. both local-

ised and polarised. Further, interactions of sputtered species with the conduction band will occur with much lower probability than with clean metals because of the lower available electron density. Thus ionisation processes which are available to metals will be much less likely for semiconductors. From the above conclusions, it will therefore be assumed throughout the experimental work of this thesis, that ion emission is governed more by bond breaking than by other processes.

CHAPTER 3

EXPERIMENTAL APPARATUS AND TECHNIQUES

### 3.1 UHV SYSTEMS

Two UHV vacuum chambers were employed in the course of the work for this thesis. Earlier experiments used a SIMS system in a UHV chamber which had been specifically designed for SIMS studies in 'ultra clean' conditions (M.G. Dowsett, 1979). These earlier experiments concern investigation of (100)GaAs substrate preparation in UHV and are reported in Chapter 5. The SIMS system had been used in previous studies of cleaved mica (M.G. Dowsett et al. 1978) and InP (M.G. Dowsett and E.H.C. Parker 1979). This chapter will concentrate on describing the second system, as the first system has been adequately described in the above references - it is also very similar to the one used for the bulk of the work. This second SIMS system was used in the studies on MBE grown PbTe (Chapter 4) and later, in the studies of surface preparation and oxygen adsorption on GaAs (to be discussed in Chapters 5 and 6).

The experimental system consisted of a UHV-MBE vacuum chamber equipped with 'in-situ' measurement of Hall coefficient and resistivity. This had previously been used in several studies of oxygen adsorption and irradiation induced effects on MBE grown (111)PbTe films (R. Kubiak 1983, S.R.L. McGlashan 1981). The chamber was suitably modified by addition of SIMS apparatus. With exception of the quadrupole mass filter (V.G. Q8), the modification involved re-location of the SIMS apparatus from the 'old' chamber to the 'new' one. An existing mass filter (V.G. Q7B), already employed for residual gas analysis, was modified by addition of an energy

filter to replace the original Q8 mass filter. Suitable ports for primary ion gun and quadrupole mass filter had already been incorporated at the design stage of the vacuum chamber.

The UHV experimental chamber was pumped by an Edwards 5" diffusion pump backed by an Edwards mechanical rotary pump. Above the diffusion pump were water- and liquid nitrogen-cooled baffles. The lower half of the system housed titanium sublimation pumps, shielded from the top half of the system by a stainless steel plate. A water cooled source assembly, for PbTe growth, was also located immediately above this stainless steel plate.

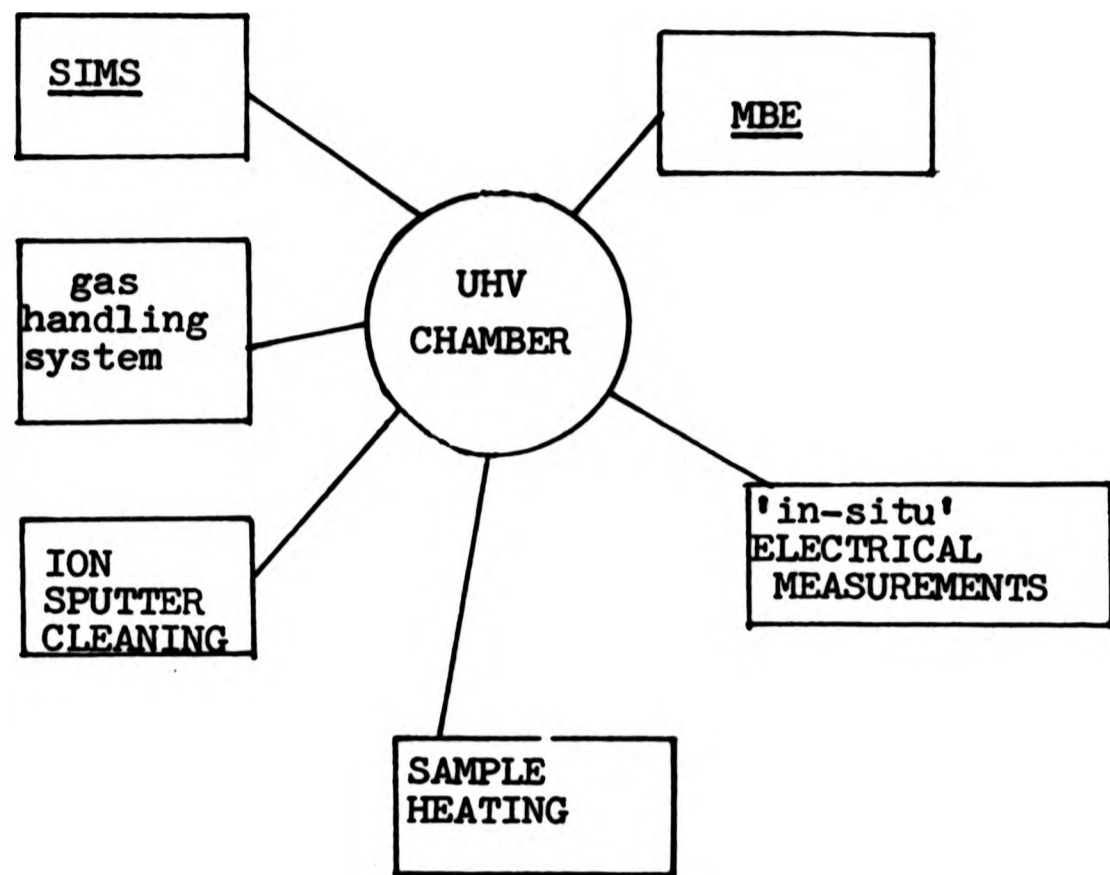
Base pressures of less than  $10^{-10}$  Torr were normally obtained after baking the UHV chamber for 12 hours. A V.G. ion gauge ( $10^{-3}$  to  $10^{-11}$  Torr range) and an LKB pirani gauge (atmosphere to  $10^{-3}$  Torr range) were used for pressure measurement. Correction factors for operating the gauges with gases other than air were obtained from manufacturers operating manuals. A stainless steel plate was fitted above the ion-gauge head to prevent direct, line-of-sight exposures of samples to gas excited by the ion gauge during gaseous exposure experiments.

Fig. 1 shows the layout of the experimental system. It can be seen that there are provisions for MBE PbTe film growth, sample heating, ion sputter cleaning, SIMS analysis and 'in-situ' electrical measurement on PbTe films.

A sample holder is supported on a stainless steel

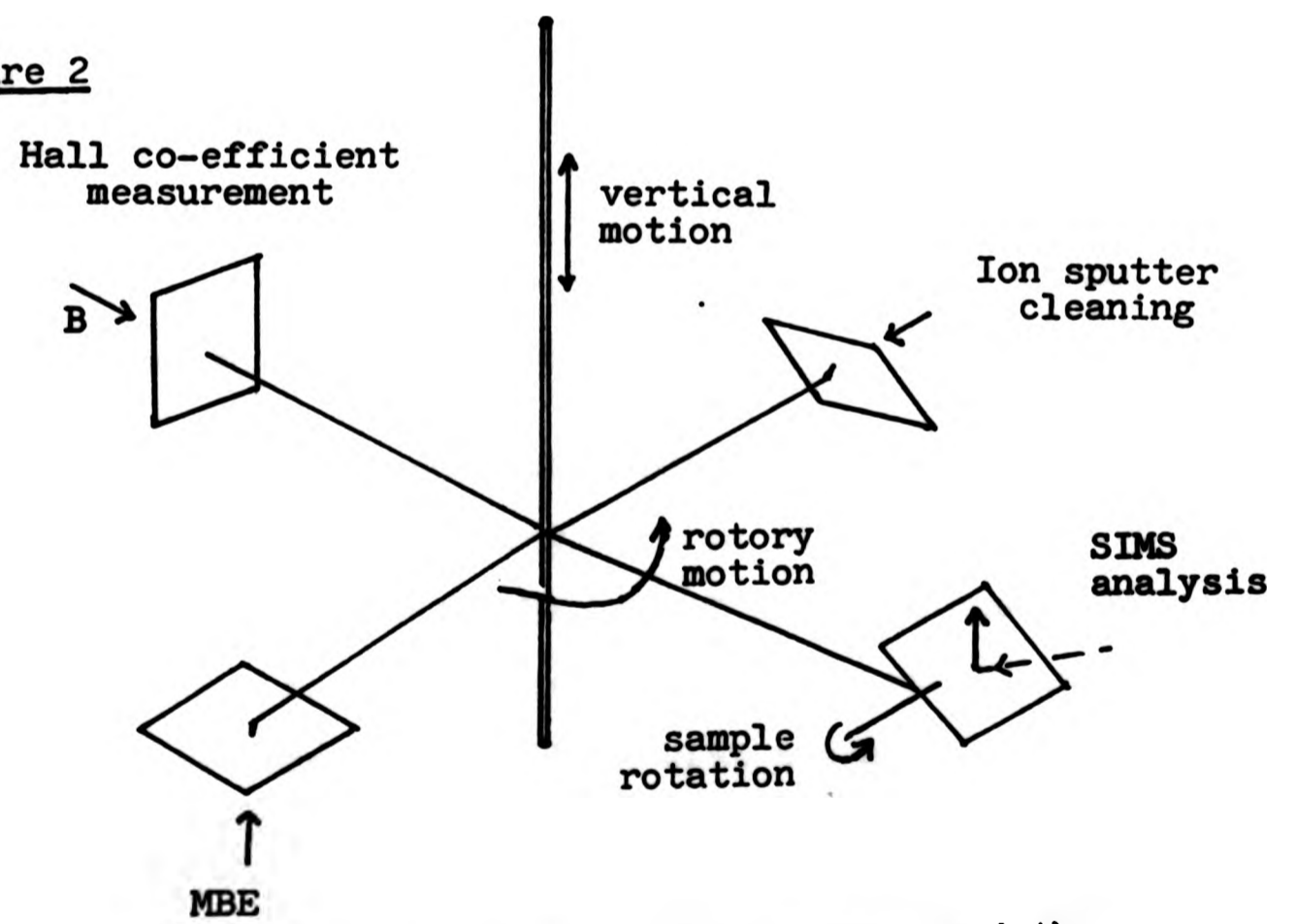


Figure 1



A SCHEMATIC OF THE EXPERIMENTAL SYSTEM

Figure 2



The 'work stations' in the UHV chamber and the directions of motion available to the sample holder

manipulator which gives the holder three directions of motion. These are depicted in Figure 2. The directions of motion are angular and vertical displacements relative to the centre axis of the vacuum chamber and sample orientation relative to the substrate holder support structure. The motions are achieved using an RD2 rotary feed through an extending bellows (V.G.Ltd.). Figure 2 also shows how these motions allow samples to be moved and oriented to the different 'work-stations' in the system, i.e. for SIMS analysis, film growth, ion sputter cleaning, and Hall effect measurement.

### 3.2 Gas-handling Systems

The original gas handling system consisted of three gas bottles connected, via ultra-high vacuum valves, to a second UHV chamber pumped in a similar manner to the main chamber, with base pressures of  $2 \times 10^{-9}$  Torr. The chamber could be isolated from its pumping path and back filled to a pressure of 200 Torr from gas bottles. Gases could then be leaked via a slow leak valve to the main chamber.

This system was used without modification for experimental work on PbTe (Chapter 4). Changing from one gas to another was, however, inefficient in the use of time and expensive high purity gases, as it involved pumping the small chamber to UHV pressures before backfilling with the next gas.

To provide more rapid change-over from one gas to another i.e. from Argon for SIMS to oxygen for gas exposure, a new simpler gas system was built for experiments on GaAs

(Chapters 5 and 6). This gas admittance system consisted of a small volume of pipe work connecting the main vacuum chamber and primary ion source - via separate slow rate leakage and isolation valves - to argon and oxygen bottles. Pipe volume was pumped out during system pump down and baking, right up to the gas bottles. When the chamber reached UHV pressures, gas admittance, isolation and leak valves were closed and the volume behind valves was filled with 1.0 atmosphere of gas via a high purity gas regulator.

### 3.3 SIMS

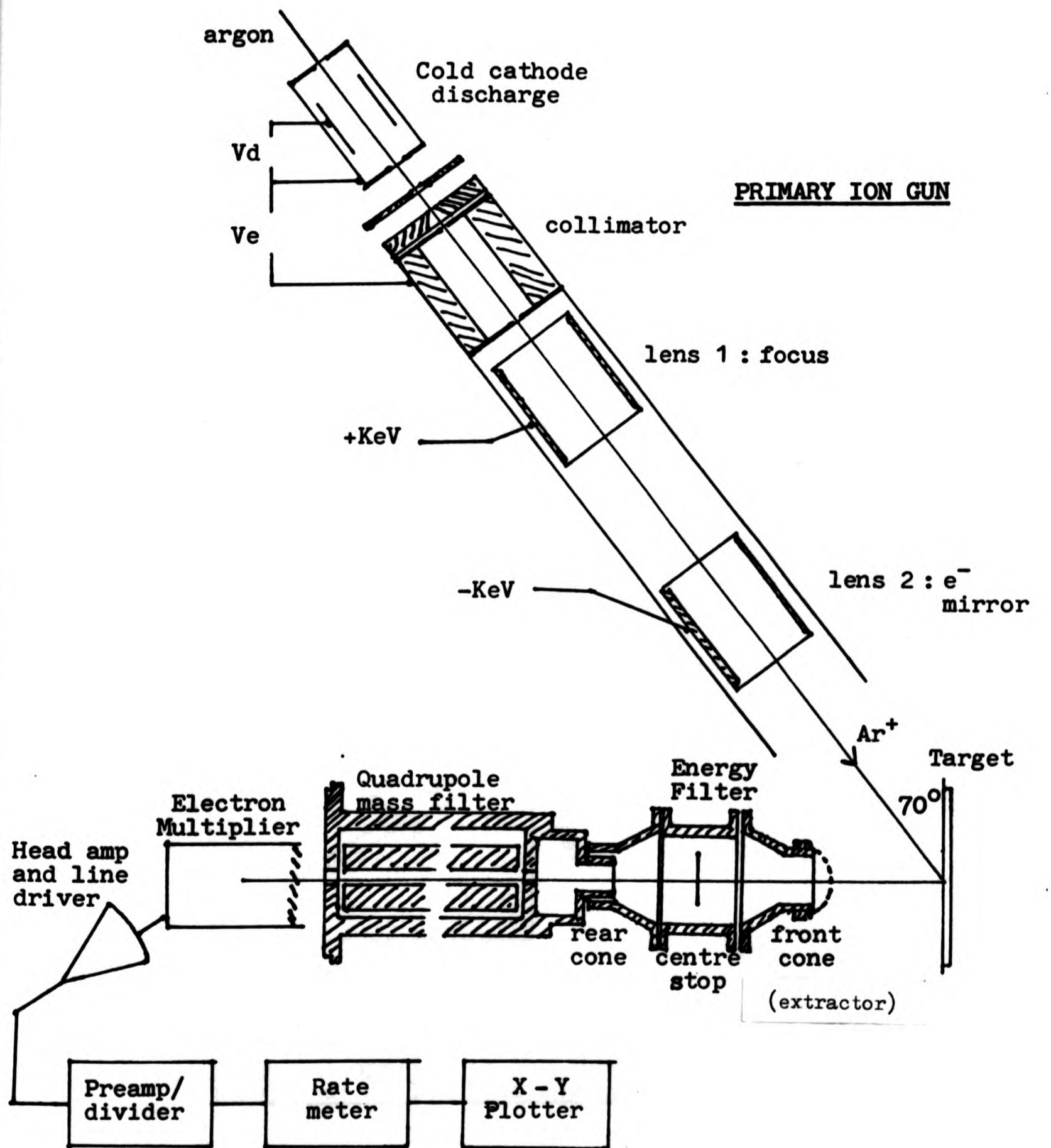
Figure 3 shows details of the secondary ion mass spectrometry system used in analysis. As can be seen, this is a complex electron optic system. Calibration will be discussed after detailing the various components.

#### 3.3.1 Primary ion gun

An A.G.2 (V.G.Ltd.) cold cathode ion gun was used for the source of primary ions. This was modified 'in house' by addition of a focusing lens and tantalum shielding in the cold cathode source (M.G. Dowsett, 1979). On relocation of the ion gun to the second UHV chamber, a tantalum lined ion beam collimator was added to improve control over beam spot size. Argon gas was supplied to the ion source via gas handling systems discussed in section 3.2.

The main electrical characteristics of the gun are shown in Figure 4. The beam energy distribution and current dependence on grid voltage are taken from Dowsett (M.G. Dowsett, 1979). The graph of maximum focused beam current was obtain-

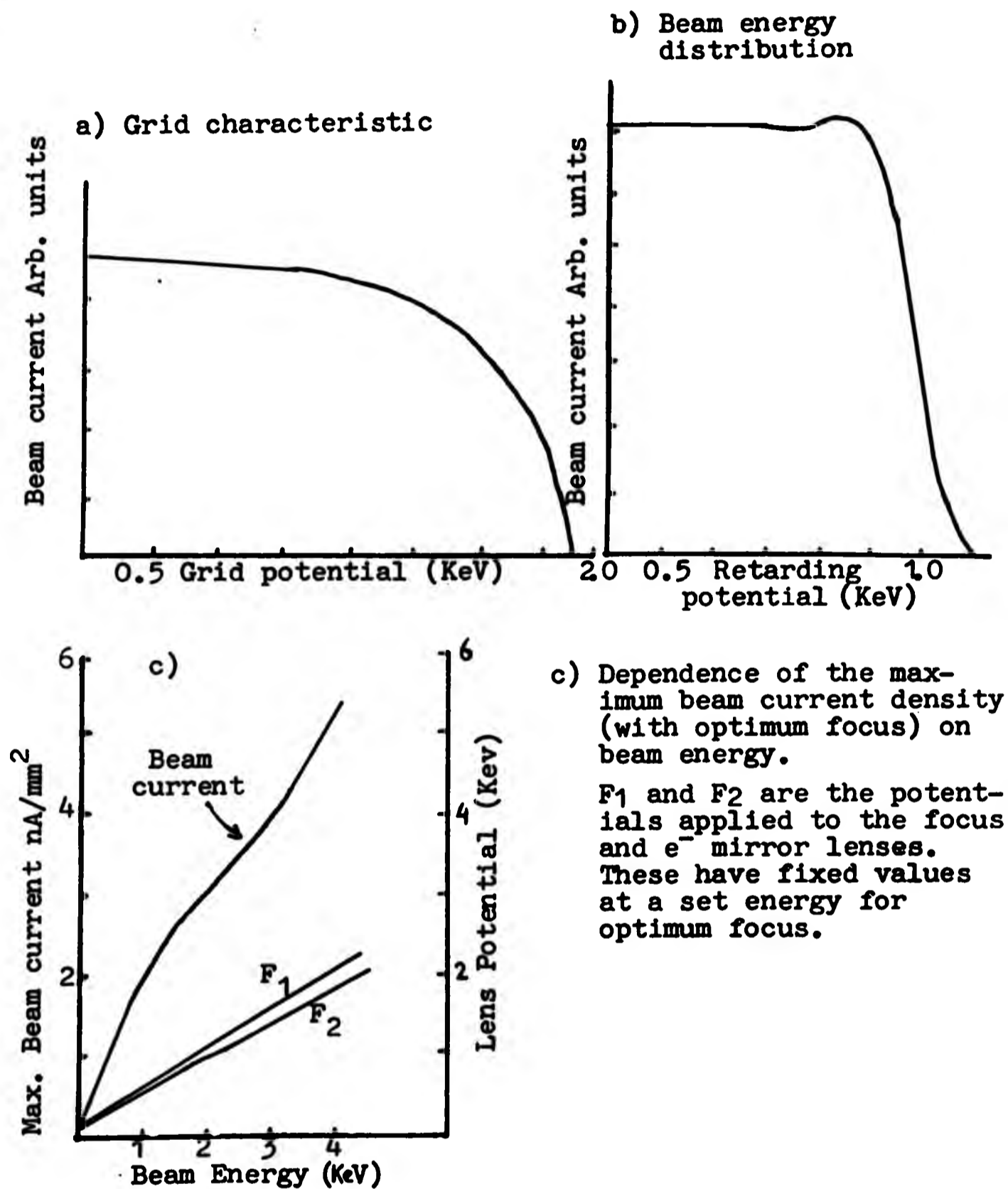
Figure 3



An outline of the SIMS apparatus

( $V_d$  is the cold cathode discharge potential and  $V_e$  is the ion acceleration potential)

Figure 4



The dependence of the primary ion current on:  
a) Grid potential (Dowsett 1979); b) a retarding potential applied to the current sensor (Dowsett, 1979) and: c) Ion beam energy.

ed by adjusting F1 (focus) and F2 ( $e^-$  mirror) for minimum spot size and maximum current density using the current sensor described later (Figure 3).

The ion gun could operate with pressures of  $8 \times 10^{-10}$  -  $5 \times 10^{-6}$  Torr of source gas measured in the main UHV system, and primary ion parameters could be adjusted in the range  $2 \times 10^{-10}$  -  $10^{-7}$  amps  $\text{cm}^{-2}$  (for beam current density), 0.7 - 3KeV (for ion energy) and 1.0 - 3.0mm dia. (for beam diameter on the target).

### 3.3.2 Primary ion current monitoring

The ion gun current was monitored on a collecting plate through a 1.0mm dia. earthed collimator. This collimator was defined by tantalum discs 2.5mm apart and oriented normal to the ion beam. Earlier calibration showed that current measurements on flat stainless steel collectors underestimate primary ion currents by 10% for 1.0KeV ions. This is due to secondary electron emission. Current measurements of the nominally 1.0mm dia. beam through the collimator gave estimates of primary ion current density at the beam centre, but underestimated total sample current by a factor of 3.5. This was due to spreading at the edges of the ion beam in the lens system. Total current measurements were also monitored during SIMS analysis of PbTe using the PbTe film surface.

### 3.3.3 Energy filters

The energy filter consists of three sections, front cone (extractor), centre stop and rear cone (Figure 3). The filter focuses ions emitted from the surface into the entrance of the quadrupole mass filter in a prescribed energy range.

Ions with energies outside this range and neutrals, are stopped by either the centre stop or side walls (Figure 3).

The filter was designed by Dowsett<sup>\*</sup> for the front cone to operate with an attracting potential, in order to extract ions from the sputter region. A potential difference between this and the centre stop then focuses the extracted ions round the stop, where a further potential difference between stop and rear cone provides an image at the quadrupole entrance. Typical operating conditions are discussed in the section concerned with calibrating SIMS optics.

#### 3.3.4 Quadrupole mass filters

A Q7B quadrupole mass filter (V.G.Ltd), was modified by the addition of an axially mounted non-line-of-sight energy filter and an electron multiplier operating in pulse count mode. This quadrupole had a very similar performance to the V.G.Q8 used in the original system. Both quadrupoles operated over a mass range of 0-300 a.m.u. Their rods were 12cm long and separated by 0.4cm. Their controllers were also very similar, providing a ramped rf potential between 0-300 volts at a frequency of 2.0MHz. The dc potential was programmed by, and proportional to, the rf potential. It also varied between 0-300 volts. dc offset could vary between 0-100 volts.

The theory of quadrupole operation has been discussed extensively in the past. The reader is directed first to a simple account by Lawson and Todd (1972) and then to the more detailed accounts by Dawson (1974, 1975). A brief description follows.

\* Dowsett, 1979.

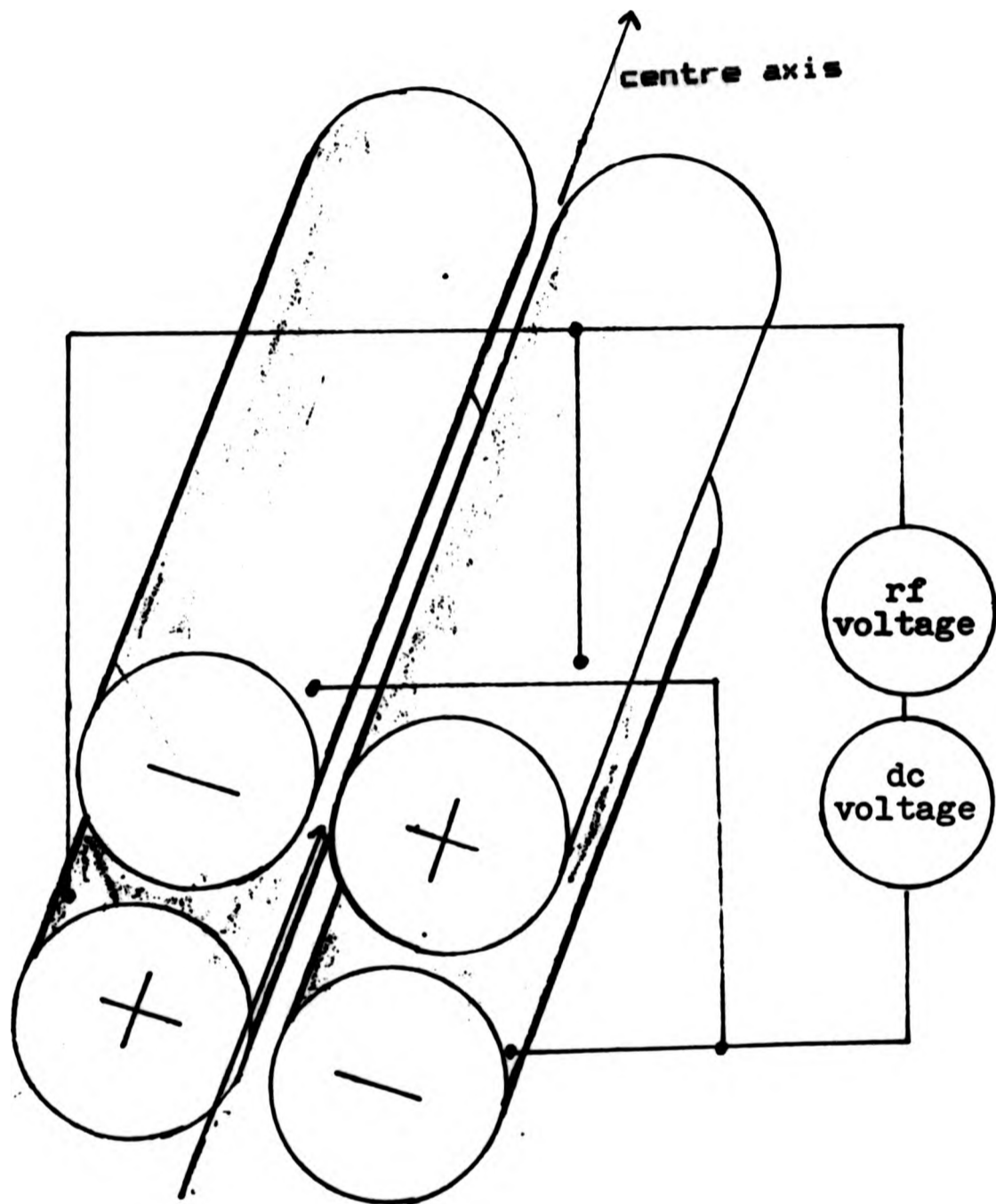
Ions entering along the centre axis of the quadrupole are subjected to a super-imposed dc and rf electric field. This field is produced by potentials applied to the quadrupole rods in the manner shown in figure 5. For an ion with a given  $m/e$  ratio, the particular trajectory is determined by the dc potential, the zero-to-peak rf potential, and the frequency of the rf. Within certain limits these trajectories are stable, or bound, and so ions are transmitted through the device. An ion with a different  $m/e$  ratio will have an unbound trajectory and will be lost, generally by collision with the quadrupole rods.

Solution of the equation of motion for ions in a quadrupole show that stable, focused trajectories occur over a range of  $m/e$  ratio. This range depends on the values of the rf and dc potentials. With constant rf frequency, the range of stability increases towards higher  $m/e$  ratio with increasing rf potential. Thus a mass spectrum can be obtained by ramping the rf potential. The width of the range of stability decreases with increasing dc potential so that this parameter controls the mass resolution. Constant resolution is achieved by keeping the ratio of the dc to rf potentials constant, as the rf potential is increased (ramped).

Because the mass filtering effect in a quadrupole is stronger for heavier ions (these are slower at a given energy and therefore 'see' more rf cycles) the transmission is a strongly decreasing function of increasing  $m/e$  ratio. For this reason, a dc offset potential is added to the ramped rf and dc potentials applied to the rods. This discriminates against lighter ions, and hence reduces the dependence of transmission on the ion mass. The above rf and dc potentials are usually referenced to a dc bias potential (pole bias), which serves to retard more energetic ions as they enter the quadrupole.



Figure 5



**A Quadrupole Mass Filter:**

Ions entering along the Z-axis are subjected to an electric field force resulting from a combination of rf and dc voltages applied to the rods in the manner shown.

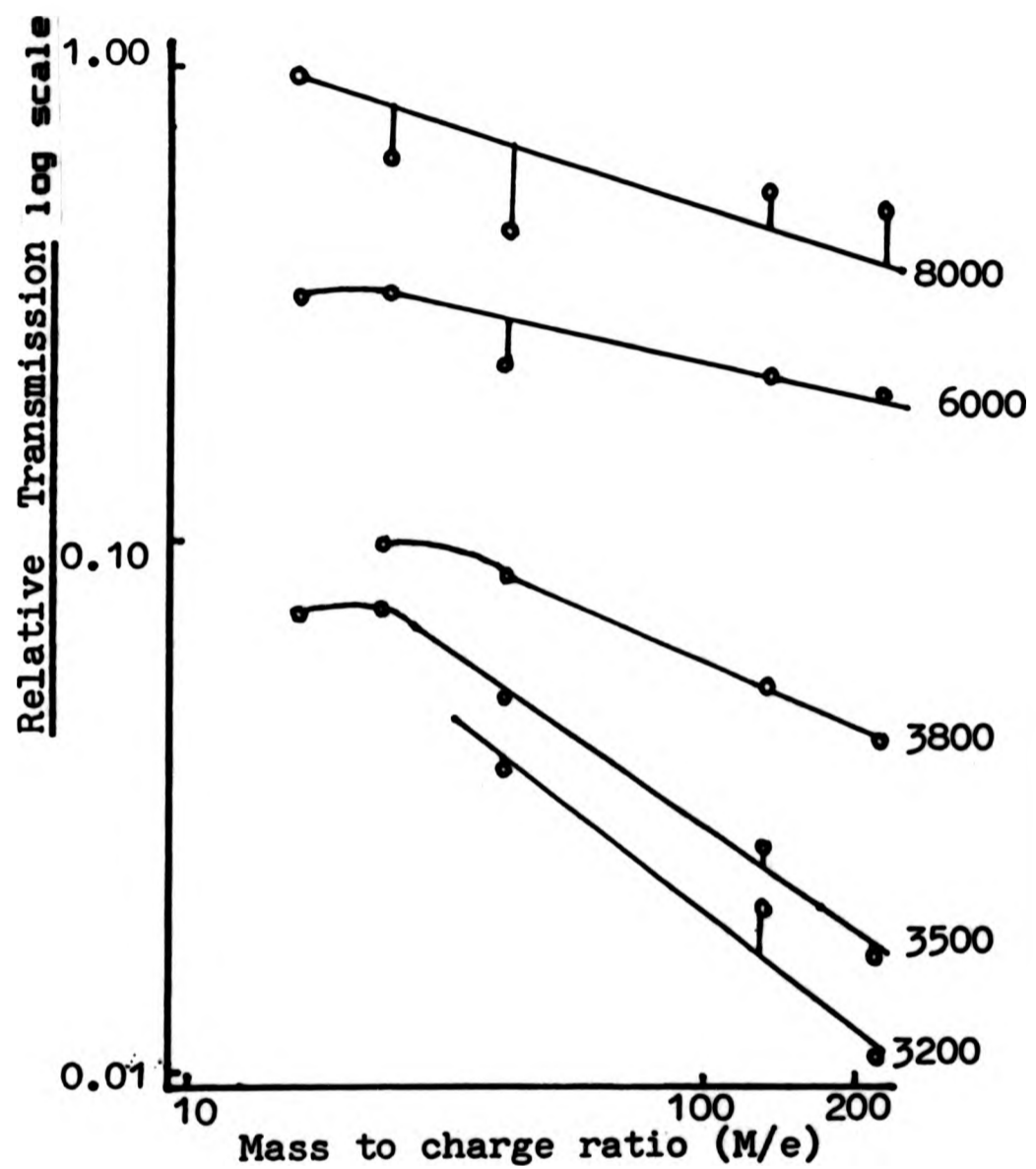
### 3.3.5 Calibration of the mass filter

Estimation of the absolute transmission of the mass filter is a complex and lengthy task, as can be seen in the work of Dawson (1974, 1975). In the present work, such calibration is not so important since the main interests are, in how signals change in response to various treatments, and what fraction of total secondary ion yield (relative transmission) is associated with a particular SIMS signal. The way in which the transmission depends on resolution (dc to rf ratio) is easier to estimate.

Several +ve and -ve mass spectra were obtained from oxidised PbTe at different settings of resolution. Attempts were made to keep all other SIMS parameters constant and to account for poor resolution of neighbouring peaks. The data from these spectra was then compiled to obtain the plots in Figure 6. This shows how the transmission depends on mass-to-charge ratio for various values of resolution setting (arb. units).

A value of resolution of 3000 would resolve single isotopes over the whole mass range. To detect signals at high mass, however, values between 4000 and 6000 were commonly used. At these higher masses, peak identification of poorly resolved signals was facilitated by high resolution spectra obtained using higher SIMS currents from oxidised surfaces. A computer program was also employed to help identify signals. This estimated the peak shape of poorly resolved signals, given isotopic data of constituent atoms and the low resolution peak shape of single isotopic species near the mass of the signal.

Figure 6



The effect of increasing resolution (i.e. dc/rf voltage ratio) on the transmission of the quadrupole filter (DC offset = 50% of f.s.d.)

### 3.3.6 Alignment determination of primary ion beam size and spatial resolution of the SIMS optics.

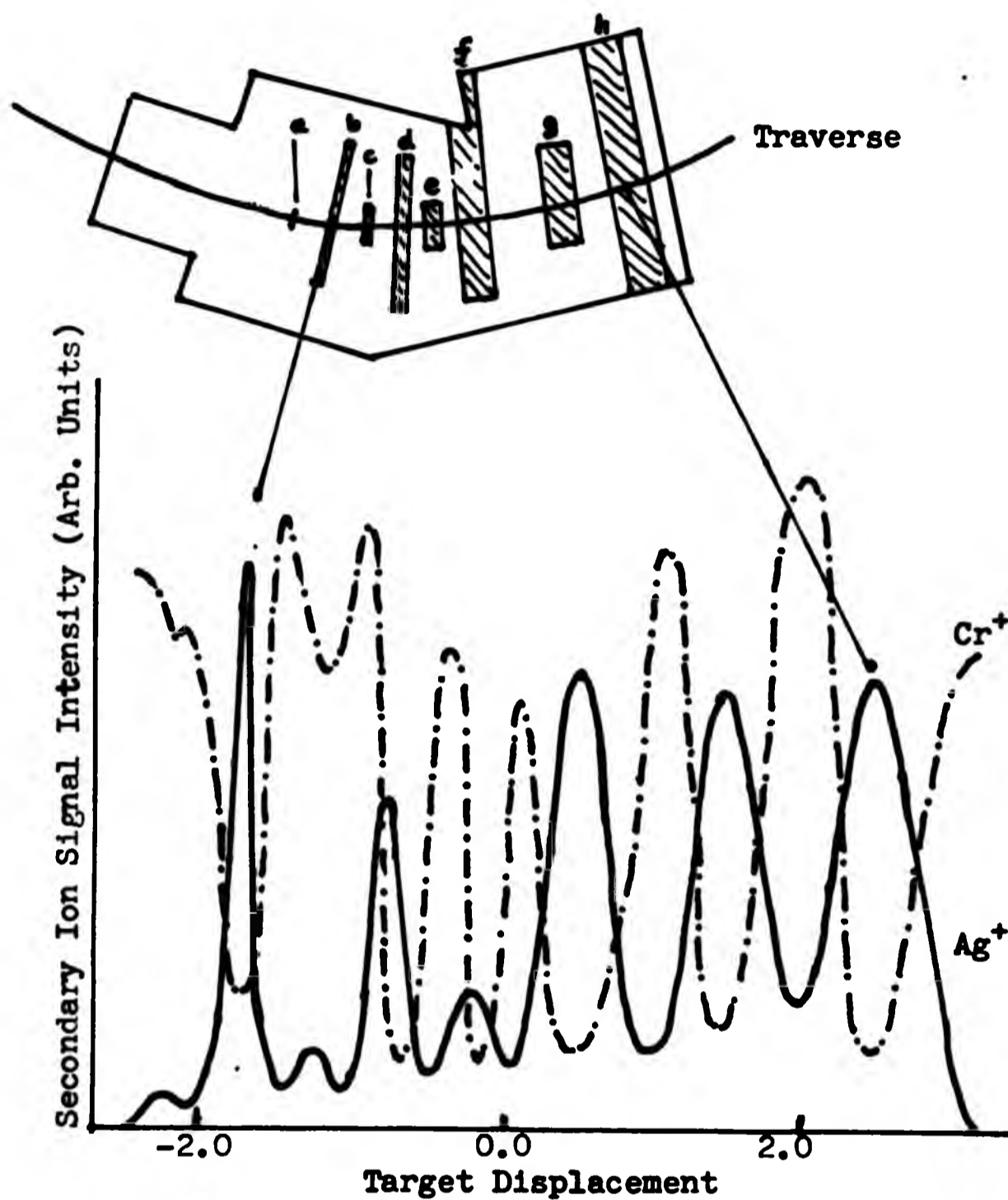
Alignment of the primary ion gun was accomplished by repeatedly optimising the intensity of secondary ion signals obtained from a PbTe film and moving the ion gun relative to the vacuum chamber. This adjustment of the SIMS gun was achieved by compressing copper gaskets which held the ion gun onto the vacuum chamber.

Ion beam diameter was first approximately determined by visual inspection of a PbTe film grown on silver. Such films showed distinct damage marks when subjected to prolonged ion bombardment ( $>1.0 \times 10^{15}$  ions-cm<sup>-2</sup>). The PbTe film showed a distinct elliptical damage zone of area  $1.3 \times 3.0$ mm<sup>2</sup> using a primary ion beam of minimum spot size.

The secondary ion optics were used as a measuring tool to determine the ion beam size more accurately. However, the secondary ion signal intensity depends strongly on the spatial dependence of the transmission characteristics of the energy filter (see section 3.5.7). Therefore, the secondary ion optics could only be used to estimate the ion beam size in the horizontal direction (in the direction of rotory motion (Figure 2) around the centre of the UHV chamber). This is the only direction of movement of the sample where the spatial relationship between the bombarded position and the secondary ion optics remains invariant (Figures 2 and 3).

A special target was constructed to estimate the ion beam size in the horizontal direction. This consisted of silver spots and lines of various sizes, deposited on a chrome film on mica substrate (Figure 7). The intensity of the Ag<sup>+</sup> signal was first optimised to obtain the maximum Ag<sup>+</sup> signal possible from each of the silver spots. This was done in order to find a traverse across the sample which passed through the centre of each spot. The target was then tracked through the ion beam and the SIMS profiles for the Ag<sup>+</sup> and Cr<sup>+</sup> signals were recorded. The profiles obtained can be seen below the drawing of the target in Figure 7.

Figure 7



The  $\text{Cr}^+$  and  $\text{Ag}^+$  signal intensity profile obtained from a resolution test pattern through the SIMS analysis position

Spot and strip sizes: a)  $0.5 \times 1.5 \text{ mm}^2$ ; b)  $1.0 \times 20 \text{ mm}^2$ ;  
c)  $1.0 \times 3.0 \text{ mm}^2$ ; d)  $2.0 \times 2.0 \text{ mm}^2$ ; e)  $2.0 \times 6.0 \text{ mm}^2$ ;  
f)  $4.0 \times 20 \text{ mm}^2$ ; g)  $4.0 \times 12 \text{ mm}^2$ ; h)  $4.0 \times 35 \text{ mm}^2$ .

(Scale of target drawing: 1:1)

The profiles show some apparently conflicting data. Firstly, the  $\text{Ag}^+$  signal from the 1mm wide strip gave the highest signal intensity, secondly, the strip gave the best defined signal and thirdly,  $\text{Cr}^+$  signals from the chrome were otherwise consistently better resolved than silver signals.

A large part of the variation in the  $\text{Ag}^+$  signal (Figure 7) can be attributed to changes in the surface induced by the ion beam while optimising the signal. The  $\text{Ag}^+$  signal was found to decrease very quickly - at a much faster rate than the  $\text{Cr}^+$ . It is thought that this fast decrease was due to a desorption of surface adsorbates, such as oxygen, with a consequential decrease in ionization of the sputtered silver atoms. Some surface diffusion of silver may have occurred either during vapour deposition when the substrates temperature would have been elevated or, as a result of ion induced damage during analysis.

The decrease in resolution across the profile suggests that there may be some variation in sample height. Because the surface of samples are oriented at  $20^\circ$  to the ion beam, small deviations in sample height produce relatively large deviations of the position of the bombarded region. This will change the relative positions of the bombarded region and the secondary ion energy filter. As will be shown in the next section, such a change away from the optimum position, results in a marked reduction in the detected secondary ion signal intensity.

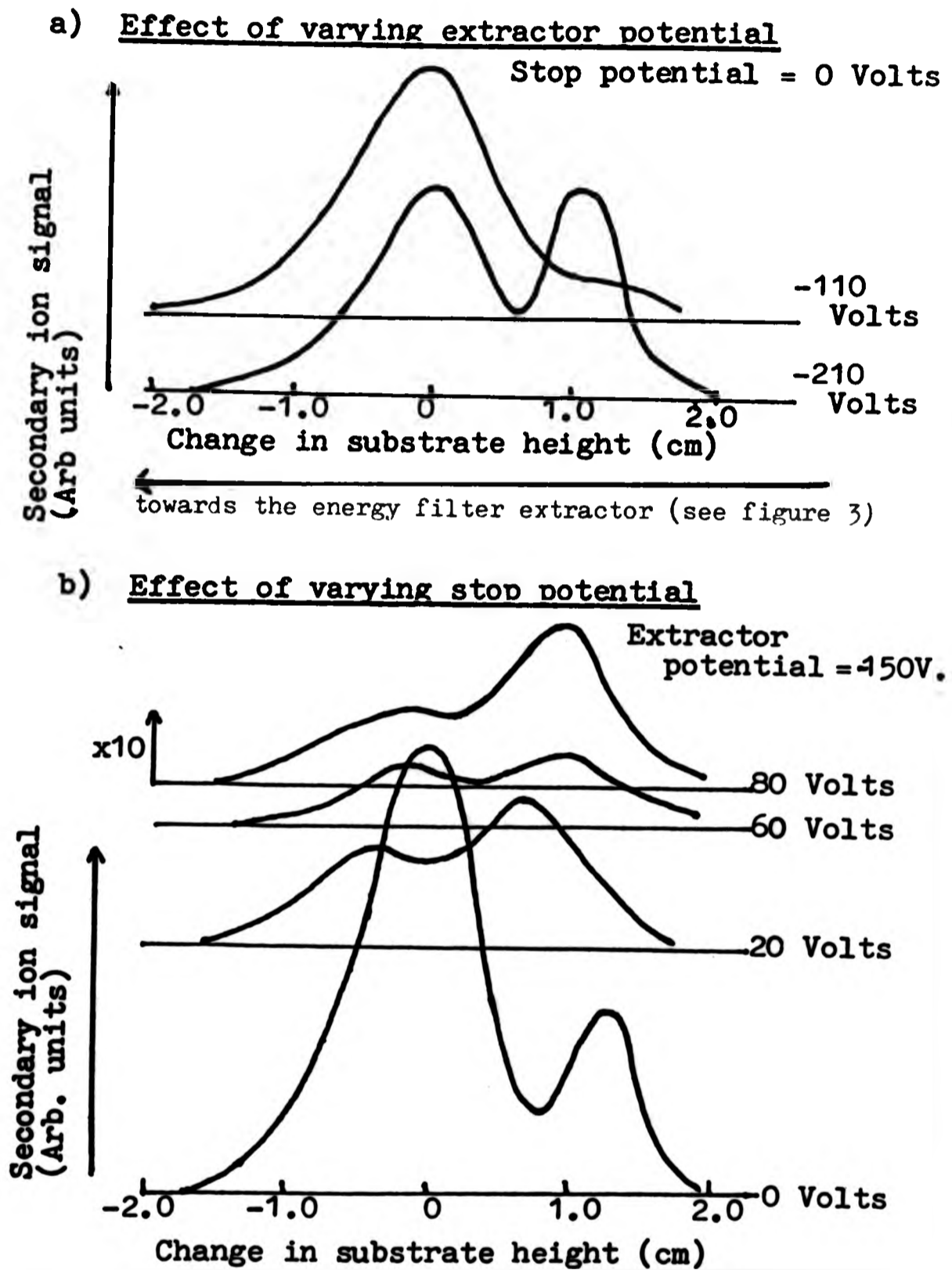
In spite of the inconsistencies mentioned above, the sharp profile of the  $\text{Ag}^+$  signal and dip in the profile of the  $\text{Cr}^+$  signal from the 1.0mm wide strip suggest that over 80% of the beam current is within the 1.0mm strip. This puts an upper limit on the size of the horizontal dimension of the ion beam of approximately 1.00mm.

### 3.3.7 The dependence of the transmission of the energy filter on ion beam position

Figures 8a and 8b show profiles for how the  $\text{Cr}^+$  signal changed with sample height. The  $\text{Cr}^+$  signal in this figure was obtained from the region of chrome between the 4.0mmx12.0mm spot and 4.0mmx35mm silver strips - see Figure 7. The centre dip in these profiles is due to the spatial dependence of transmission. It corresponds to the ion beam hitting the surface directly under the centre stop of the energy filter. The stop potential is zero for the profiles in Figure 8a, so that focusing is solely due to the potential difference between extractor and stop. Notice that for the lower extractor voltage (-100volts), the peaks are asymmetric, peaking where the sample is nearest to the extractor. Higher voltage (-210volts) decreases the difference between the two peaks. i.e. Sample height becomes less important.

Figure 8b shows how profiles varied with positive voltage on the stop and constant extractor voltage (-150volts). With a low positive potential, (20Volts), the transmission maximum is moved from near the extractor towards the lower peak. Higher voltages (20Volts-80Volts) result in loss of much of the secondary ion signal because the lower energy component of the  $\text{Cr}^+$  signal is retarded by the stop. In practise,

Figure 8



The dependence of energy filter transmission on sample height



both extractor and stop potentials were varied to suit sample height.

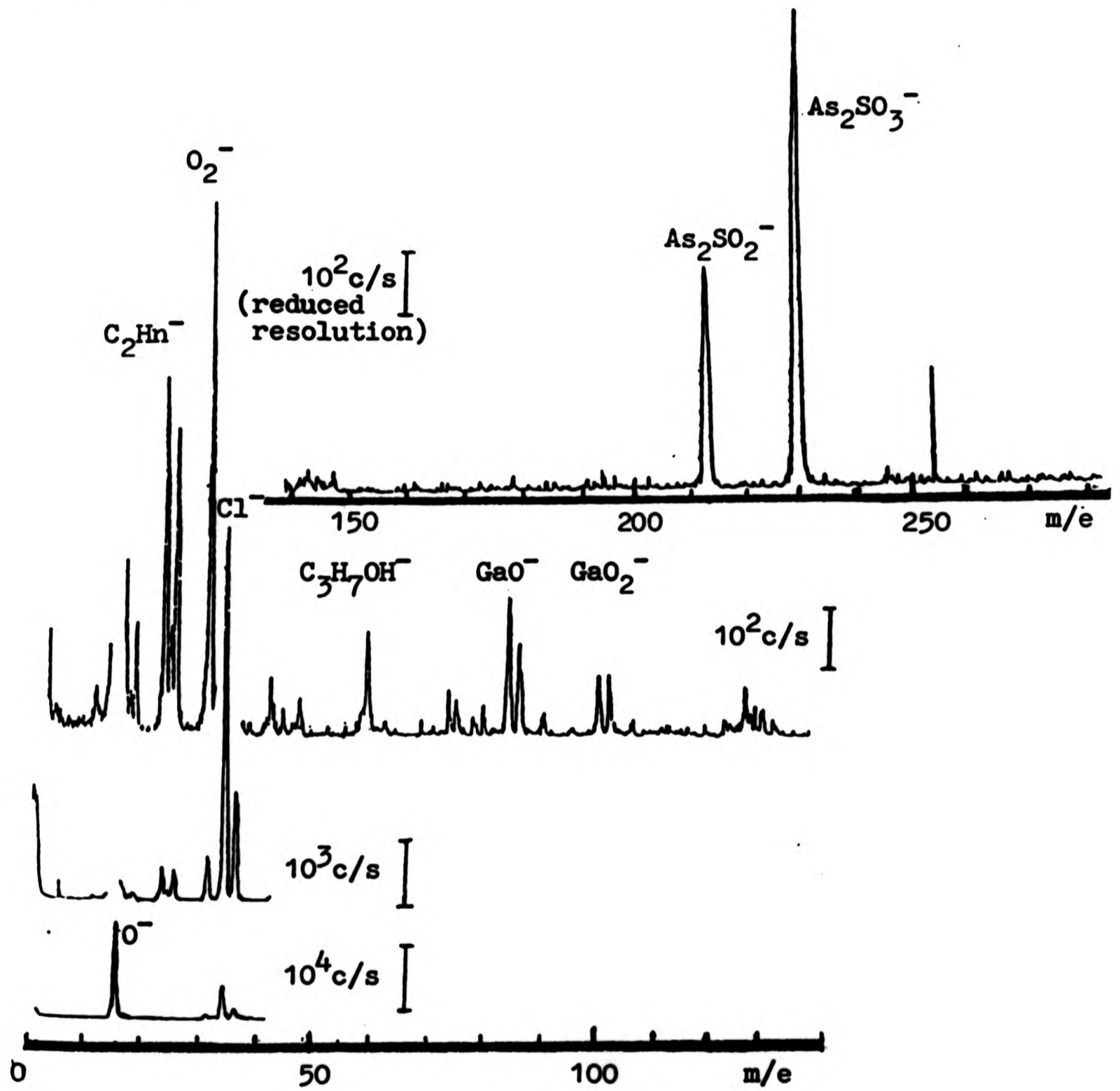
There was little need to change energy filter settings during experiments, provided sample height remained approximately the same. High secondary ion energies did not present a problem, because secondary ion energy peaked below 15eV for most surfaces investigated and only increased from this level for  $O^-$  ions from strongly oxidised surfaces.

#### 3.3.8 Secondary ion mass spectra

For most of the analysis in the thesis, the primary ions used in SIMS analysis consisted of 1.0 KeV  $Ar^+$  ions incident at  $70^\circ$  to the sample norm. This ion beam formed a  $1.3 \times 3.3 \text{ mm}^{-2}$  ellipse on the analysis area. The maximum dose used in each analysis was  $3 \times 10^{14} \text{ ion-cm}^{-2}$ . This corresponds to relatively 'low dose' SIMS. For each SIMS analysis, a fresh area of film was always used. Secondary ions were collected normal to the target, and ions with energies in the range 0-10eV were mass analysed. All mass spectra in a study were taken under the same conditions so that absolute intensities from different substrates and stages of preparation were comparable.

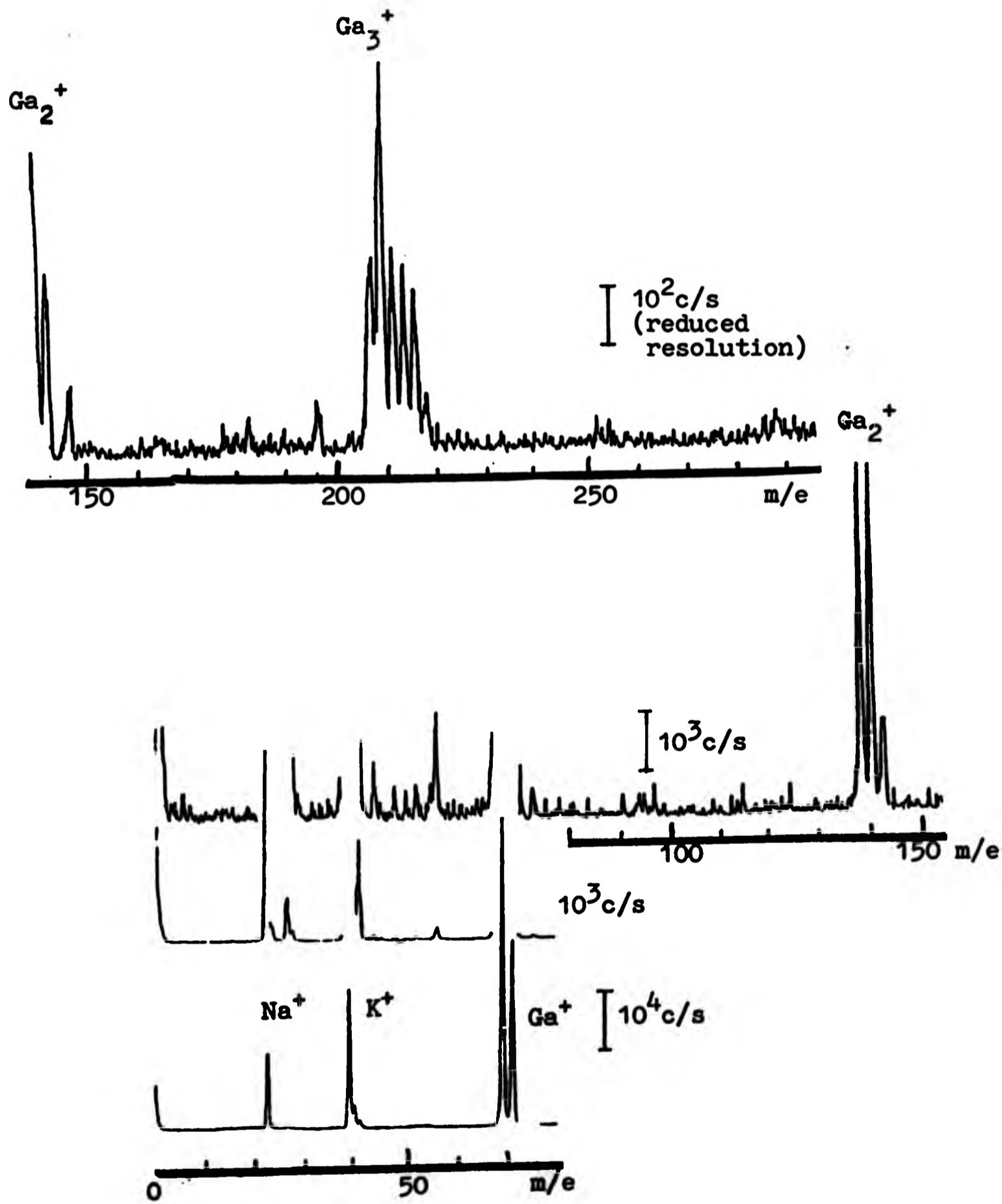
Figures 9a and 9b show SIMS spectra, as recorded from the surface of oxidised (100)GaAs substrates. These spectra were obtained under typical 'low dose' SIMS conditions. Notice that the major peaks and isotopes are easily discernable over the complete mass range using a relatively low current density of  $6 \times 10^{-10} \text{ amps - mm}^{-2}$ .

Figure 9a



A typical negative ion SIMS spectrum from an oxidised GaAs surface.

Figure 9b



A typical positive ion SIMS spectra from an oxidised GaAs surface

### 3.3.9 Differences between the original and relocated SIMS instrument

The SIMS instrument discussed in this chapter gave a performance that was similar to the apparatus used in the earlier studies using the first experimental chamber (M.G.Dowsett, 1979, M.G. Dowsett et al., M.G. Dowsett and E.H.C. Parker 1979). Operating conditions for SIMS analysis were also similar. These were the main differences: slightly lower primary ion energies (0.7KeV) were employed; beam shape was less well defined and; the mass dependent transmission of the quadrupole mass filter was different. Therefore, direct comparisons could not be made of spectra from the two systems. It was possible, however, to make comparisons of relative changes found in signal intensities, as is done in Chapter 5.

### 3.4 Ion sputter cleaning gun

A V.G. AG1 ion gun was used for ion sputter cleaning of (100)GaAs. Preparation for ion sputter cleaning of substrates consisted of out-gasing all ion gun electrodes by electron bombardment from the filament during vacuum system 'bake out' and by running the gun continuously overnight before use. Total current measurements were obtained on substrates mounted on a molybdenum block of area  $2.5 \times 2.5 \text{cm}^2$ , biased to a positive potential (approximately 150 volts) to prevent secondary electron emission. Ion beam size was approximately  $3 \text{cm}^2$ . This was determined with the current sensor used for the V.G. AG2 ion gun. During sputtering, substrates were oriented at  $45^\circ$  to the ion source, with the beam centred on the middle of the substrates.

### 3.5 Sample heating and MBE growth

#### 3.5.1 Sample heating in UHV

The substrate heater/holder assembly for PbTe consisted of two copper plates with approximate dimensions of 2.5cm x 5.0cm x 0.25cm, held together by four molybdenum fixing screws. The plates had milled tracks on one side, approximately 2mm apart, in which quartz sleeved tungsten heater wire was placed. The top plate also had a 1.0mm hole to accommodate a chromel-alumel thermocouple. Mica substrates with predeposited silver contacts were fixed to the substrate holder with tantalum clips and aquadag. Contact to substrates was obtained by compressing tantalum strips onto silver connections. All connections for heater, thermocouple and sample measurement, were taken to fused quartz feedthroughs via glass bead insulated copper and tungsten wire.

Identical sample holders were used for GaAs in both vacuum chambers. Substrates were soldered with indium (Metal Research, Cambridge) onto a 0.125" thick molybdenum block of area 3cm x 5cm (99.9%, Noriba Ltd.), held onto a substrate heater/holder with tantalum clips (Metal Research, Cambridge). The substrate heater assembly consisted of 0.1mm thick molybdenum foil sandwiched between fused quartz plates (99.9%, Thermal Syndicate Ltd.,) held with molybdenum fixing screws onto a stainless steel support structure. This structure also supported a tantalum foil reflector on the reverse side of the quartz plates to the molybdenum block. A chromel-alumel thermocouple positioned in a 1.0mm dia. hole drilled in the molybdenum block was used to estimate

substrate temperatures. A current of 5.0 amps at 12 volts in the molybdenum foil heater gave a substrate temperature of 580°C.

### 3.5.2 Growth by MBE of thin semiconducting films

(111)PbTe films were grown in the same manner as has been previously reported by Kubiak (1983) and McGlashan(1981). Briefly, the films were grown by a modified form of the triple temperature technique (C.T. Foxton and B. Joyce 1973). Both Pb and Te fluxes were derived from a single open boat quartz tube source of 99.999%PbTe of 150-200 m particles prepared from p-type, Te rich, single crystal PbTe (Koch Light Chemicals). Before growth, both source and substrate were taken to temperatures well above the growth temperatures to desorb volatile contaminants. During growth, the molecular beams impinged on a mica substrate (Mica Muscavite Supplies Ltd.) at a temperature of 250°C and a quartz film thickness monitor (Edwards FTM 4,2) - both at the same distance from the source. Doping levels in the film which were determined by Pb in the molecular beam (S.R.L. McGlashan 1981), could be controlled by the changing rate of film growth ( $0.51\text{sec}^{-1} - 3\text{\AA}\text{sec}^{-1}$ ). This gave carrier concentrations between intrinsic levels of  $2 \times 10^{16}\text{cm}^{-2}$  and strongly n-type doped films of  $10^{19}\text{cm}^{-2}$ . The resulting PbTe films showed degraded mobilities which could be improved towards bulk values by annealing at 280°C for a few minutes. A magnetic field was generated external to the vacuum system for Hall co-efficient measurements.

Previous studies on characterisation of these native films conclude the following: 1) Carriers are uniformly distributed throughout the film; 2) Hall mobility is independent of carrier concentration; 3) near bulk values of mobility for very thin films (500Å), suggest that the PbTe surfaces correspond to near specular scattering.

Previous structural analysis shows that the main defects are double-positioned grain boundaries and dislocations lying approximately perpendicular to the film surface. These are characteristics of PbTe grown on mica (E.H.C.Parker and D. Williams 1969). The boundaries form loops which generally enclose domains of single orientation.

The UHV preparation for MBE and the growth and measurement of (100)GaAs layers is described in detail elsewhere (J. Grange 1979, B. Meggitt 1980). A Langmuir source assembly which had been used previously for PbTe deposition was employed to provide an As<sub>4</sub> flux during GaAs substrate heating. The charge for the source consisted of granules of alpha arsenic in an open quartz tube boat. This assembly resided in a graphite lined source heater, surrounded by a liquid nitrogen shroud.

CHAPTER 4

A SIMS STUDY OF OXYGEN RETENTION ON PbTe FILMS  
GROWN BY MBE ON MICA SUBSTRATES



CHAPTER 4

A SIMS STUDY OF OXYGEN RETENTION ON PbTe FILMS  
GROWN BY MBE ON MICA SUBSTRATES

#### 4.1 INTRODUCTION

This chapter presents the results of a SIMS study of oxygen retention on (111)PbTe films grown by molecular beam epitaxy MBE. Such a study has become necessary because of the conflicting picture left by past studies of how oxygen is adsorbed from low pressure exposures. Much of the confusion is now known to have stemmed from the way in which samples have been prepared for oxygen exposures, and from the use of electron beam irradiation, i.e. during Auger spectroscopy. This interferes strongly with oxygen adsorption. SIMS analysis on MBE grown PbTe offers the possibility of observing directly the adsorption of oxygen, while producing a minimum of damage to a surface. The use of MBE to grow thin PbTe films, produces films which have a well defined response to oxygen which is easily reproduced.

Early investigations of oxygen adsorption have relied mostly on measurements of Hall coefficient and resistivity. It is the differences that have been found in such measurements, which have given rise to different pictures of how oxygen is adsorbed. At the time, these differences appeared to be associated with differences in surface preparation used by various experimenters. This could not be checked directly with electrical measurements for, although electrical measurements are very sensitive to interactions of the PbTe surface with oxygen, they are incapable of providing the kind of detailed surface information that is essential for understanding interaction mechanism(s) (Malane and Zemel 1969, Green and Lee 1966, Parker and Williams 1976, Egerton

Juhasz 1969). This kind of information can only be obtained by probing the surface with a surface analytical technique like SIMS, which has the potential to give direct verification of the presence of oxygen and how it is bonded to the surface.

The results of electrical studies show that surface preparations fall into groups which give a different response to oxygen. In the first group, surfaces are prepared from air-exposed films by cleaning with ion sputtering and anneal in UHV. For these films, oxygen exposures at approximately  $10^{-3}$  Torr produce p-type behaviour. This has been explained in terms of electron trapping, resulting in depletion/inversion at the surface (Melane and Zemel 1969). The second group, on MBE grown (111)PbTe films (Parker and Williams 1976, 1977), show a more complex behaviour where the pressure of exposure determines the dominant mechanism for oxygen adsorption. Low pressure oxygen exposure results in an irreversible reduction of n-type carrier concentration to intrinsic levels and constant mobility at near bulk values ( $1700\text{cm}^2(\text{VS})^{-1}$ ). This electrical response has been interpreted in terms of oxygen retention on excess Pb atoms which are sustained by diffusion of Pb interstitials from the film - this is referred to as 'the mobile defect model' (Parker and Williams 1976). At higher oxygen exposure pressures  $P(\text{O}_2) > 10^{-2}$  Torr, these films show p-type behaviour with implied band bending. A large part of this doping appears to be associated with the surface as it can be reversed by returning films to UHV.

Surface analysis of sputter cleaned but unannealed surfaces with LEED, AES, UPS and XPS (Sun et al. 1978), has indicated that ion bombardment induced damage anneals out at room temperature to provide suitable surfaces for oxygen adsorption experiments. Examination of MBE grown PbTe films however, shows that this surface is particularly sensitive to e-irradiation and ion bombardment at doses which are typical of AES analysis and sputter cleaning. Recent studies have shown that both these fluences modify the electrical properties of native, and oxygen exposed MBE grown films and change the response of these to further oxygen exposure (Kubiak et al. 1982, McGlashan et al. 1979). This sensitivity of the MBE grown PbTe surface suggests that oxygen adsorption on films prepared by sputter cleaning, as the first group of studies mentioned, is dominated by factors associated with the preparation methods used, rather than by inherent properties of the clean unperturbed PbTe surface. Further, because of the sensitivity of PbTe, the application of surface analysis techniques which depend on electron or ion bombardment are themselves brought into question. For example, AES has been shown to be unsuccessful at detecting the presence of adsorbed oxygen on MBE grown PbTe where electrical analysis has indicated the presence of a substantial oxygen coverage (McGlashan et al. 1979). This inability of AES to detect oxygen suggests that adsorbed oxygen is desorbed by the electron beam before its presence can be registered in the AES spectra.

In the present study, SIMS is evaluated as a surface

analysis technique for PbTe surfaces. The original aims of the study were to determine whether SIMS could be used to test the 'mobile defect model' for oxygen adsorption mentioned earlier. Electrical measurements in preliminary tests showed, however, that surface damage also occurs during SIMS analysis and that this damage is sufficient to modify oxygen adsorption behaviour. Unlike the cases discussed above, damage produced during SIMS analysis does not completely dominate oxygen adsorption kinetics, but, it is sufficient to complicate adsorption of oxygen and make interpretation of SIMS spectra from such surfaces extremely difficult. 'In-situ' electrical measurements do help, however, to sufficiently enable experiments which investigate, not the direct adsorption of oxygen, but the desorption of oxygen that occurs during SIMS analysis. The experiments are partially successful in that they show that changes in  $O^-$  and  $Pb^+$  SIMS signals and film conductance, after low pressure oxygen exposures, are related. They suggest that before damage is introduced by SIMS analysis, O and Pb are initially bonded together and that during SIMS analysis, fragmentation of such bonds are responsible for changes in electrical properties. The results of the study are consistent with the 'mobile defect model' for oxygen adsorption.

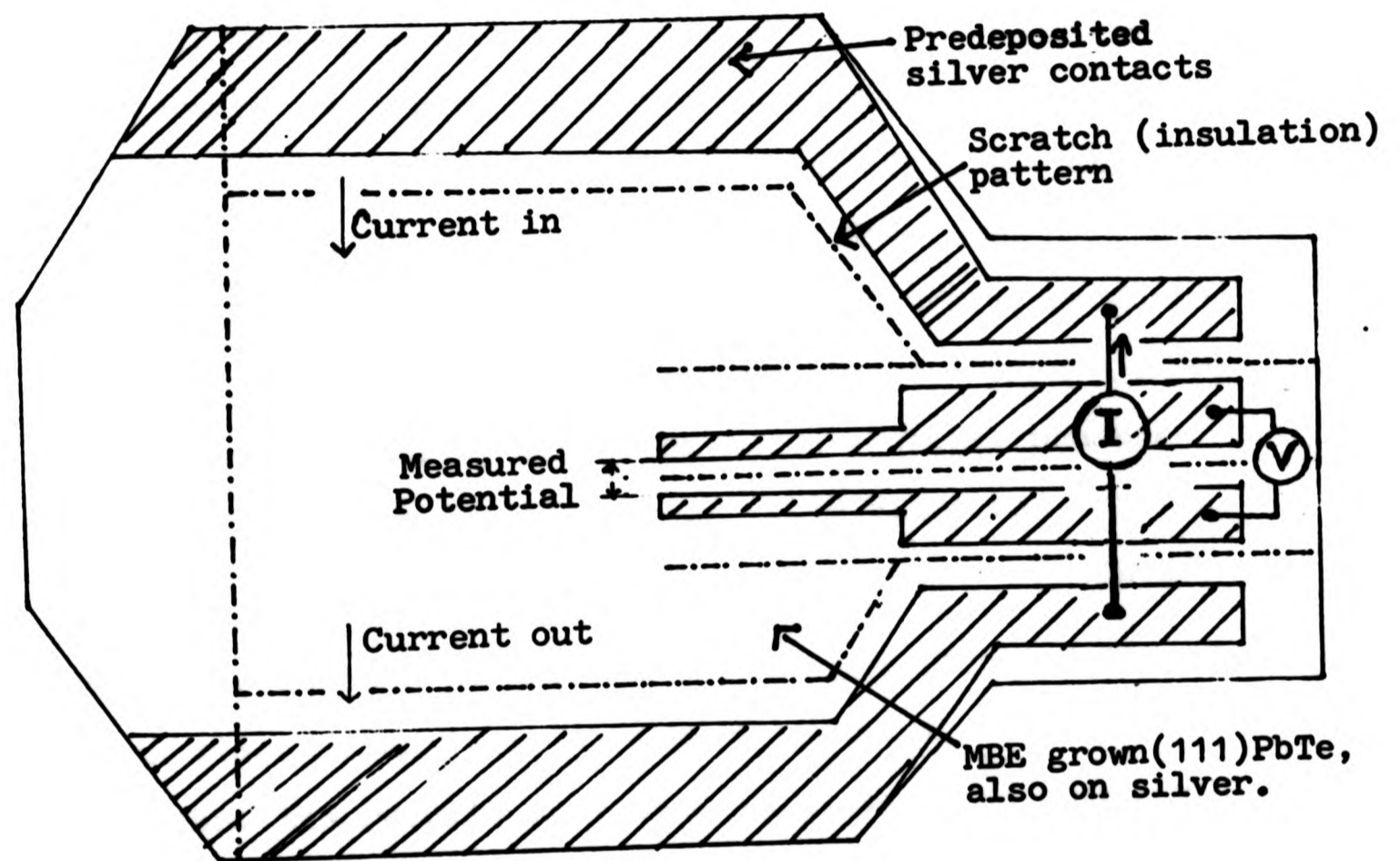
## 4.2 Experimental

Experiments were performed in a stainless steel UHV vacuum chamber which is described together with provisions for MBE PbTe film growth, SIMS analysis and 'in-situ' assessment of electrical properties, in Chapter 3.

### 4.2.1 Film growth and substrate structure for 'in-situ' electrical assessment of PbTe films

Fig. 1 shows the structure of the PbTe films used for the bulk of the experimental work. The figure shows that PbTe is deposited over the entire area of a cleaved mica substrate on which silver connections have been previously deposited. An electric current, used to induce potential gradients in the film, is constrained to enter and exit the film at specific points by shallow scratch marks scribed in the mica before PbTe deposition. The coverage of PbTe is poor over the steps produced by the scribing and measurements show that the scratch marks give good electrical isolation. A constant current flows through the two outside contacts shown in the figure (for electrical measurements.) The potential resulting from this current across the two innermost contacts is measured. Measurements of film conductivity and mobility using this arrangement, agreed with measurements on films in past studies using different procedures to define the film for electrical measurements (Kubiak et al. 1982, McGlashan et al. 1979, Parker and Williams 1976, 1977). In these studies, PbTe films have been defined by depositing PbTe through a molybdenum mask to give in a van der Pauw (1958) shaped film. Such a procedure

Figure 1



Structure of the PbTe on mica films

This structure allows 'in-situ' electrical measurement of Hall co-efficient and resistivity.

could not be used here because preliminary trials showed that any exposed mica would charge up under the influence of the primary ion beam and deflect the ion beam from the point of analysis.

#### 4.2.2 Experimental analysis

PbTe films were grown in the manner described in Chapter 3. After growth, they were subjected to oxygen exposure in the range  $2 \times 10^{-6}$  Torr to 1.0 Torr. Before and after the oxygen exposures, the films were analysed with SIMS, and Hall coefficient measurements were obtained. Electrical conductance of the films was continuously monitored. Oxygen exposures were accumulative, i.e. SIMS and electrical measurements were obtained from 'as grown' PbTe films and from the same films after successive, accumulated oxygen exposures. SIMS and electrical parameters and the procedures followed at each stage of analysis were kept the same, in order to ensure that the results from each stage could be compared. This experimental procedure and the parameter settings used are detailed below.

##### 'low dose' SIMS analysis

'low dose' SIMS spectra were obtained in a background pressure of  $5 \times 10^{-8}$  Torr of Ar gas with a residual UHV pressure of typically  $2 \times 10^{-10}$  Torr. Primary ion beam intensities ( $2.0 \times 10^{-10}$  amp-mm<sup>-2</sup>), and analysis times (300 sec) were kept to a minimum. Major peaks that were present in the secondary ion spectra were recorded first, to ensure that any changes induced in these by the analysis were minimised.



No area of a film was subject to SIMS analysis more than once.

These precautions were only partially successful in limiting the effects of SIMS analysis on the surface. Typically, the above analysis would produce a change in major SIMS signals like  $Pb^+$  of  $\approx 30\%$ . Analysis also changed film conductance. This had a complex dependence on the history of oxygen exposure and ion bombardment of a sample.

SIMS analysis of sputter removal of adsorbed oxygen layers  
Changes observed in the main SIMS signals were recorded during more prolonged SIMS analysis where the total dose received in a area was  $4 \times 10^{14}$  ions-cm<sup>-2</sup>. Here, SIMS spectra were repeatedly recorded. A relatively fast scan rate of 100 seconds was used in recording spectra to ensure that an adequate number of data points were recorded from each SIMS signal to ensure that fluctuations in the response of these would not be missed.

#### Electrical measurements

The Hall coefficient of films was recorded just prior to SIMS analysis and the conductance of the films was recorded continually. Absolute values of these electrical measurements from surfaces which had previously been analysed with SIMS are of dubious quality. This is because the electrical measurements only give an accurate reflection of changes in the film properties when these changes are distributed uniformly through the film. There are indications that in some circumstances, the effects of ion bombardment

induced defects are transmitted, by diffusion, through PbTe films. An earlier reported example of this is global changes in electrical properties observed with local electron irradiation in AES analysis (McGlashan et al. 1979).

Limitations of the experimental analysis.

The above method of analysing the PbTe surface has two problems associated with it. Firstly, oxygen adsorption occurs on surface defects induced by ion bombardment during earlier SIMS analysis. It will be shown that although no region of film was analysed more than once, the damage produced by SIMS significantly affects oxygen retention. This problem could have been overcome by preparing freshly grown films for each oxygen exposure. Unfortunately, however, this was not possible due to insufficient time in the experimental programme.

The second problem is that the SIMS instrument is not capable of monitoring how SIMS signals vary during oxygen exposure. Such capability would have required a much more sophisticated and expensive SIMS apparatus than that used in the current study. This problem is alleviated to some extent by investigating the desorption of oxygen and other effects of ion bombardment during SIMS analysis. Several studies concerned with oxygen adsorption on metals have shown that changes in SIMS signals during SIMS analysis of adsorbed oxygen layers can be related to the form of adsorption initially present on the surface (Dawson 1977, Wittmaack 1979, Yu 1977, 1978). A specific example of this is the case of sputter removal of adsorbed oxygen from

molybdenum (Winograd et al. 1978) where sputter removal of oxygen is shown as being reversible with adsorption.

#### 4.3 Results

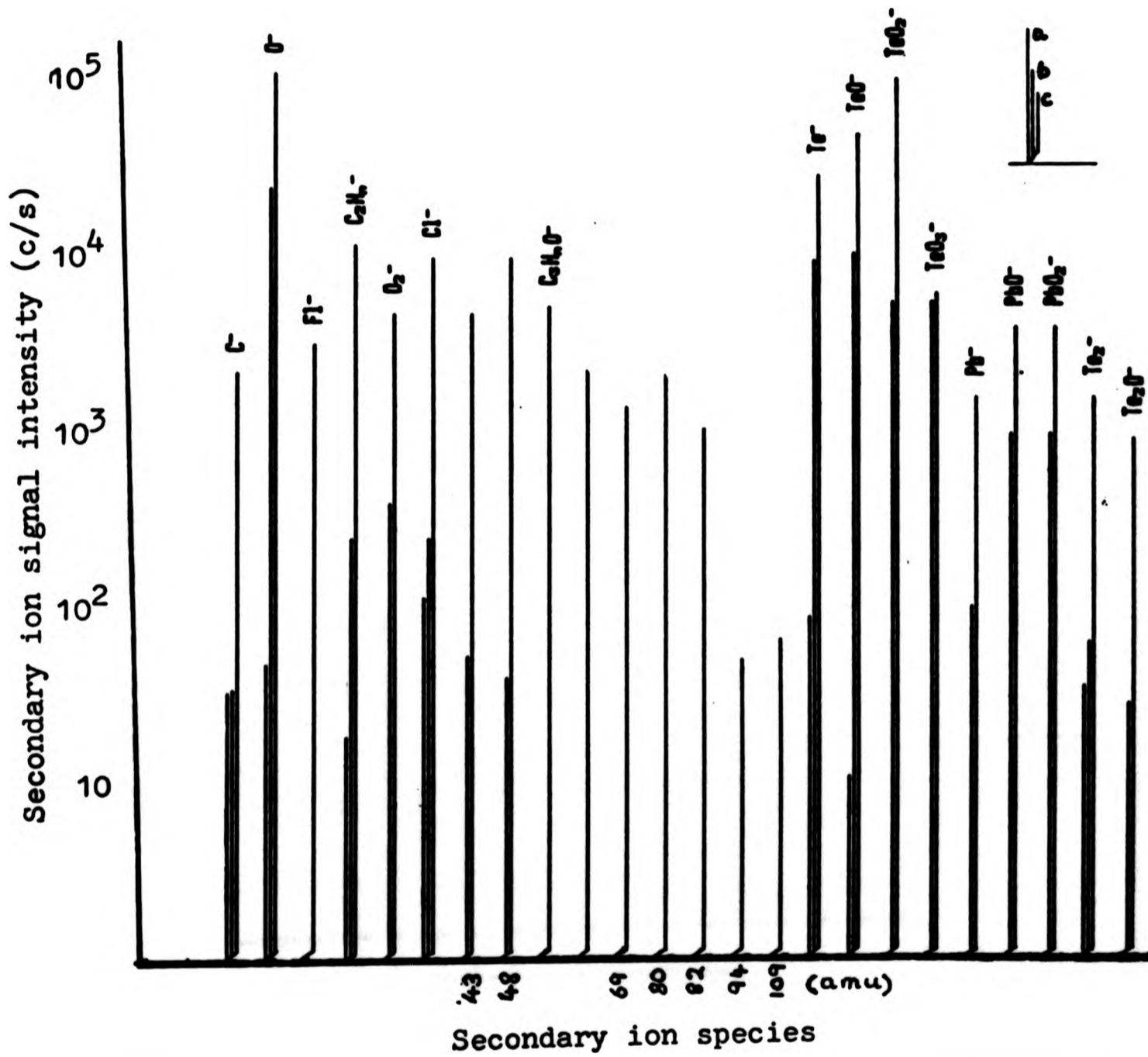
##### 4.3.1 The sensitivity of SIMS analysis to oxygen on the PbTe surface.

Figs. 2a and 2b show comparative SIMS spectra from as-grown (111)PbTe and the same surface, after oxygen exposure and after air exposure.

Consider Fig. 2a first. Notice the very large changes that are induced by the exposures in the negative ion signal intensities of  $O^-$  and many of the oxygen containing signals. In particular, it can be seen that  $TeO^{2-}$  which is not detected from the fresh grown film, is more than a factor of  $10^4$  bigger on the air exposed surface. The small  $O^-$  signal from the freshly grown film is thought to be due to oxygen adsorbed from the residual gas ( $2 \times 10^{-10}$  Torr) over a relatively long period (24 hours) before SIMS analysis. Both these observations show that SIMS has adequate sensitivity to oxygen for surface investigations.

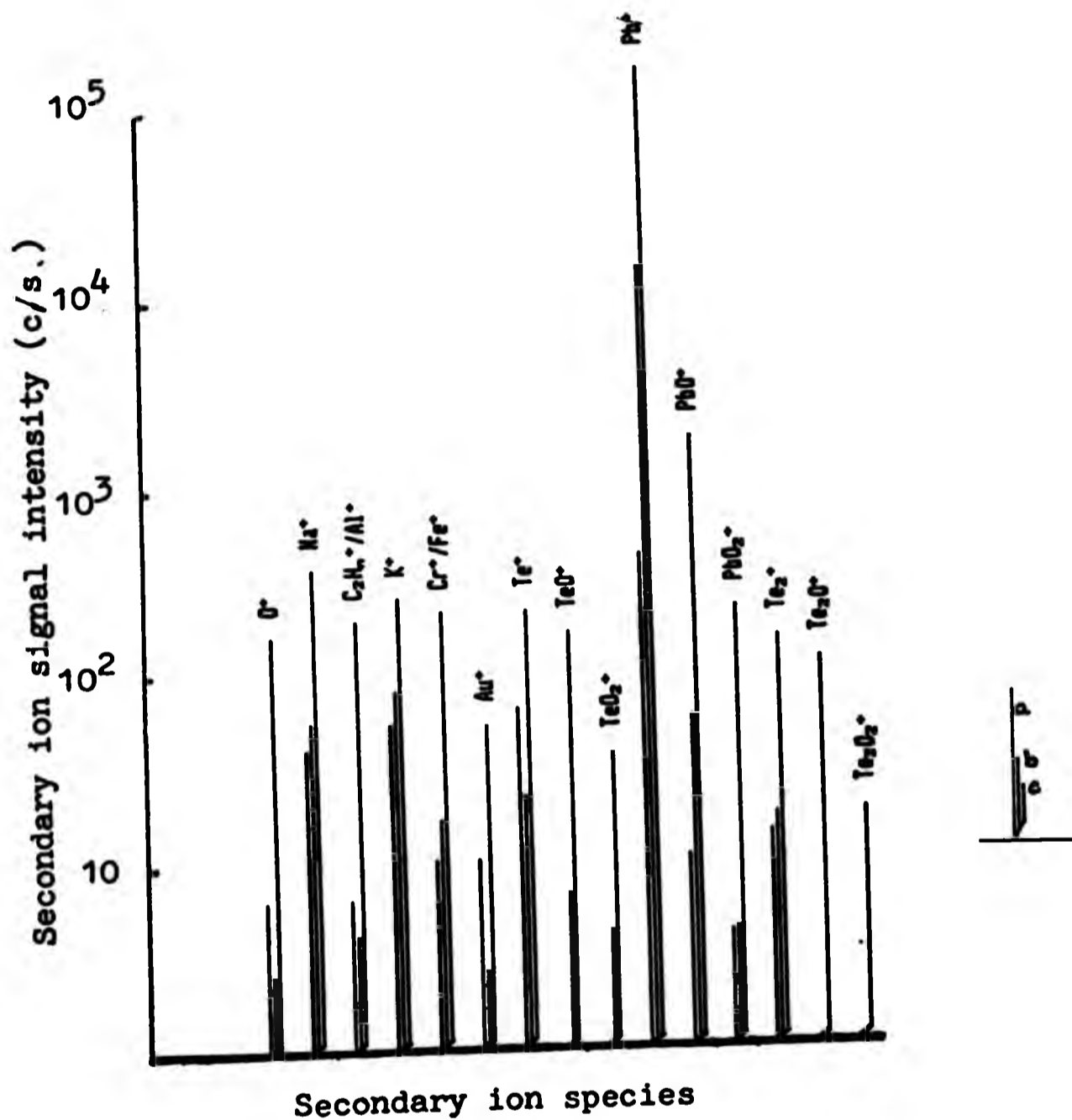
Fig. 2a also shows that the main signals to respond to oxygen in the negative ion spectra are  $O^-$  and tellurium related signals. This suggests that, either oxygen is more strongly associated with Te, or SIMS is less sensitive to oxygen associated with Pb in negative ion spectra. The fact that no Pb related signals are found in the negative ion spectra from the freshly grown film suggests that the latter suggestion is true. Other points that suggest a

Figure 2a



The effect of oxygen exposure and air exposure on -ve secondary ion signals. From MBE grown PbTe.  
 a) Freshly grown PbTe; b) after oxygen exposure of  $1.7 \times 10^9$  Lang. at 1.0 Torr; c) after air exposure of  $6.0 \times 10^9$  Lang. at  $6 \times 10^{-3}$  Torr.

Figure 2b



The effect of oxygen and air exposures on +ve secondary ion signals. From MBE grown PbTe. a) Freshly grown PbTe; b) after oxygen exposure of  $1.7 \times 10^9$  Lang. at 1.0 Torr; c) after air exposure of  $6.0 \times 10^9$  Lang. at  $6 \times 10^{-5}$  Torr.

low sensitivity to Pb related signals are that, in another study (Hewitt and Winograd 1978), the  $\text{PbO}^-$  signal has been observed to give particularly low secondary ion yields near the limits of detectability of SIMS. Further, it has been suggested that Te has a preferentially high sputter yield (Kubiak et al. 1982), in order to explain modifications which occur in electrical properties on PbTe films bombarded with low energy (300eV,  $\text{Ar}^+$ ) ions.

Some estimate of the sensitivity of SIMS to oxygen adsorbed at high pressures can be made by comparing the changes in SIMS signals shown in Fig. 2a, with an expected surface coverage of oxygen. For the air exposed surface this can be assumed to be in the region of 1.0 monolayer. Fig. 2a shows that for the primary ion current used ( $5 \times 10^{10}$  amps), a secondary ion signal intensity of approximately 10 5c/s is obtained for the  $\text{O}^-$  SIMS signal. The sensitivity to oxygen is therefore approximately  $10^{-5}$  of a monolayer coverage. The sensitivity to oxygen in the  $\text{O}^-$  signal is not expected to remain constant over the whole range of oxygen coverage.

The many hydrocarbon related signals which can be seen in the figure for the air exposed surface are thought to be due to backstreaming from the diffusion pump. The pump was turned off during this exposure.

Fig. 2b shows that the positive ions respond differently. Many of these remain near the levels detected on the fresh grown film even after the large exposure ( $1.7 \times 10^9$  Langmuirs)

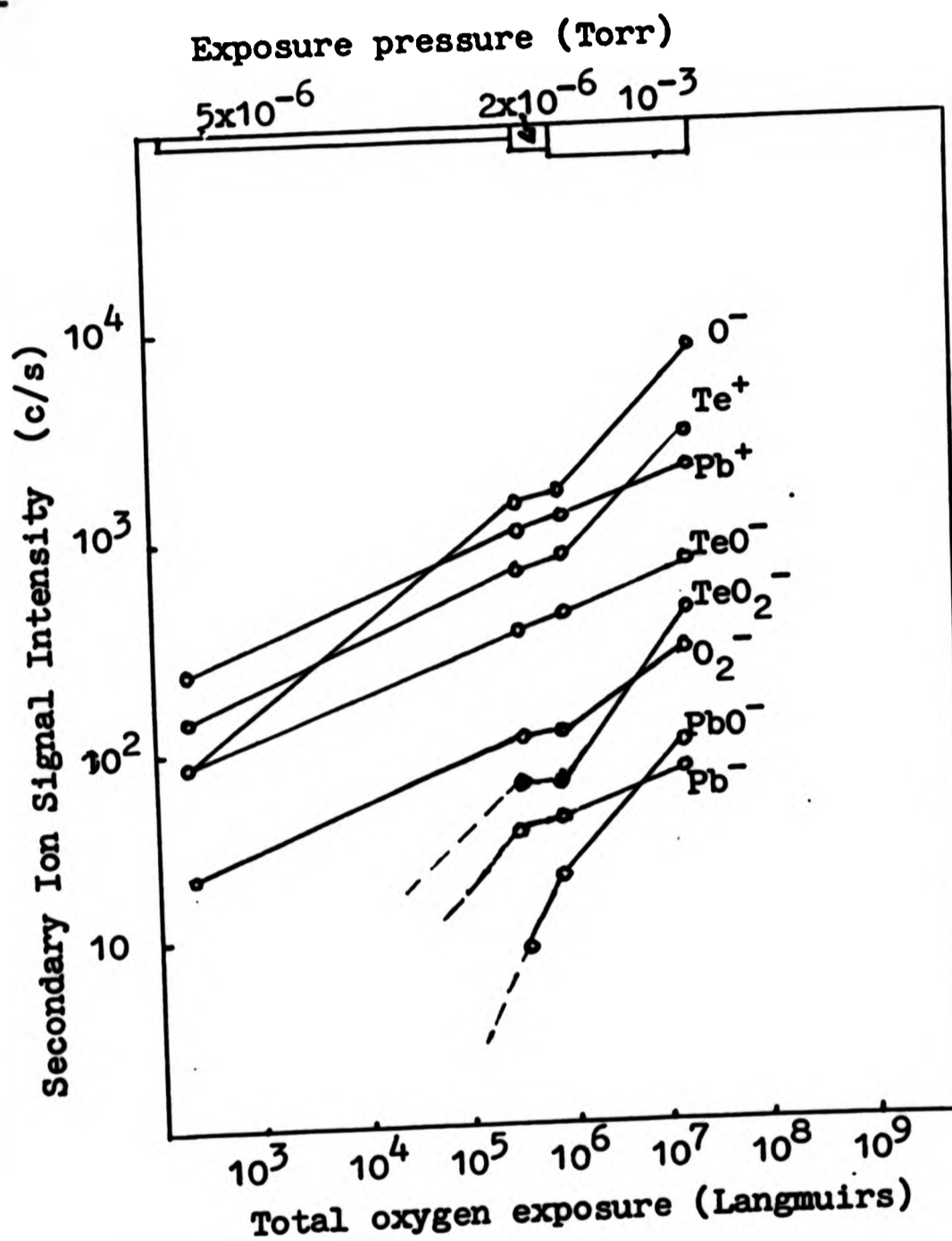
at the relatively high pressure ( $P(O_2)=1.0\text{Torr}$ ) used. These signals show a response which is only comparable to that of the negative ions after air exposure.

Similar, differing behaviour of positive and negative ions has been found in oxygen exposure studies on metals, (Winograd et al. 1978, Benninghovan et al. 1978), and the binary compound semiconductors GaAs - see Chaps. 5 and 6, and InP (Dowsett et al. 1977, 1978). In these studies, the  $O^-$  signal increases monotonically with oxygen coverage (Benninghovan et al. 1978). Positive ion signals often decrease and rarely have a simple relationship with oxygen coverage except at very low coverage (10% of a monolayer). Other similarities with spectra from GaAs and InP are, the very low negative ion yields observed from clean surfaces and, similar residual contaminant and film related signal intensities.

#### 4.3.2 Response of SIMS signals to low pressure oxygen exposures

Fig. 3 shows the response of the signal intensities of the negative and  $Pb^+$  signals to three accumulated low pressure oxygen exposures. The response of each signal is plotted as a function of total, accumulated exposure (Langmuirs). Pressures used, and the range of the various exposures, are indicated in the top legend. Responses of positive ions other than the  $Pb^+$  signal are not included in the figure because significant changes only occur in these after high pressure air exposure.

Figure 3



Response of the main secondary ion signals detected from MBE grown PbTe to accumulated, low pressure oxygen exposures.



After the first oxygen exposure ( $5 \times 10^{-6}$  Torr), it can be seen that the  $O^-$  signal and several signals containing Te and Pb respond to oxygen. This trend continues through the further exposures.

Because both signals containing Pb and Te respond to oxygen, the data in Fig. 3 gives very little insight into how oxygen is adsorbed. As in our discussions of Figs. 2a and 2b, the higher signal intensities for signals containing Te gives no indication that Te is preferentially associated with oxygen. The signals with Pb may have resulted from processes which give much lower secondary ion yields. This is supported by the fact that both the  $Pb^-$  and  $PbO^-$  signals only appear after oxygen exposure and are not present on the spectra from the freshly grown film. These species, or their precursors, may be sputtered from the freshly grown film but have secondary ionization probabilities which are too low for SIMS to detect their emission. On the other hand, both the  $Te^-$  and the  $TeO^-$  signals are detected from the freshly grown film indicating that the secondary ion yield for these signals is much higher.

A similar exercise to the one used in estimating the sensitivity of SIMS to oxygen after air exposure, can be employed here to estimate the sensitivity after low pressure exposure. An expected surface coverage for oxygen can be estimated from the 'mobile defect model' (Parker and Williams 1976). The model predicts that films used in the

present study, typically 2000Å thick and doped to  $5 \times 10^{18} \text{ cm}^{-3}$  with excess lead, should adsorb about 10% of a monolayer of oxygen on saturation of the low pressure adsorption process. Electrical measurements show that the adsorption process nears saturation after the first exposure at  $5 \times 10^{-6}$  Torr, (Fig. 3). This figure shows that a  $\text{O}^-$  SIMS signal intensity of approximately  $10^3 \text{ c/s}$  is obtained for this exposure. The sensitivity of the  $\text{O}^-$  signal to oxygen with the primary ion current used ( $5 \times 10^{10}$  amps) is, therefore, between  $10^{-3}$  and  $10^{-4}$  of a monolayer coverage.

#### 4.3.3 The response of SIMS signals and film conductance to ion bombardment after low pressure oxygen exposure - ( $10^{-6}$ Torr)

The data presented in Figs. 2a, 2b and 3, and discussed in the previous sections shows that, although SIMS has adequate sensitivity to oxygen, merely monitoring and comparing SIMS spectra obtained before and after oxygen exposure is not a fruitful approach for determining how oxygen is adsorbed on the surface. One other factor that hinders interpretation of the data in these figures, is surface damage that is accumulated during SIMS analysis. The effect of surface damage modifies the normal electrical response of the PbTe films to oxygen and the measurements show that surface defects gradually dominate the oxygen adsorption behaviour of later oxygen exposures.

The remaining results presented in this study are all concerned with how ion bombardment influences the PbTe surface, especially by desorption of oxygen adsorbed during oxygen

exposures. The present section deals with the restricted case of the influence of ion bombardment on the PbTe surface, after the low pressure oxygen exposure at  $5 \times 10^{-6}$  Torr on the freshly grown PbTe film. This is the only case where surface damage from earlier SIMS analysis can be neglected.

The results for this case, consist of an interesting comparison between the response of SIMS signal intensities and the response of the electrical film conductance during ion bombardment. This comparison identifies secondary ion signals which are associated with the generation of donor type defects which occurs during the ion bombardment.

#### Response of the SIMS signals

Figure 4 shows the way in which the main SIMS signals, detected after low pressure exposure to oxygen, changed during ion bombardment. To help compare their behaviour, the signals are plotted relative to their level on commencement of analysis to ion bombardment. With exception of the  $\text{TeO}_2^-$  signal, it can be seen that the response of the signals can be split into two portions - an initial response where the signals decrease quickly with ion bombardment dose and a different response, after more prolonged bombardment, which shows an exponential, decreasing dependence with time. Such an exponential response indicates sputter removal of fragments from a finite source. (Dawson 1977, Yu 1977, 1978)

Provided variations in secondary ionisation probabilities can be neglected during the change in the SIMS signals, this behaviour can be characterised by an effective cross-section

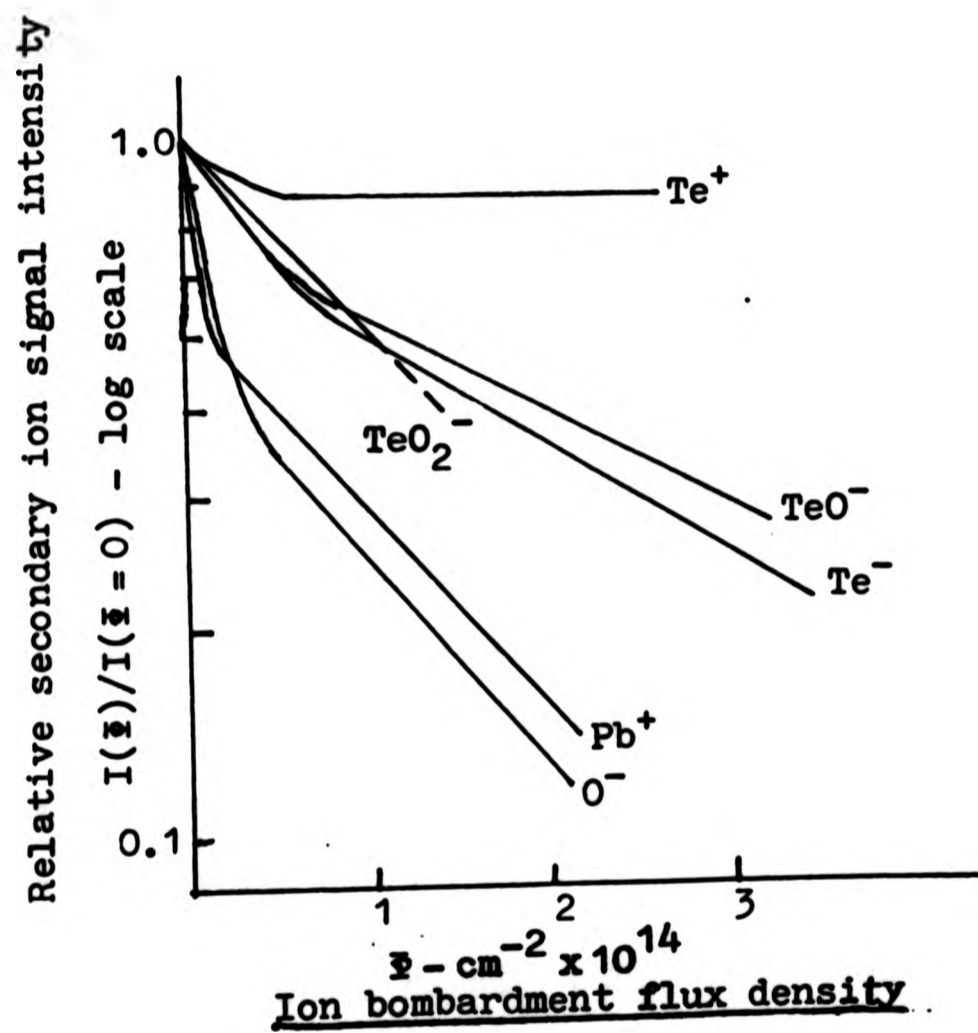
$\rho_d(\text{cm}^{-2})$  for destruction or desorption of the parent species of the ion. Cross-sections are related to the primary ion flux received by the surface,  $\Phi(\text{ions cm}^{-2})$ , and the secondary ion signal intensity  $I(\Phi)$ , before and after dose  $\Phi$  by:

$$\rho_d = \frac{-1}{\Phi} \ln \left[ \frac{I(\Phi)}{I(\Phi=0)} \right] \quad \text{Equation 4.1}$$

It can be seen from Equation 4.1 that the cross-sections describe the probability of destruction by the ion beam, of the bonding arrangements from which secondary ions are derived. It must be stressed that this assumes that secondary ionisation probabilities do not vary. A case where this would not be true is when ions result from recombination. Then the cross-section would have an added factor which would reflect the probability of recombination.

Figure 4 shows that the  $\text{Pb}^+$  and  $\text{O}^-$  signals behave similarly during analysis and respond most sharply to the ion bombardment. This strongly suggests that they come from the same source on the surface and that this source has relatively weak bonding compared to the source of the other signals. The  $\text{TeO}_2^-$  signal has a response which is similar to the latter part of the response of the  $\text{O}^-$  signal. It is thought, however, that the source of this signal is present at only very low coverage. This is indicated by the much lower signal intensity for the  $\text{TeO}_2^-$  signal on commencement of ion bombardment (20c/s), compared with that of the  $\text{Pb}^+$  and  $\text{O}^-$  signals ( $10^3\text{c/s}$ ).

Figure 4



The effect of ion bombardment on SIMS signal intensities after low pressure oxygen exposure  
oxygen exposure:  $5 \times 10^{-6}$  Torr,  $3.6 \times 10^6$  Lang.

It can be seen that the response of other signals is significantly different to that of the oxygen. Both the  $\text{Te}^-$  and  $\text{TeO}^-$  signals behave similarly to each other and the  $\text{Te}^+$  signal is insensitive to the ion bombardment.

#### Response of the film conductance

In general, the electrical conductance of films increased towards saturation values during SIMS analysis. This effect was strongest and most easily observed during SIMS analysis after the oxygen exposure on the freshly grown PbTe. The fact that this oxygen exposure produced the biggest changes in carrier concentration, removing most of the excess n-type carriers which were originally present in the film, implies that the effects of ion bombardment may be the opposite to those of oxygen adsorption. i.e. While the effect of oxygen exposure is to remove donor defects from the film, the increase in film conductance during ion bombardment suggests that the main effect of ion bombardment is to release these donors back into the film.

In the above situation, where carriers are generated from a limited source of donor defects, the rate of change in film conductance can be expressed in terms of a cross-section for carrier generation, similar to that described for SIMS signals and the incident ion flux intensity. This gives a relationship which is similar to that described above for depletion from a limited source of secondary ions. This relationship (Equation 4.2), assumes that carriers generated at the surface, diffuse throughout the film.

No justification is given for this assumption except that in the 'mobile defect model', the donor defects are originally present in the film bulk and are depleted by a diffusion mechanism. The derivation of Equation 4.2 is not trivial, so it is derived in an Appendix 4.1. This relationship allows us to compare the electrical response directly with the response of the secondary ions.

$$\sigma_d = \frac{-1}{\bar{x}} \ln \frac{\dot{v}(\bar{x})}{\dot{v}(\bar{x} = 0)} \quad \text{Equation 4.2}$$

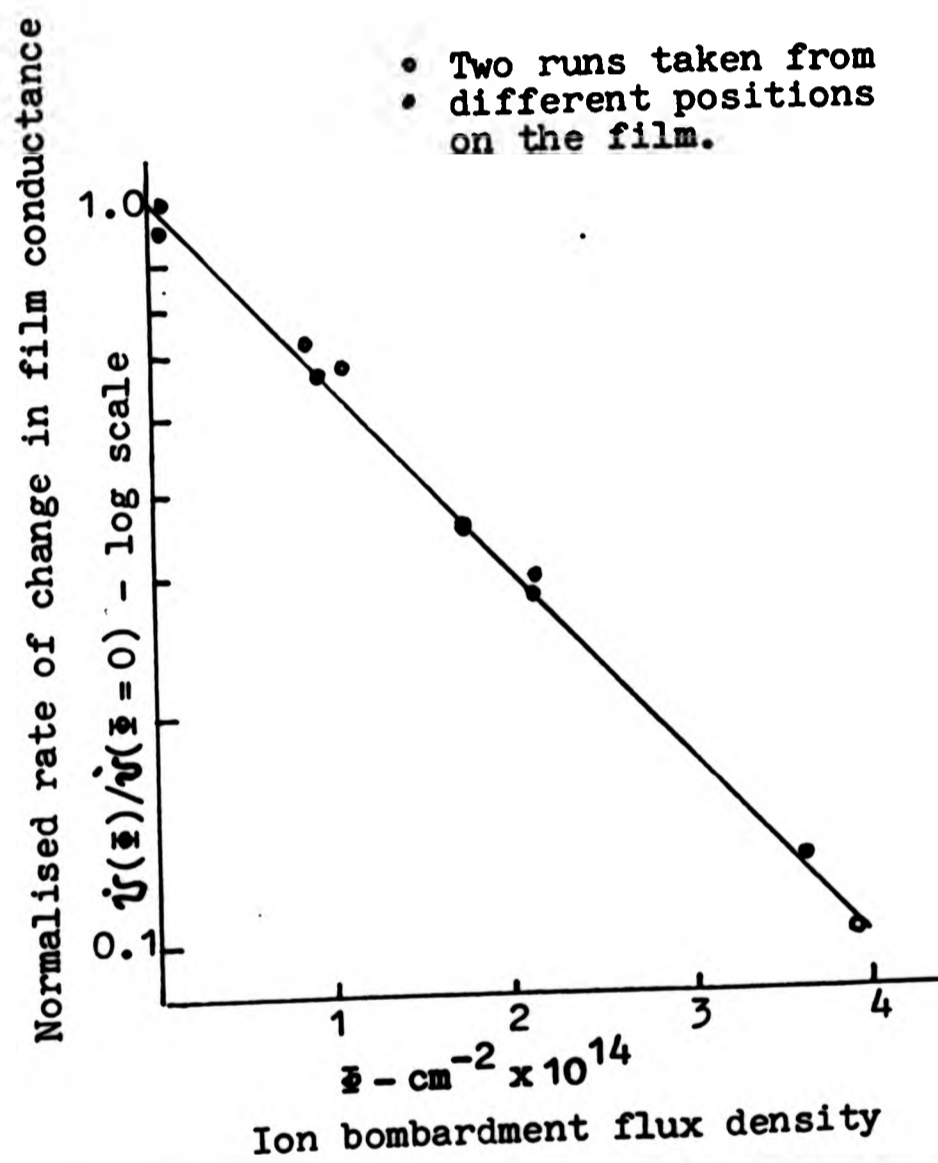
$\dot{v}(\bar{x})$  is the rate of change of film conductance with respect to the primary ion flux ( $\bar{x}$ ) received by the surface and  $\sigma_d$  is the destruction/desorption cross-section for the species being depleted at the surface in the generation of the mobile defects.

Figure 5 shows the data for the change in conductance expressed in terms of Equation 4.2. This data was obtained by numerical differentiation of the continuously sampled film conductance. Notice that there is clear agreement between the data obtained from two different areas of the film and with Equation 4.2.

#### Comparison of the response of the SIMS signals and the film conductance

Comparison of the slopes of the SIMS signals in Fig. 3 and the slopes for the rate of change in the film conductance in Fig. 4 shows that there is close agreement in the value for the destruction cross-section of the parent species of

Figure 5



The effect of ion bombardment on the rate of change in film conductance after low pressure oxygen exposure.  
oxygen exposure  $5 \times 10^{-6}$  Torr,  $3.6 \times 10^6$  Lang.



the donor defects induced by ion bombardment, and the cross-sections of the  $Pb^+$  and  $O^-$  signals ( $\lambda_d=5 \times 10^{-15} \text{ cm}^2$ ). The slope of the response of the  $TeO_2^-$  signal also agrees well with that of the electrical response, but as discussed earlier, the signal is unlikely to correspond to a high surface coverage.

This agreement in the response of the  $Pb^+$  and  $O^-$  signals with that of the film conductance is strong evidence for concluding that the source of the donors and the  $Pb^+$  and  $O^-$  SIMS signals are one and the same. This source can be envisaged as consisting of oxygen atoms weakly bound to lead atoms with the donors resulting from fragmentation of this parent species.

The results of the above analysis of oxygen desorption during ion bombardment compliment the 'mobile defect model' for oxygen adsorption.

#### 4.3.4 An assessment of the influence of ion bombardment induced surface damage on the response of the PbTe surface to oxygen exposure.

The preceding section discussed the effects of ion bombardment for the specific case of bombardment induced oxygen desorption from the undamaged PbTe. This section is concerned more with the way in which ion bombardment modifies the PbTe surface and changes oxygen adsorption. The first part of the assessment consists of a summary of differences observed in the response of electrical measurements to oxygen exposure compared with the response that would be expected from undamaged PbTe films. This summary provides a background for the

second part of the assessment which is concerned with SIMS analysis from oxygen adsorbed on such modified surfaces.

Response of electrical measurements - during SIMS analysis

During SIMS analysis the electrical conductance of native, oxygen exposed and air exposed films increases towards saturation values. This change reverses slightly on removal of the ion beam. The effect is essentially local, i.e. it can be repeated with the same result, by bombarding any other area on the film. The previous section considered a specific case of this in some detail. Such detailed analysis of the response after further oxygen exposures was not possible, however, because the absolute changes observed in film conductance are not large enough to provide plots (like that in Fig. 4) of the rate of change of film conductance with respect to ion bombardment dose.

The response of electrical measurements - during Oxygen exposures

In the previous section it was also stated that the response of undamaged PbTe film to initial low pressure oxygen exposure at  $5 \times 10^{-6}$  Torr is the same as that observed in previous studies. This is not the case, however, after further oxygen exposures where the surface has been exposed to ion bombardment and has surface damage produced by SIMS analysis. A gradually increasing deviation from the normal response to oxygen exposure shows that the surface damage produced by SIMS is accumulated. Eventually, after repeated oxygen exposures and SIMS analysis, the surface damage is seen to completely inhibit any response to a lengthy exposure to air

( $10^{-3}$  Torr, 284 hours) which has no effect on a residual n-type film conductance. This is in marked contrast to the p-type response normally produced by such exposure (Parker and Williams 1976). P-type conduction could be induced by high pressure oxygen exposures in films with only moderate ion induced damage.

The changes in carrier concentration produced by SIMS are accompanied by a gradual degradation in carrier mobility. Where damage was slight, this degradation could be reversed by low pressure oxygen exposure.

The kinetics of carrier removal during oxygen exposures are also different on film surfaces modified by SIMS analysis. The kinetics (response of the carrier concentration) are complex and although there are some similarities with kinetics on electron damaged films (AES) (McGlashan et al. 1979), and low energy ion damaged films ( $\text{Ar}^+$ , 300 eV) (Kubiak et al. 1982), the carrier removal does not conform with either case.

One can surmise that differences between the behaviour observed here and that produced by low energy ion bombardment and electron irradiation, can be attributed to the higher energy ions used in SIMS analysis and to the fact that the ion bombardment is not homogenous, but perturbs the surface locally. It seems likely that no one defect is responsible for the observed effects, but rather, that a range of electrically active defects are generated, possibly Frenkel and Shottky pairs.

The response of SIMS signals - during SIMS analysis

The electrical results presented above show that after SIMS analysis of the initial oxygen exposure, film properties and mechanisms of oxygen retention become increasingly governed by defects induced during further SIMS. It is shown that these defects interact with oxygen, so it can be expected that results of SIMS analysis should reflect this.

In SIMS analysis, significant changes occur in the secondary ion signals from native, oxygen exposed and air exposed surfaces. Moving the film relative to the ion beam indicates that changes are essentially local in nature and persist over the time scale of the analysis, typically two hours.

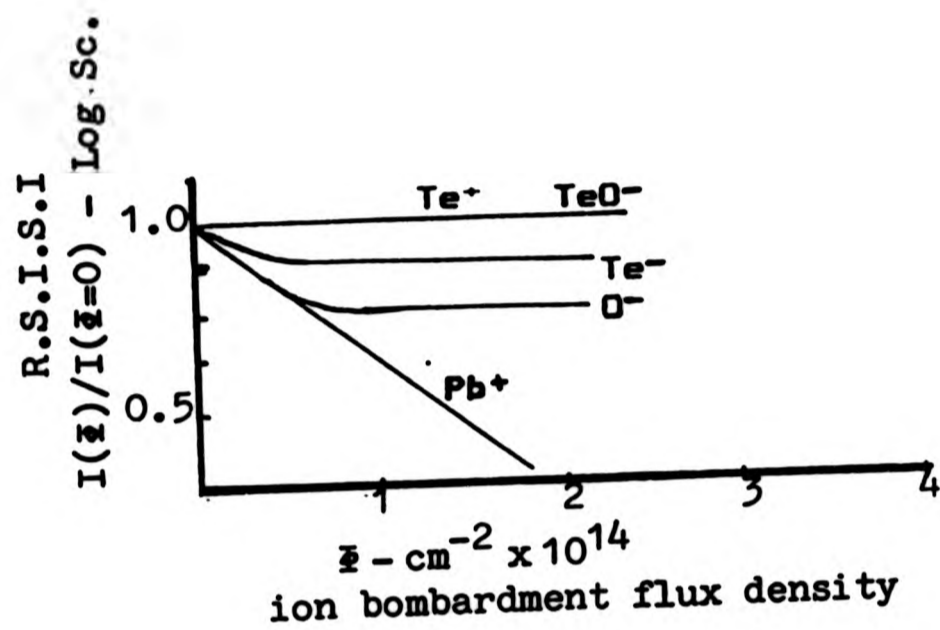
Figure 6a-d show similar plots to that in Figure 4. In this case, the plots show the response of the main secondary ion signals after further oxygen exposure/SIMS analysis cycles.

As can be seen, there are significant variations in the changes induced by ion bombardment for the various oxygen exposures. Notice that there is a definite trend in the response of signals towards higher exposure. The response of the signals appears to fall into three categories: 1)  $O^-$ ,  $Pb^+$  and  $TeO_2^-$  which show behaviour which changes with oxygen exposure; 2)  $Te^-$  and  $TeO$  which show behaviour which, after initial changes, is independent of the oxygen exposure; and 3)  $Te^+$  which after initial changes, appears relatively independent of oxygen coverage and ion bombardment. These three categories will be discussed with a view to determining the source of the ions and hence, the dominant form(s) of oxygen

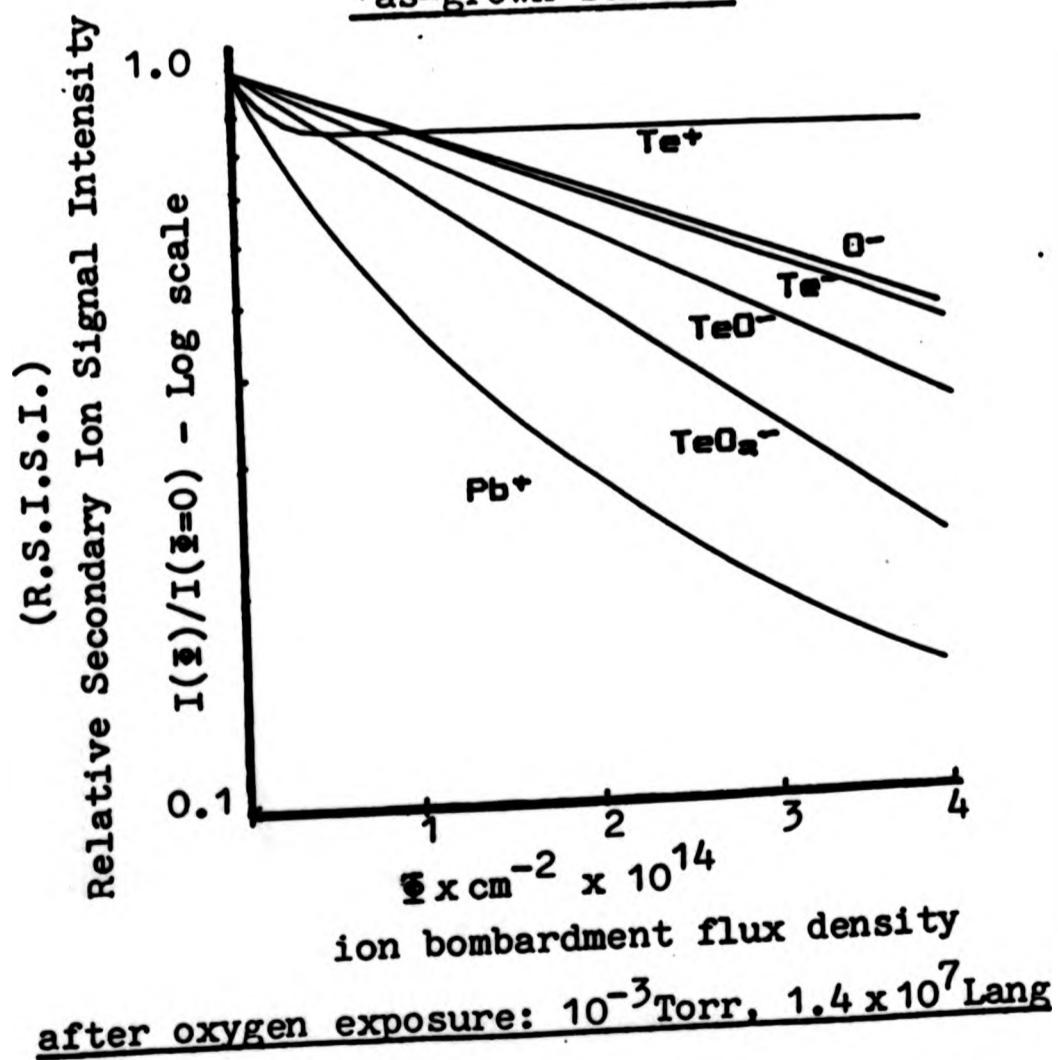
Figures 6 a - d

The effect of ion bombardment on SIMS signal intensities after accumulated oxygen exposures.

(a)



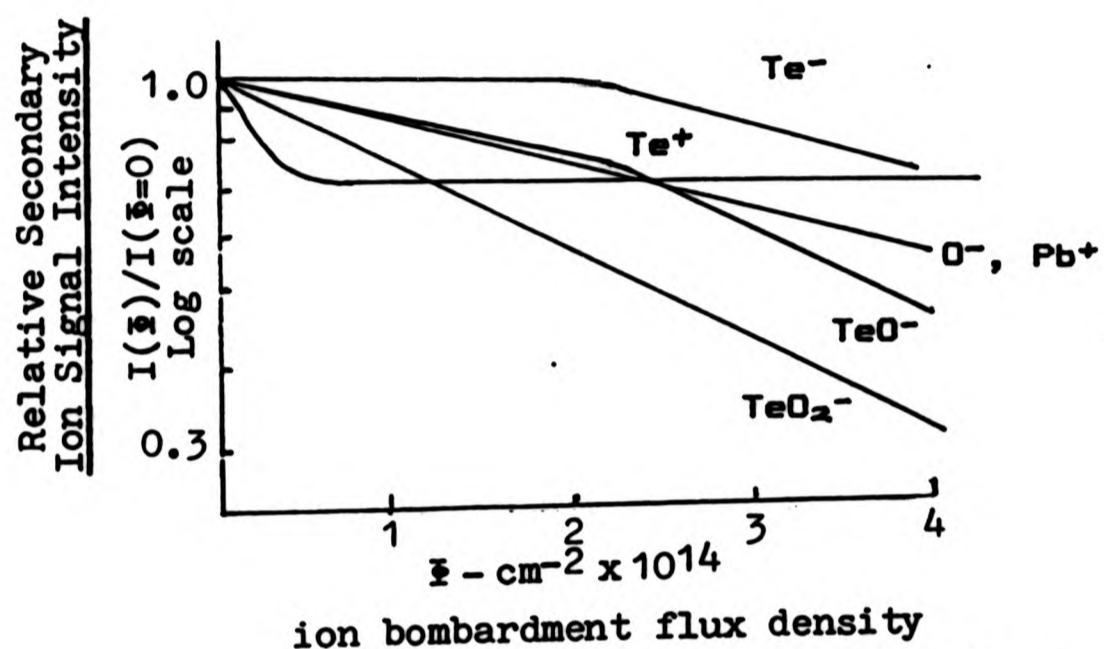
(b)



Figures 6a - d

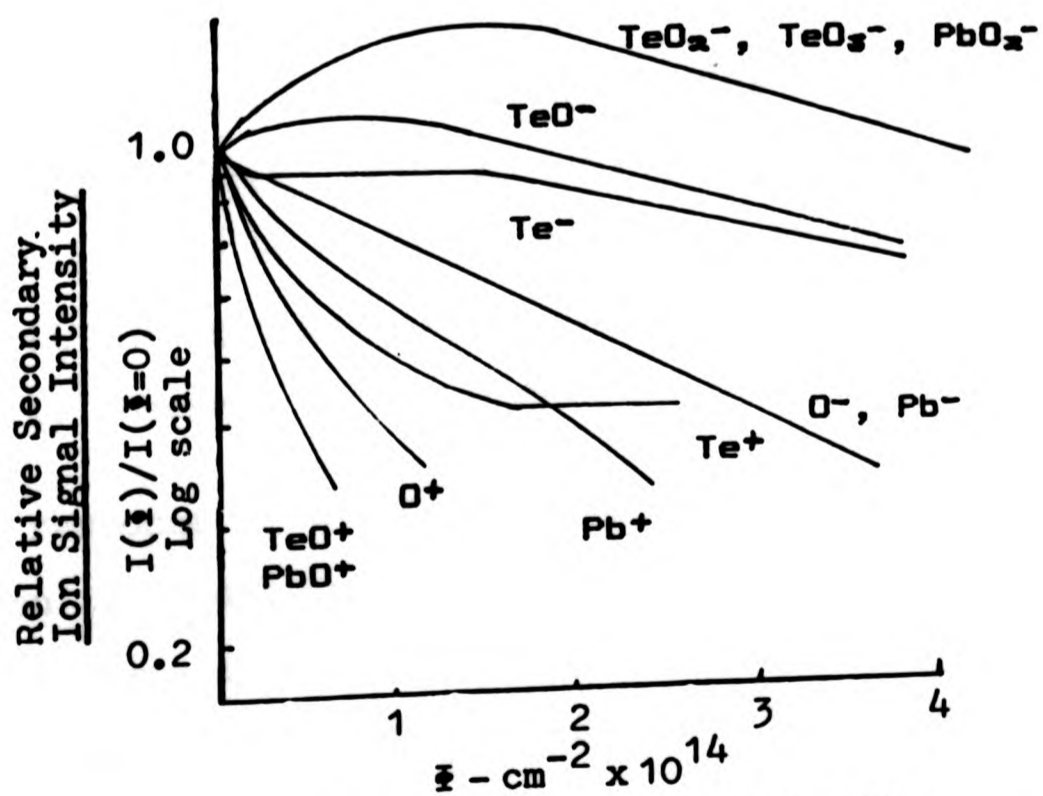
The effect of ion bombardment on SIMS signal intensities after accumulated oxygen exposure - cont.

(c)



ion bombardment flux density  
after oxygen exposure:  $1.0 \text{ Torr}, 1.8 \times 10^9 \text{ Lang.}$

(d)



ion bombardment flux density  
after air exposure:  $3.6 \times 10^{-2} \text{ Torr}, 6 \times 10^9 \text{ Lang.}$

adsorption present on the surface before SIMS analysis.

The behaviour of the  $Pb^+$ ,  $O^-$  and  $Te^-$  signals

Notice that the slope for the  $Pb^+$  signal tends from a high value on the 'as grown' surface to a low value on the air exposed surface. This indicates that the bonding between Pb atoms on the surface becomes stronger after successive oxygen exposures. The behaviour of this signal from the 'as grown' surface is interesting in its own right because after initial changes, it is the only signal from this surface which is influenced by ion bombardment. This makes the source of this signal a likely candidate for the donor defects which, electrical measurements show, were created during analysis.

As can be seen in the figures(6b-d), the  $O^-$  and  $Pb^+$  signals no longer show the association apparent in Figure 4. The response of the  $Pb^+$  deviates significantly from that expected for a limited source. The exposure at 1.0Torr (Fig. 4c), appears to make a transition towards the more complex behaviour observed on the air exposed surface. The source of  $Pb^+$  is substantially different from the source at lower oxygen exposures. This is to be expected, as the kinetics for carrier removal during this exposure show some indications of the normally observed p-type response.

The absolute response of the SIMS signals to oxygen indicates that oxygen is bonded on the air exposed surface to Te and Pb atoms. There is strong support for this view in the similar response of the  $PbO_2^-$ ,  $TeO_2^-$  and  $TeO_3^-$  signals

during SIMS analysis of the air exposed surface.

The behaviour of the  $\text{Te}^-$  and  $\text{TeO}^-$  signals

Figure 4 shows the initial responses of  $\text{Te}^-$  and  $\text{TeO}^-$  are similar to that of the  $\text{TeO}_2^-$  signal for low pressure exposure. This indicates that the three signals are derived from the same surface species and consequently some Te-O bonding results from low pressure oxygen exposure. However, it is unlikely that the predominant form of oxygen retention is associated with this response. Figure 4 shows that the source for this initial response is soon depleted and replaced by a response with lower cross-section. Further, the source of  $\text{O}^-$  and  $\text{Pb}^+$  ions is not depleted even though the cross-sections for this source are much higher.

Two points indicate that the source of the  $\text{Te}^-$  and  $\text{TeO}^-$  signals corresponds to adsorption on the ion damaged surface. Firstly, apart from the initial behaviour for low pressure exposures,  $\text{Te}^-$  and  $\text{TeO}^-$  are relatively independent of oxygen exposure. This indicates that the source(s) of these ions is not related to differences in the forms of adsorbed oxygen. Secondly, Figure 6 shows the behaviour of the signals after the exposure at  $10^{-3}$  Torr, remains the same throughout bombardment. This suggests that the oxygen contained in the  $\text{TeO}_2^-$ ,  $\text{TeO}^-$  and  $\text{O}^-$  signals is originally adsorbed in a manner which is not affected by ion induced damage, i.e. on an ion damaged surface.



### The behaviour of the Te<sup>+</sup> signal

The independence of the Te<sup>+</sup> signal, after initial changes, suggests that its main source is independent of the effects of oxygen exposure and ion induced damage. It is thought that it is sputtered from sites related to the unperturbed PbTe film and, with the ion energies employed (1KeV), there is some probability that it is derived from the sub-surface (Yu 1977). The increasing initial change in this signal with accumulated oxygen exposure may be related to the coverage of oxygen.

### Summary

Analysis of the response of -ve ion SIMS signals, during SIMS analysis from oxygen adsorbed at various exposure pressures, shows: 1) Different forms of oxygen retention appear to operate at low and high pressure regimes; 2) at low pressures ( $<10^{-3}$ Torr), adsorption is associated with the Pb<sup>+</sup> SIMS signal which in its turn is associated with mobile donor defects; 3) at higher pressures ( $>10^{-3}$ Torr), adsorbed oxygen is associated with Pb and Te atoms, probably in a compound oxide; 4) SIMS analysis produces surface re-siding defects which have a major influence on further adsorption.

### 4.4 Conclusions

Although the present study is not definitive in determining the nature of oxygen retention on (111)PbTe films, analysis with SIMS is remarkably successful in comparison with previous studies. This is particularly true considering the

relative simplicity of the SIMS apparatus.

The ability to detect oxygen adsorbed at low pressures is a significant result in itself, as electron irradiation in AES analysis desorbs this oxygen too quickly to monitor its presence (McGlashan et al. 1979). Also significant is the strong indication that low pressure adsorption corresponds to the earlier proposed 'mobile defect model' (Parker and Williams 1976). There is evidence that a compound oxide forms at higher exposure pressures. SIMS has the ability to differentiate between the different phases of oxygen retention and, to some extent, determine their source.

The damage produced by ion bombardment in SIMS analysis has, however, proved to be a difficult problem - not only in the sensitivity shown by electrical conductance measurements to the low doses employed, but also in the effects which bombardment has had on further oxygen adsorption.

Several factors suggest that these difficulties of SIMS analysis on PbTe will also apply to other single crystal semiconductor surfaces. The first of these factors is that the destruction cross-sections of secondary ion signals during SIMS analysis are similar to published values for cross-sections from adsorbed layers on metal surfaces (Dawson 1977, Yu 1978), thus indicating that PbTe may be no more prone to surface damage than metal surfaces. Secondly, it has already been reported that electron bombardment as used in AES, modifies local oxygen adsorption on GaAs (Ranke and Jacobi 1975).

Considering the effects of electron and ion bombardment on PbTe outlined in this study, it is likely that similar effects will be observed with GaAs. Although the destructive effects of SIMS analysis severely hampered attempts to investigate oxygen adsorption on PbTe, the analysis shows that a definitive study should be possible using more sophisticated apparatus which is currently available (Yu 1977). The main requirements are to improve overall sensitivity. This can be effected by using a quadrupole mass spectrometer with higher transmission and also, by providing facilities for faster data recording of only those mass peaks which are of interest. Other improvements would be a facility to record the energy spectrum of secondary ions to help differentiate species and a means of recording mass SIMS signals during oxygen exposure. This would be a great improvement on the present situation where SIMS signals can only be recorded after oxygen exposure.

#### APPENDIX 4.1

$$\rho_d = -(I)^{-1} \times \ln \frac{\dot{v}(\bar{x})}{\dot{v}(\bar{x}=0)} \quad \text{Equation 4.2}$$

The above equation is given in section 4.3.3 relating the destruction cross section ( $\rho_d \text{ cm}^2$ ) for depletion of a limited source of donor type defects, to the rate of change of electrical film conductance ( $\dot{v}(\bar{x}) \text{ ohm}^{-1} \text{ cm}^2$ ) with respect to the primary ion flux ( $\bar{x} \text{ ion-cm}^{-2}$ ). The change in film conductance is caused by the liberation into the film, of donor defects from the surface by ion bombardment.

This appendix is concerned with the derivation of the above relation. The equation is derived using the following model:

A primary ion flux ( $\bar{x} \text{ ion-cm}^{-2}$ ) bombards a limited source of donor defects ( $N_s \text{ cm}^{-2}$ ) causing destruction of this source at a rate that is proportional (the destruction cross section  $\rho_d \text{ cm}^2$ ) to the surface concentration of the source on the surface. The differential equation expressing this is given in Equation 4(a).1 .

$$\frac{dN_s(\bar{x})}{d(\bar{x})} = -\rho_d \bar{x} N(\bar{x}) \quad \text{Equation 4(a).1}$$

The destruction of the source gives rise to donor type defects. If the following assumptions are accepted, the increase in film conductance produced by the generation of the donor defects is simply related to the decrease in the concentration of the source ( $N_s(\bar{x}=0) - N_s(\bar{x})$ ), by Equation 4(a).2.

The assumptions are: a) that the destruction of each source site generates donors which diffuse throughout the whole film bulk (or across the whole film surface), quickly enough to assume that the increase in carrier concentration is homogeneous; and b) that the change in the mobility in the region of the ion bombardment can be neglected.

$$\mathcal{U}(z) = \mathcal{U}(z=0) + K x (N_s(z=0) - N_s(z)) \quad \text{Equation 4(a).2}$$

(where K is a constant of proportionality)

$K(\text{cm}^2\text{-ohms}^{-1})$  is the increase in film conductance produced by the destruction of one site of the source of the donor defects. It includes the following factors: a) the ratio of the bombarded area to the volume of the film; b) the number of donor defects produced per destroyed source site; c) the number of electrons added to the conduction band per donor defect; and d) the mobility.

Integrating Equation 4(a).1 and substituting the resulting relation for the depletion of the source into equation 4(a).2 gives Equation 4(a).3 .

$$\mathcal{U}(z) = \mathcal{U}(z=0) + K x N_s(z=0) x (1 - e^{-\rho d x z}) \quad \text{Equation 4(a).3}$$

Solving equation 4(a).3 for  $\rho d$  gives the equation 4(a).4 below.

$$\rho d = -\bar{x}^{-1} \times \ln \left[ \frac{\mathcal{V}(\bar{x}=0) + K \times N_s(\bar{x}=0) - \mathcal{V}(\bar{x})}{K \times N_s(\bar{x}=0)} \right]$$

Equation 4(a).4

It can be seen in equation 4(a).4 that the destruction cross-section is not simply related to the film conductance and the primary ion flux (I). This is because it depends on the initial surface density of the source of the defects,  $N_s(\bar{x}=0)$ , and the constant of proportionality, K (which are unknown quantities). It can also be seen that the above relation is not amenable to graphical determination of  $\rho d$ .

Differentiating equation 4(a).3 however, gives the relation in Equation 4(a).5 which is more useful for graphical analysis.

$$\frac{d\mathcal{V}(\bar{x})}{d(\bar{x})} = \rho d \times (K \times N_s(\bar{x}=0)) \times e^{-(\rho d \times \bar{x})}$$

Equation 4(a).5

This equation is expressed in the more familiar form of Equation 4.2 by substituting the identity given below in Equation 4(a).6 into Equation 4(a).5 to give Equation 4(a).7. (Equation 4(a).6 gives the rate of change of the film conductance with respect to the primary ion flux at the onset of bombardment.)

$$\frac{d \mathcal{V}(\bar{x}=0)}{d(\bar{x})} = \rho d x \cdot (K \times N s(\bar{x}=0))$$

Equation 4(a).6

$$\rho d = -(\bar{x})^{-1} \times \ln \left[ \frac{\dot{\mathcal{V}}(\bar{x})}{\mathcal{V}(\bar{x}=0)} \right]$$

( where  $\dot{\mathcal{V}}(\bar{x}) = \frac{d(\mathcal{V}(\bar{x}))}{d(\bar{x})}$  )

Equation 4(a).7

CHAPTER 5

A SIMS ASSESSMENT OF (100)GaAs SURFACE PREPARATION  
FOR MBE AND ADSORPTION STUDIES



## 5.1 INTRODUCTION

This chapter reports the results of a SIMS investigation into methods used to prepare suitable (100)GaAs surfaces for growth of thin epitaxial films by Molecular Beam Epitaxy (MBE) and for adsorption studies.

The requirements of the preparation process for MBE film growth are exacting because MBE requires chemically stable and atomically clean surfaces (Cho and Arthur 1975). Although actual details of the preparation methods used by different groups vary, they mostly consist of a two stage cleaning process. The first stage consists of chemically etching the surface of substrates in an oxidising etch (S. Lida and K. Ito 1971). This cleans the surface of impurities and leaves a thin protective oxide layer. The second stage consists of the removal of this protective oxide layer in the MBE growth chamber at UHV pressures. This stage normally involves thermal desorption of the oxide in a low pressure atmosphere of  $As_4$ . The  $As_4$  prevents depletion of arsenic from the top monolayer(s) of the surface.

The efficacy of preparation procedures has been studied extensively in the past using chemical, (Chang et al. 1977 ) optical (Wilmsen and Kee, 1978) and vacuum based (Ploog and Fisher 1977, Lawrence et al. 1979) surface analysis techniques.

Studies using AES (Chang et al. 1977, Ploog and Fisher 1977, Lawrence et al. 1979, Arthur 1974, Drathen et al. 1978, Wilmsen and Kee 1978), RHEED (Lawrence et al. 1979),

LEED (Arthur) and ESCA/XPS (Wilmson and Kee, 1978) show that, within the limits of the sensitivity of these techniques, the thin oxide layers appear to be removed completely by heating to  $570^{\circ}\text{C} - 580^{\circ}\text{C}$  in an  $\text{As}_4$  flux (Cho and Arthur, 1975). This heating leaves surfaces which LEED and RHEED show to have well defined electron diffraction patterns, characteristic of good crystallographic quality. Uebbing (1970) has shown however, that heating by itself leaves tenacious carbonyl impurities. Attempts to remove carbon by ion sputter cleaning causes crystallographic damage and this is not easily removed by annealing (Lawrence et al. 1979).

Secondary ion mass spectrometry has two main advantages for investigating surface preparation. The first of these is its high sensitivity especially in the presence of oxygen. The second advantage is the ability of SIMS to detect chemical groupings.

A recent study which used SIMS to compare wet and dry oxides formed on amorphous GaAs is a good example of its sensitivity to different chemical groups (L.L. Kazmerski and P.J. Ireland 1980). In this study, SIMS analysis from wet oxide shows  $\text{GaO}^+$  and  $\text{AsO}^+$  signals which correspond to Ga-O and As-O bond related shifts in AES and XPS energy spectra. This indicates the presence of a mixed oxide of gallium and arsenic. On the dry oxide, only the presence of  $\text{Ga}_2\text{O}_3$  is identified. The SIMS spectra also show that secondary ion signals for contaminants are also very different, with wet oxides showing metal and halogen signals which are not found on the dry oxide.

A useful reference for the present work is provided by an earlier study on substrate preparation carried out by Ploog and Fisher (1977). They show positive ion SIMS spectra from 'as grown' MBE GaAs films with very little As related signals. This indicates that signals containing As atoms have low secondary ion yields. Further, the positive spectra presented show unassigned signals which are fairly easily assigned as corresponding to  $\text{GaO}^+$ ,  $\text{In}^+$ ,  $\text{GaAsO}^+$ ,  $\text{As}_2\text{O}^+$ ,  $\text{Ga}_3^+$  and  $\text{Ga}_2\text{As}^+$ . The presence of secondary ion signals containing oxygen in the spectra indicates that SIMS can detect oxygen uptake on GaAs even from the residual gas.

In the present study SIMS is used to investigate several aspects of surface preparation. The aims of the study are to determine, in order of priority: 1) the efficacy of the procedures used in the laboratory to prepare substrates for MBE; 2) a cleaning schedule that is suitable for preparing substrates for oxygen adsorption studies; 3) differences that result from heating substrates in vacuo and in low pressure  $\text{As}_4$  ambient; and 4) the effects of ion sputter cleaning.

## 5.2 Experimental

### 5.2.1 UHV chambers and SIMS instrumentation

The UHV chambers and SIMS instrumentation used in this study are described in Chapter 3.

### 5.2.2 The preparation of substrates before loading into the UHV chamber

A total of eight (100)GaAs substrates, five with an oxide layer produced in wet-chemical-etching and three with oxide produced by air-exposure of MBE grown (100)GaAs layers, were used in the study. All the substrates were of approximately  $4.0\text{cm}^2$  in area.

The wet chemical etching of substrates was performed by two persons who were skilled in substrate preparation for MBE growth (B.T. Meggitt 1979, J. Grange 1979, 1980). These people also carried out the loading of substrates into the UHV vacuum chamber. This procedure was followed to ensure that the methods used for substrate preparation were as identical as possible to the methods used by these individuals in preparing substrates for their own work - the growth and characterisation of MBE GaAs films. The ultimate test of suitability of films prepared in this manner (actually growing films on the substrates) was not possible. This would have involved major modifications to the vacuum chamber.

The substrates were supplied, cut to a nominal thickness of 0.8 mm and etched to remove surface damage. Unfortunately some suppliers were not forthcoming in describing the etch used, but it is similar to the lap polish in 2% bromine in methanol used on substrates supplied by R.S.R.E. (Malvern).

The preparation of the substrates for loading in the UHV chamber consisted of: 1) removing a protective wax layer in hot trichloroethylene; 2) washing in de-ionised distilled water; 3) etching in  $15:1:1 \text{H}_2\text{SO}_4:\text{H}_2\text{O}_2:\text{H}_2\text{O}$  at  $40^\circ\text{C}$ ;

4) rinsing in distilled water; 5) drying either by rinsing in I.P.A. followed by evaporation of the I.P.A. (which has a tendency to leave drying stains), or blow-drying with dry  $N_2$  gas; and finally 6) soldering onto a sample heater/holder with indium metal at  $115^\circ C$ . The substrates, located on the holder, were then loaded into the vacuum chamber. The etch in  $H_2SO_4:H_2O_2:H_2O$  is known to leave the surface with a protective oxide, rich in the arsenic oxide  $As_2O_5$ . Gallium oxide ( $Ga_2O_3$ ) is more soluble in an acidic pH (S. Lida and K. Ito 1971).

The substrates on which MBE films were grown were prepared in the same manner as detailed above, with one difference. They were loaded into a MBE growth chamber instead of the SIMS chamber. These substrates were immediately transferred to the SIMS chamber after film growth. This ensured that the films received a minimum of contamination from the laboratory.

The experiments on substrates which involve the use of  $As_4$  overpressure were performed in the modified PbTe MBE growth chamber detailed in Chapter 3. The experiments on other substrates were performed in the chamber of the original SIMS system. This is outlined - also in Chapter 3. After loading substrates into the UHV chamber, the chamber was pumped to UHV pressures and baked at  $200^\circ C$  for 24 hours. This was done to remove water vapour.

### 5.2.3 Experimental procedure

#### Experiments involving the use of $As_4$ flux

Four substrates were used in this part of the study, three of these with air-exposed MBE layers and the fourth with a chemically prepared oxide layer. These four substrates were subjected to a treatment which consisted of two cycles of substrate heating to  $580^{\circ}C$  for 10 minutes in  $2 \times 10^{-6}$  Torr of  $As_4$ , and ion sputter cleaning with  $Ar^+$  ions of energy 350eV and dose  $10^{16}$  ions  $cm^{-2}$  for 30 minutes. This was completed by reheating substrates in  $As_4$ . Positive and negative SIMS spectra were obtained before and after each stage of treatment.

#### Experiments without involving the use of $As_4$ flux

SIMS spectra were obtained from substrates before and after heating to  $580^{\circ}C$  for 10 minutes. During heating, the pressure rose from  $10^{-10}$  Torr to  $5 \times 10^{-8}$  Torr and residual gas analysis showed that the desorbed vapour consisted mainly of water and  $As_n$  ( $n = 1, 2, 3, 4$ ). One substrate was sputter cleaned with  $Ar^+$  ions (300eV,  $3 \times 10^{15}$  ions  $cm^{-2}$ , 10 min) before heating at  $580^{\circ}C$ .

#### SIMS analysis

The conditions for SIMS analysis have been described in Chapter 3. One point to note is that SIMS spectra obtained using the different SIMS apparatus are not directly comparable. It is only possible to compare relative changes in secondary ion signal intensities in SIMS spectra obtained from using the two SIMS instruments.

The identification of signals in SIMS spectra was aided by the known isotopic ratios of Ga and In and by association of SIMS signals which responded to surface preparation treatments in a similar manner. In the SIMS spectra presented as data in this study, the peak heights of signals (designated  $CH_n$ ,  $C_2H_n$  and  $C_3H_n$ ) are the arithmetic mean of signals with typical values of  $n = 1, 2, 3$ .

### 5.3 Results

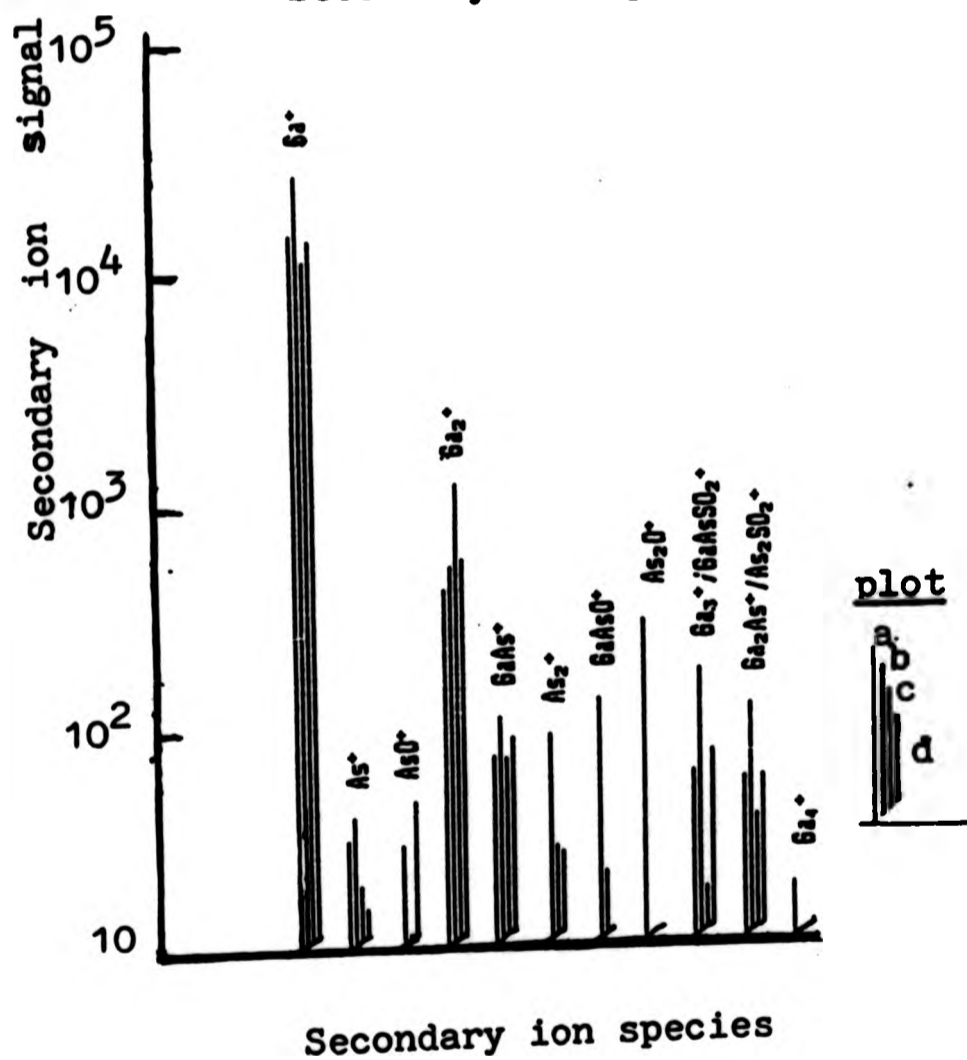
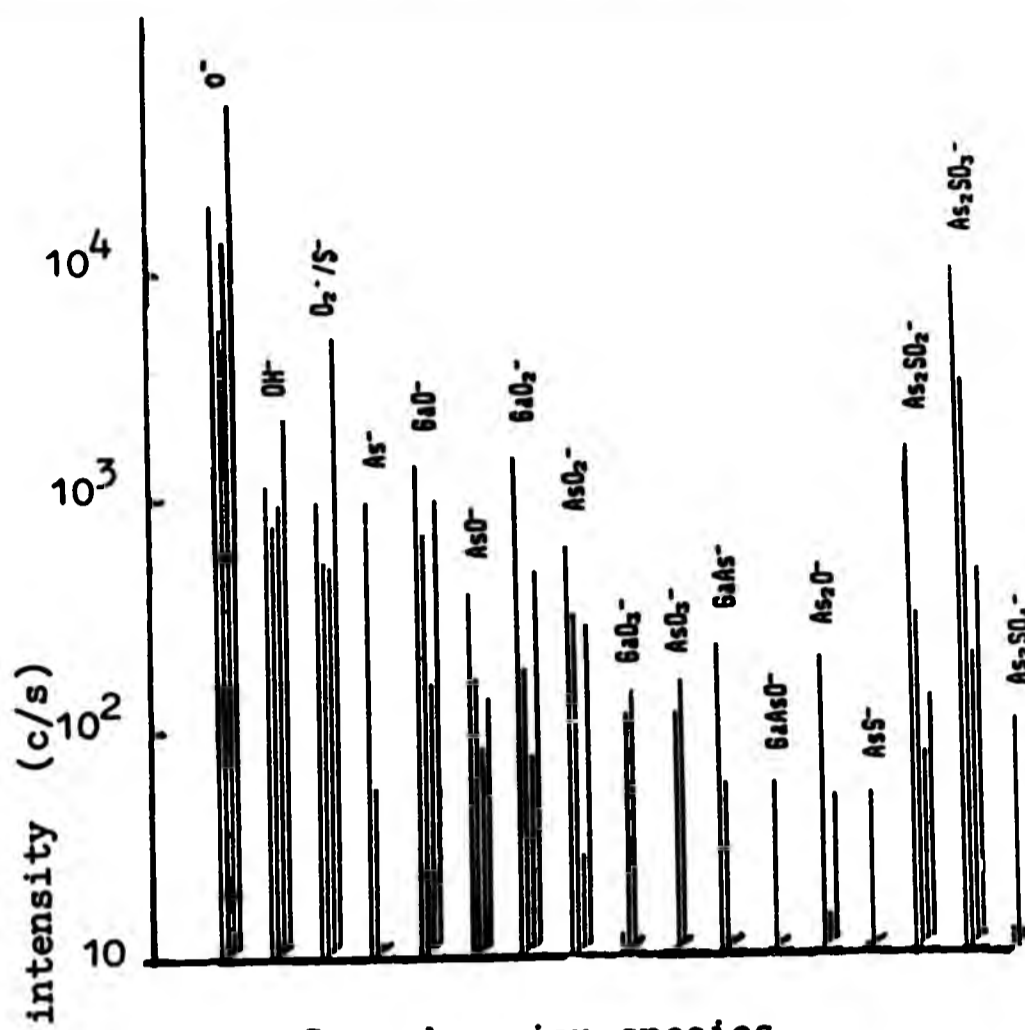
#### 5.3.1 Identification with SIMS of contamination and its sources, on the surface of wet-chemical-etched (100)GaAs substrates

The SIMS spectra from four chemically etched (100)GaAs substrates are plotted comparatively in Figures 1a and 1b. The spectra show that there are large variations in the signal intensities. These variations are presumably indicative of uncontrolled factors in the wet-chemical preparation.

There are many more signals in the spectra than in comparable AES spectra. Only oxygen and carbon contamination are observed in AES spectra from similar surfaces (K. Ploog and A. Fisher 1977, G. Lawrence et al. 1979).

The SIMS spectra show that signals containing oxygen and carbon appear in abundance. Oxygen appears in oxide and sulphate SIMS signals. (The sulphates presumably arise from the wet-chemical-etching). Carbon appears in the form of hydrocarbons. These hydrocarbons are possibly due to the use of iso-propanol in the substrate preparation. Other sources of carbon cannot be discounted because similar

Figure 1a

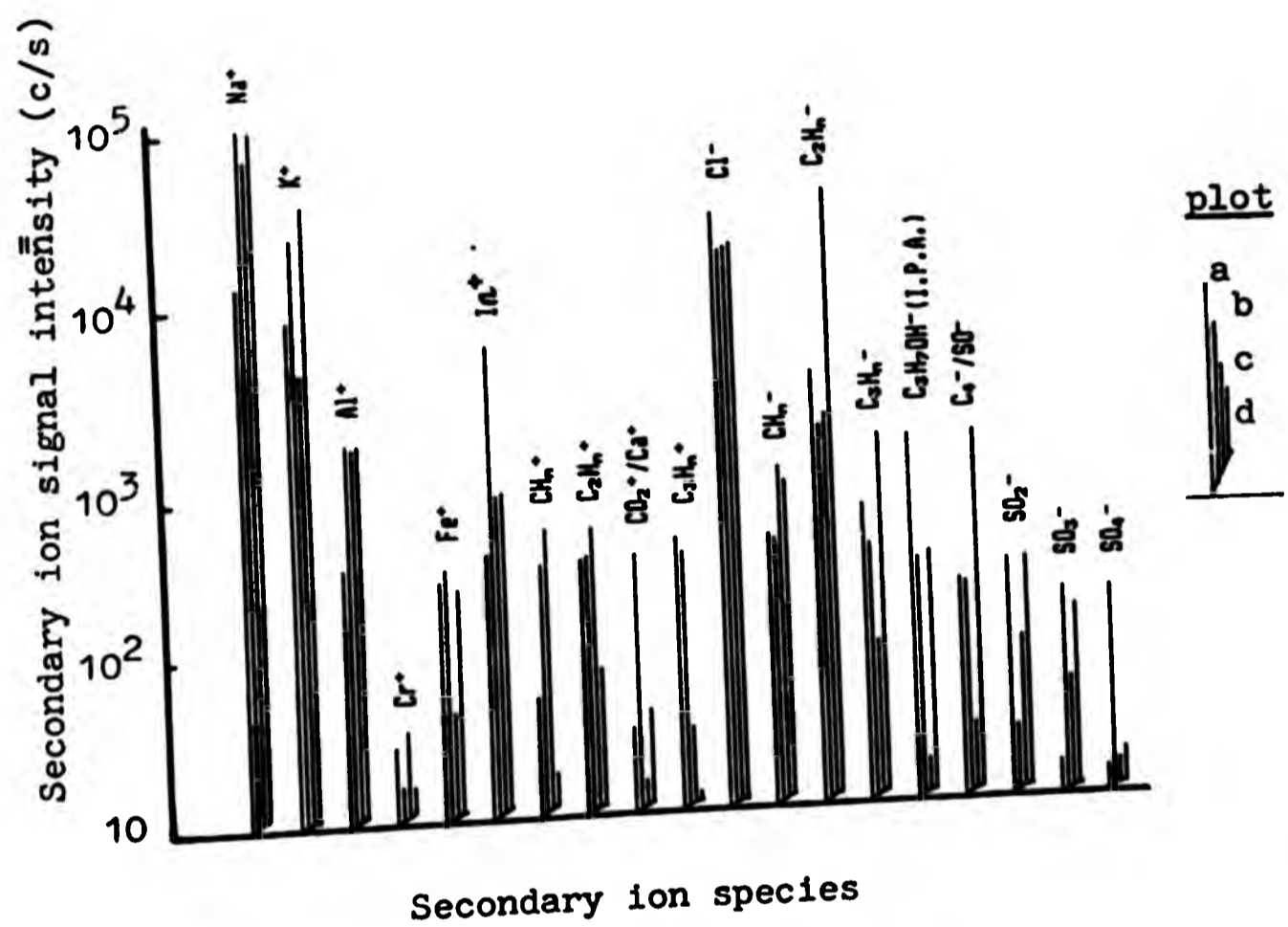


SIMS spectra from four chemically etched (100)GaAs substrates.

(Variations in peak height are indicative of uncontrolled factors in wet-chemical etching.)



Figure 1b



SIMS spectra of contaminant signals from  
four chemically etched (100)GaAs substrates.  
(Variations in the spectra are indicative  
of uncontrolled factors in wet-chemical  
etching.)

intensities of signals containing carbon atoms are obtained from air-exposed MBE grown films (Figure 2). Additional major contaminants include Na and K - common contaminants on surfaces - probably associated, in this case, with NaOH, KOH chlorine and other hydrated products.

One major problem in identifying signals in the plots arises because of a series of mass interferences between the sulphur atom (S), and the peroxide radical ( $O_2$ ). This threatens clear identification of many signals. The problem is most acute for the signals assigned  $As_2SO_n^-$  ( $n=1,2,3,4$ )

Estimates of the dependence of the transmission of the quadrupole mass filter on mass-to-charge ratio show that the transmission of the  $As_2SO_3^-$  signal at 230 a.m.u. is between 1.0% - 5.0% of the transmission for  $O^-$  at 16 a.m.u. (Dowsett et al. 1978). It can be seen from Figure 1a that this means that the  $As_2SO_3^-$  signals account for a large part of the oxygen detected from the surface. It is important to know whether this signal arises from arsenic sulphate or from arsenic oxide (in which case it would be assigned as  $AsO_5^-$ ).

To help overcome this difficulty in assigning the  $As_2SO_3^-$  signal, a comparison of oxide from a chemically etched substrate and an air-exposed MBE film was obtained with SIMS. The presence of sulphates could be reasonably discounted on the MBE film.

In this comparison a chemically etched substrate and an air-exposed MBE film were analysed in the same experiment,

mounted 1.0 cm apart on the same sample holder. This ensured that differences found in the SIMS analysis could be attributed to the substrate history before the substrates were soldered onto the sample holder.

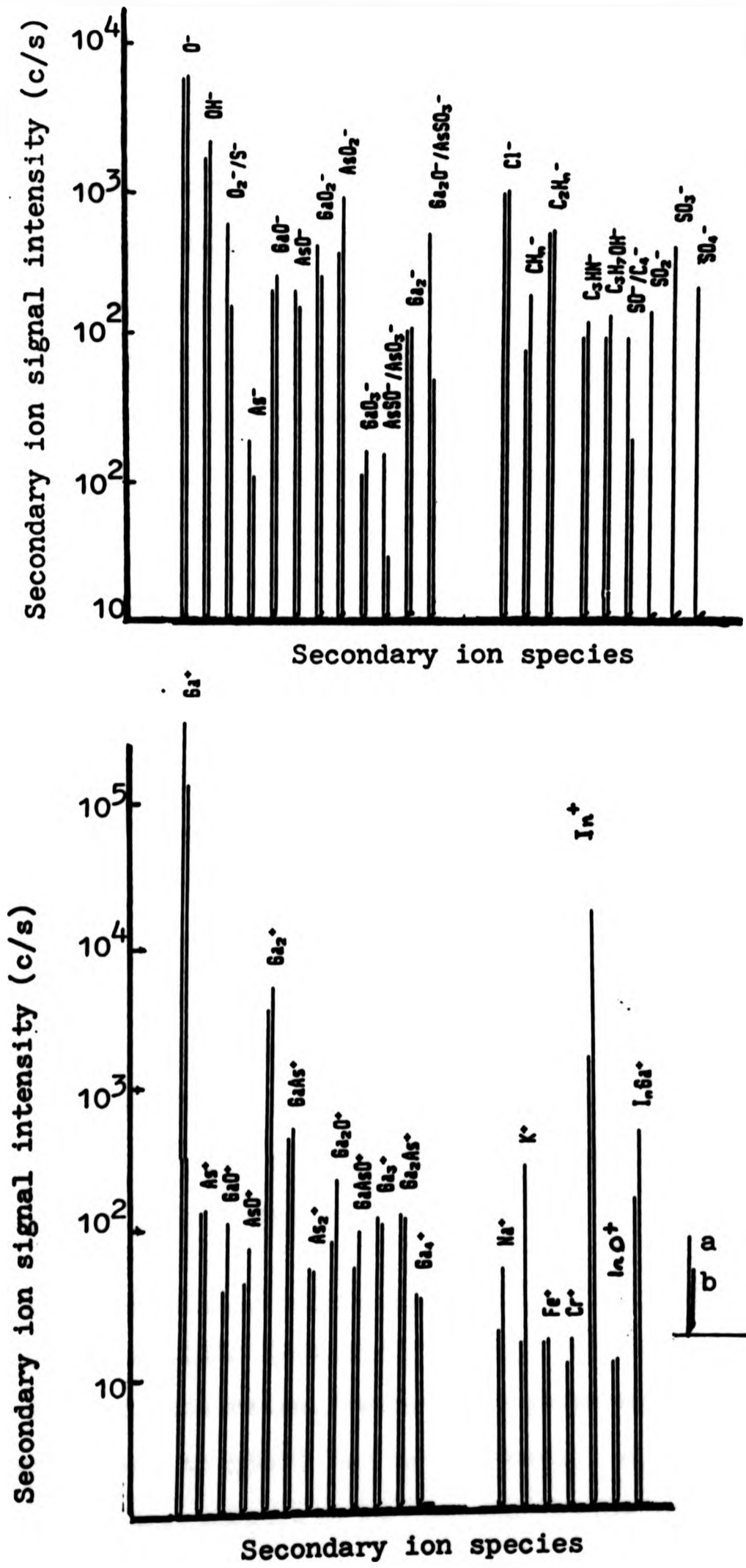
Figure 2 shows plots which compare the SIMS spectra obtained from the two substrates. It can be seen that the spectra are quite similar, but differ significantly in one aspect. Only signals assigned as  $SO_n^-$  ( $n=2,3,4$ ) appear in the spectra from the etched substrate. This supports the proposition that there are sulphates present on the etched substrate. The higher signal intensities from the etched substrate of other signals (assigned as  $S^-/O_2^-$ ,  $SO^-/C_4^-$ ,  $AsSO^-/AsO_3^-$ ,  $AsSO_3^-/Ga_2O^-$ ) is additional supportive evidence of the presence of sulphates.

The above comparison is not conclusive, but it is considered to be strong enough evidence to assume that sulphates are present on the chemically etched substrates and that the  $As_2SO_3^-$  and the other sulphate related signals in Figure 1a and 1b are in fact, properly assigned.

The large variation in the intensities of SIMS signals containing sulphur in Figure 1a and 1b, shows that the wet-chemical-etch leaves a variable amount of sulphate. This possibly relates to lack of control over p.h. and/or etch temperature, as these factors have the most influence on the solubility of arsenic sulphate in the etch solution (S. Lida and K. Ito 1971).

In Figure 1b, the variation in the SIMS signals containing

Figure 2



The difference between SIMS spectra from a)chemically etched (100)GaAs;and b) air exposed MBE grown (100)GaAs.

carbon atoms does not seem to show any clear relationship to the pre-vacuum history of the substrates, i.e. to the use of I.P.A. or  $N_2$  gas to dry the substrates in the final stages of substrate preparation. Notice also, in Figure 2, that the signals containing carbon and the  $Cl^-$  signal, from both the chemically etched and the air-exposed MBE film, are of similar intensity. Such levels of carbonaceous contamination would not be expected from the air-exposed MBE film. This result shows that, in general, there is a lack of correlation between carbonaceous SIMS signal intensities and sample history.

A possible source of contamination is the vacuum chamber itself. It is thought that contamination most likely occurs while the UHV chamber is baked to remove water vapour. During the bake, the liquid nitrogen 'cold trap' (which normally prevents back-streaming of oil from the diffusion pump into the vacuum chamber) is heated to  $180^\circ C$ . The resultant back-streaming, and diffusive 'crosstalk' between the substrates, are considered to be the most likely sources of carbonaceous contamination (M.G. Dowsett et al. 1977).

#### 5.3.2 A SIMS evaluation of surface preparation for MBE

Figures 3a and 3b show plots from SIMS spectra obtained from two chemically etched substrates, before and after heating them in the UHV chamber to  $580^\circ C$  for ten minutes. During this heat treatment, one substrate was heated in low pressure ( $10^{-6}$  Torr)  $As_4$ . This substrate was prepared in as similar a manner as possible to the substrates prepared before

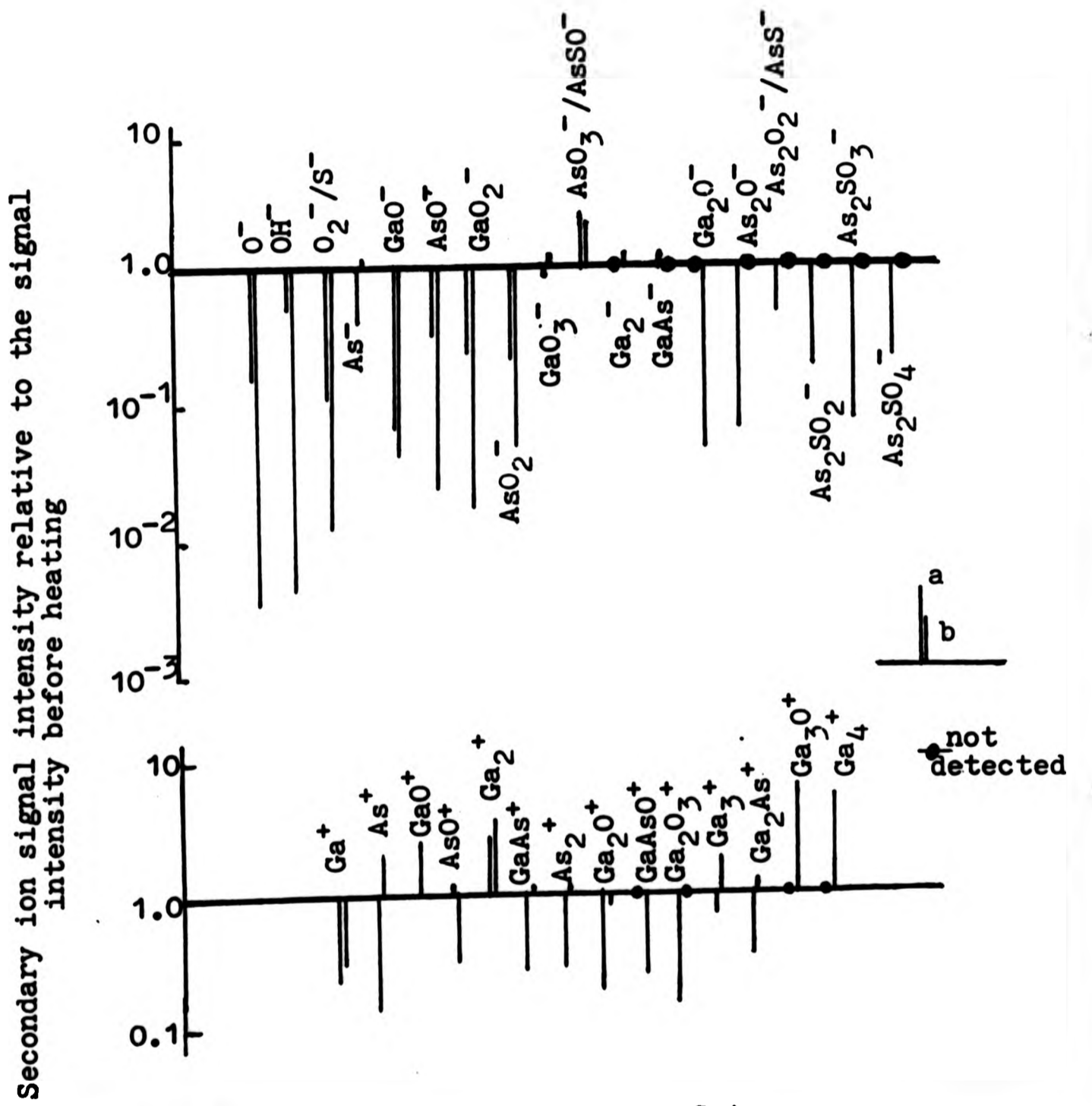
the growth of MBE films in this laboratory. The other substrate was heated at UHV pressures ( $10^{-10}$  Torr). The data from this substrate is included in the Figures 3a and 3b to provide a comparison with which to assess the efficacy of heating in  $As_4$ .

The peak heights of signals in the figures are relative peak heights. They are the ratio of the SIMS signal intensities found after heating, divided by the signal intensities found before heating. The data is presented in this manner because absolute comparisons of the SIMS signal intensities from each substrate cannot be made. This is due to the fact that the substrates were analysed in different UHV chambers with different SIMS apparatus.

The most evident feature in Figure 3a is that heating in  $As_4$  results in much larger reductions in the SIMS signals containing oxygen atoms than by heating in UHV alone. For example, the  $O^-$  SIMS signal intensity reduces to 0.4% of its SIMS signal intensity found before heating in  $As_4$ , while this signal only reduces to 20% of its level before heating in UHV. This result shows that as well as playing its intended role of inhibiting As depletion, heating in  $As_4$  also facilitates the removal of oxygen.

It has already been determined (in section 5.3.1) that the wet chemical-etch process leaves a variable amount of sulphate contamination on the surface. Most of the remaining differences in the response of the signals from the two substrates are considered to be attributable to a higher initial

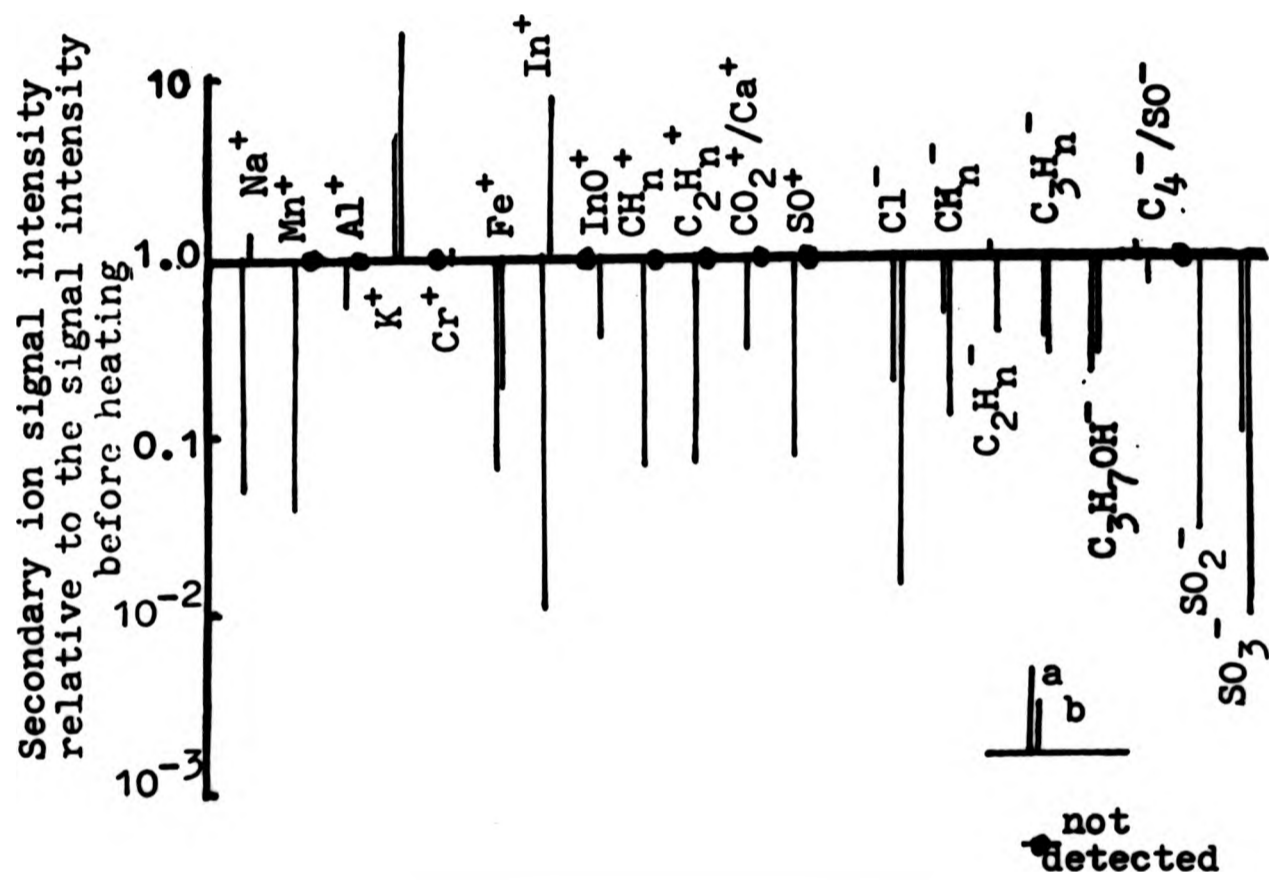
Figure 3a



The effect of heating on oxide and GaAs related SIMS signals.

a) heated in UHV; b) heated in  $As_4$ .

Figure 3b

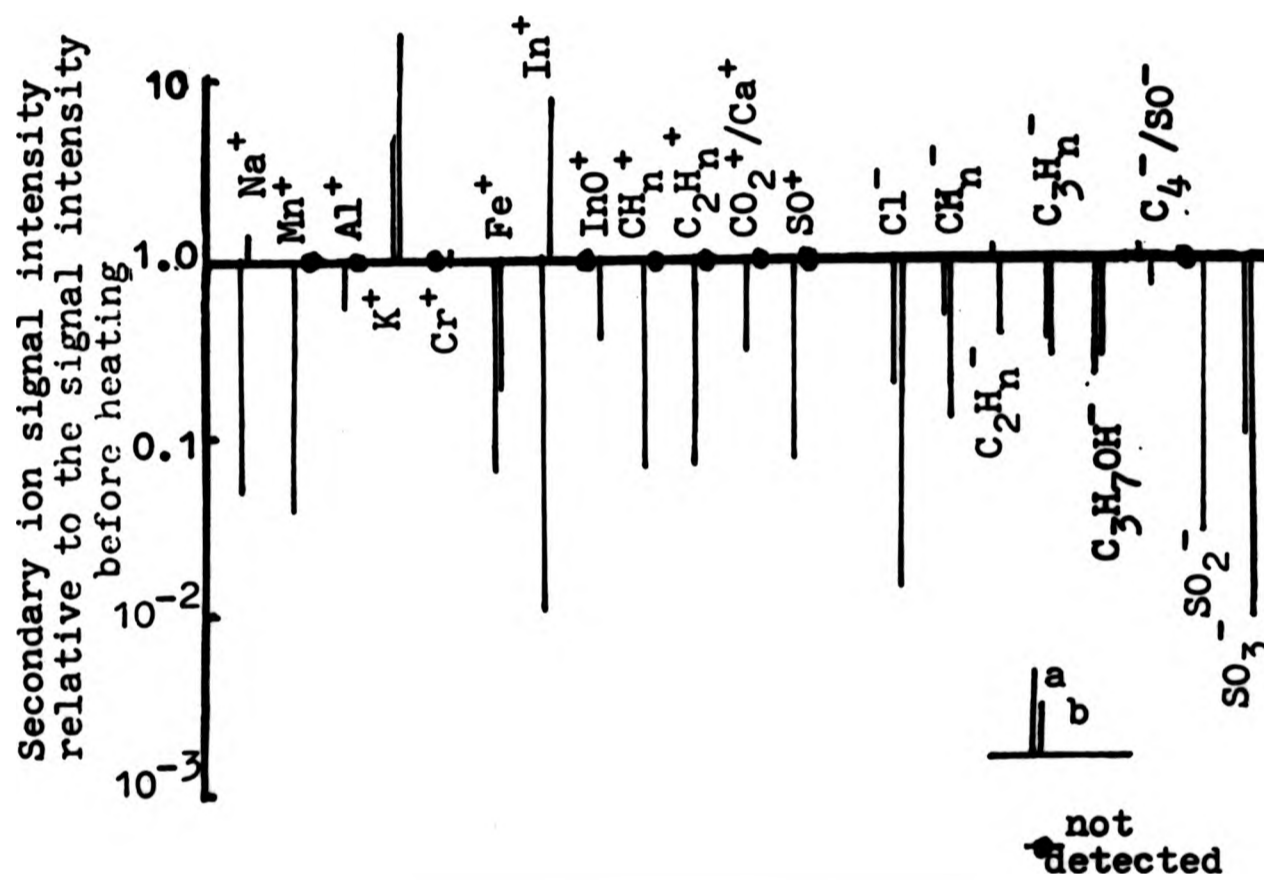


The effect of heating on contaminant related SIMS signals.

a) heated in UHV; b) heated in As<sub>4</sub>.



Figure 3b



The effect of heating on contaminant related SIMS signals.  
a) heated in UHV; b) heated in As<sub>4</sub>.

coverage of sulphate contamination on the substrate heated in UHV.

Figures 3a and 3b show that the sulphate related signals from the substrate heated in UHV are reduced by a similar amount to the  $O^-$  signal. Plot b of Figure 1a shows the mass spectra obtained from this substrate before heating. It can be seen that after the signals in Figure 1b are reduced by the amounts shown in Figure 3b, the sulphate related signals still represent a major source of the oxygen (and sulphur) on the surface after heating. This shows that after heating, the residual contamination is probably primarily made up of sulphates.

A similar exercise can be carried out to determine the effects of sulphates on the substrate heated in  $As_4$ . Plot a in Figure 2 shows the mass spectrum from this surface obtained before heating. The only evidence of sulphate related signals in this figure are the  $SO_2^-$  and the  $SO^-$  signals (and possible the  $C_4^-/SO^-$ ,  $AsO_3^-/AsSO^-$  and the  $GaO_2^-$  signals). After heating, all that is detected is the  $AsO_3^-/AsSO^-$  signal.

(The  $GaO_2^-$  signal is assigned as  $GaO_2^-/AsSO_3^-$  before heating - see plot a of Figure 2. The double assignment of this signal in Figure 2 arises from mass interference between  $Ga_2O^-$  with masses at 154, 156 and 158 amu and  $AsSO_3^-$  with mass 155 amu. Before heating, both species were definitely in the SIMS spectra but could not be resolved adequately to determine separate signal intensities for each. After

heating the signal could be resolved properly, and this showed the signals to be  $\text{Ga}_2\text{O}^-$ .)

Notice that the  $\text{GaO}^+$  and  $\text{GaO}_2^+$  SIMS signals increase as a result of heating in  $\text{As}_4$ . This, and the fact that the  $\text{Ga}_2\text{O}^-$  signal is the only signal detected from this surface above 150 amu (where the transmission of the mass filter is quite seriously diminished - Figure 6 in Chapter 3), suggests that the form of the residual oxide is a tenacious oxide of gallium.

Such a conclusion is made tentatively however, because the behaviour of positive ion signals does not generally follow oxygen coverage in as simple a manner as negative ion signals. (The more complex behaviour for positive ions can be seen in the studies of oxygen adsorption on PbTe in Chapter 4 and on GaAs in Chapter 5).

The behaviour of the  $\text{AsSO}_3$  signal is of interest. It can be seen in Figure 3a that this is the only signal in the negative spectra which increases after heating. This effect is observed for both substrates. It is likely that the signal results from the thermal breakup of arsenic sulphate.

Figure 3b shows how the contaminant signals responded to heating. The figure shows that heating in  $\text{As}_4$  produced marginally greater reductions in the  $\text{CH}_n^-$ ,  $\text{C}_2\text{H}_n^-$ ,  $\text{C}_3\text{H}_n^-$  and  $\text{C}_3\text{H}_7\text{OH}$  signals than heating in UHV. These SIMS signals reduced to levels between 10% and 50% of the intensities observed before heating. The reductions in these signals

are comparable with reductions reported for AES carbon signals (C 272eV) (K. Ploog and A. Fisher 1977).

Figure 3a shows that heating in UHV results in reductions in the  $\text{As}^+$ ,  $\text{GaAs}^+$ ,  $\text{As}_2^+$  and  $\text{Ga}_2\text{As}^+$  SIMS signal intensities to near or below the detection limit of the SIMS apparatus. Notice that no corresponding reductions occur after heating in  $\text{As}_4$ . This is evidence that the substrate heated in UHV is depleted of arsenic.

The air exposed MBE layers responded in a similar manner to the etched substrate heated in  $\text{As}_4$ . The other chemically etched substrates heated in UHV, also responded in a similar manner to the one reported here.

SIMS has shown in this section that even heating substrates in  $\text{As}_4$  leaves a significant amount of oxygen on the surface. This has consequences for MBE film growth because the process used here is as identical as possible to the process used to prepare substrates for MBE studies. RHEED and LEED analysis on substrates prepared for MBE and films grown thereon, have shown little evidence of imperfections in structure which could be attributed to surface contamination. This shows that the sensitivity of SIMS is probably greater than the sensitivity of these techniques in detecting contaminant related surface defects. Further, SIMS is shown to be sufficient for monitoring surface preparation for MBE.

### 5.3.3 Surface preparation for oxygen adsorption studies

In this section, SIMS is used to evaluate two surface preparation techniques used in oxygen adsorption studies. The first one consists of ion sputter cleaning followed by heating in UHV. This approach has often been used to prepare the surface of chemically etched polar GaAs substrates surfaces (Ploog and Fisher 1977, 1979 and Ludeke and Koma 1976).

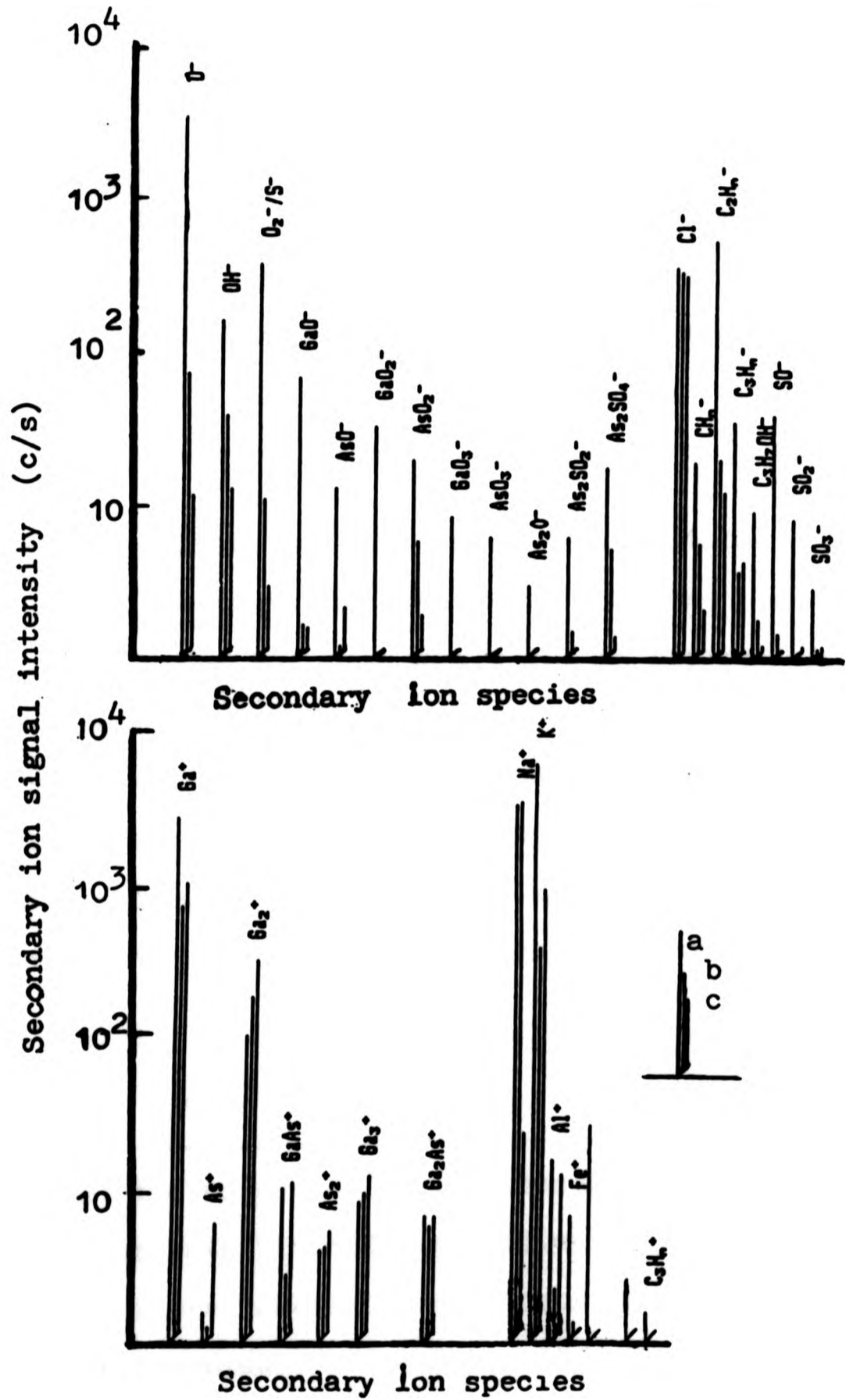
The second preparation technique consists of two repeated cycles of heating in low pressure  $As_4$  and ion sputter cleaning with a final heating in  $As_4$ . The purpose of this procedure is to produce substrates which appear atomically clean as far as SIMS analysis is concerned. The rationale behind the process is that, while ion sputter cleaning is essential (to remove carbonaceous contamination), the surface damage produced by sputtering will be less for substrates which are heated (annealed) in  $As_4$  than for substrates which are heated UHV.

The actual details of substrate preparation are given in the experimental section 5.2.3

#### Ion sputter cleaning and subsequent heating chemically etched (100)GaAs in UHV

Figure 4 shows how SIMS signal intensities from a chemically etched substrate (plot a), responded to ion-sputter cleaning with  $3 \times 10^{15}$  ion  $cm^{-2}$   $Ar^+$  ions (350eV) (plot b), and finally to heating in UHV at  $580^\circ C$  for 10 minutes. It can be seen that ion sputter cleaning by itself, produces marked reductions in all the signal containing oxygen, sulphur and carbon atoms.

**Figure 4**



The effect of ion sputter cleaning and subsequent heating in UHV on SIMS signals from chemically etched (100)GaAs.  
 Plots: a) from chemically etched substrate; b) after ion sputter cleaning c) after heating in UHV. 106

The figure also shows that heating results in further decreases in all the remaining oxide and sulphate related signals. Notice that only 0.35% of the original  $O^-$  SIMS signal intensity remains after heating. This shows that the residual level of oxide contamination after this treatment is probably as low, or even lower than that which results from heating in  $As_4$ . Notice that heating does not produce a further decrease in the negative carbonaceous signals.

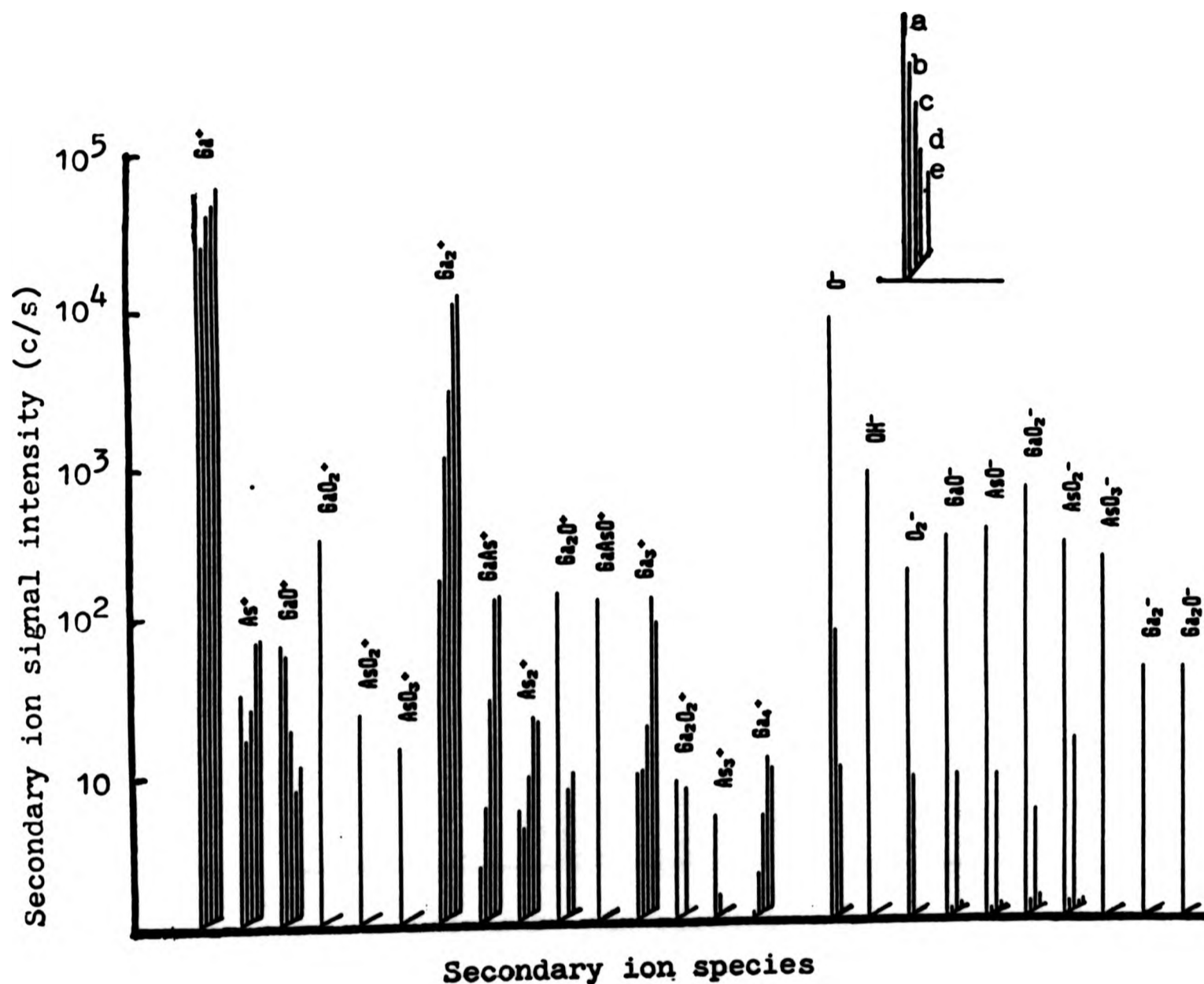
It is very difficult to compare the above results with those of past studies. This is because the 'ion dose' (not the density of the ion dose), the ion dose energy and an approximate value of the temperature to which substrates are heated are often the only parameters quoted for substrate preparation (Ranke and Jacobi 1976, 1979, Ludeke and Koma 1976). The data presented in the present analysis is in agreement with these studies to the extent that they report preparation.

#### Surface preparation by repeated heating in $As_4$ and ion-sputter cleaning

Since it is found that the effects of this cleaning procedure are very similar for both the MBE and chemically etched surfaces, it is considered adequate to discuss the results from only one of these examples.

Figures 5a and 5b show the SIMS spectra obtained from an air exposed MBE grown film after the various stages of preparation. The overall effectiveness of the cleaning process is immediately apparent in the response of all the SIMS signals. It can be seen that almost all of the oxide related

Figure 5a



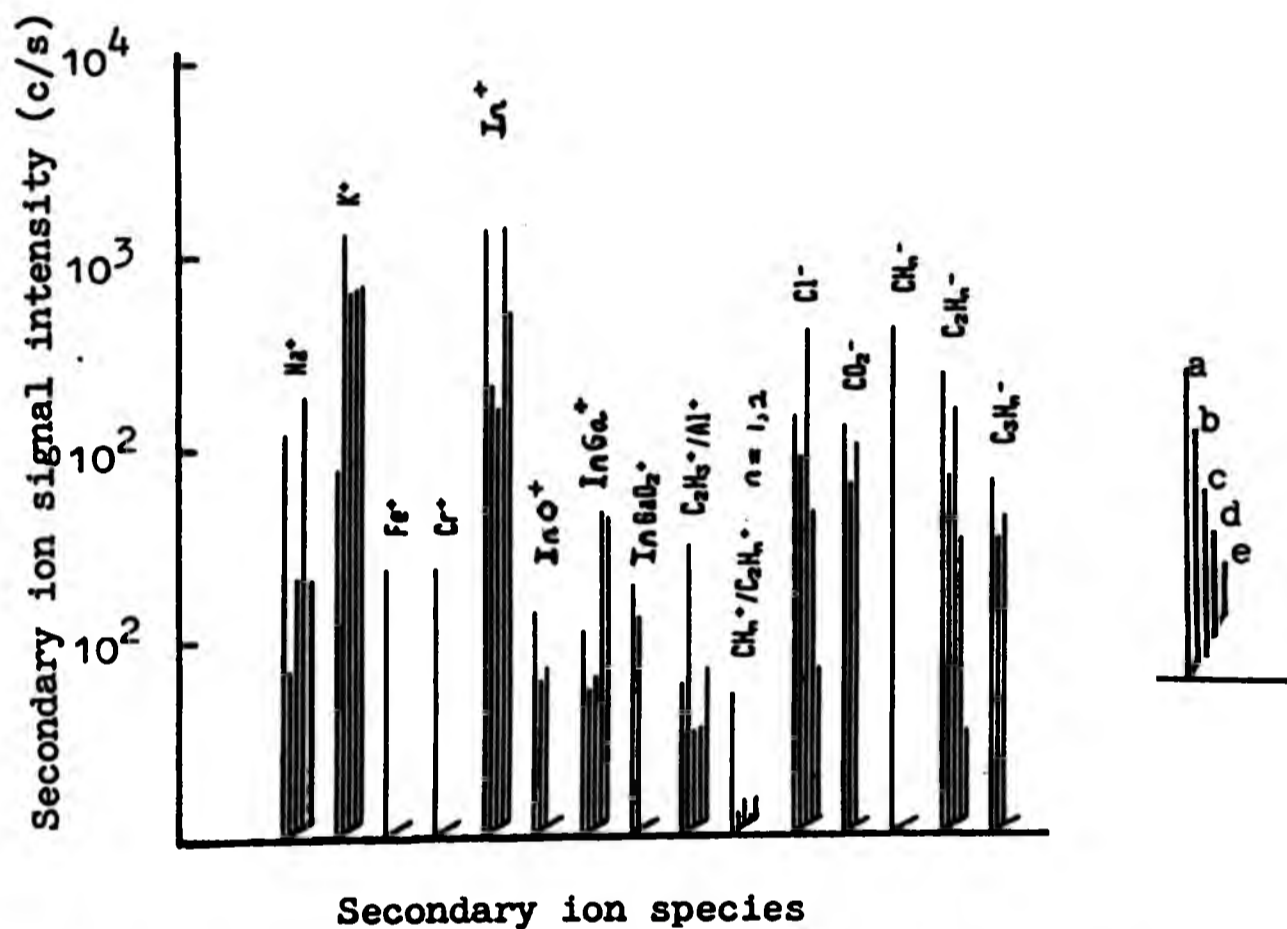
The effect on oxide and GaAs related SIMS signals of repeated cycles of heating in As<sub>4</sub> followed by ion sputter cleaning.

Plots: a) oxide on air-exposed MBE GaAs film; b) after heating in As<sub>4</sub>; c) after ion-sputter cleaning and re-heating in As<sub>4</sub>; d) after further ion-sputter cleaning; e) after final heating in As<sub>4</sub>.

(The heat treatment consisted of heating to 580°C for 10 minutes in 10<sup>-6</sup> Torr of As<sub>4</sub>. Ion-sputter cleaning consisted of bombardment with Ar<sup>+</sup> ions. The ion dose was 10<sup>16</sup> ions-cm<sup>-2</sup> and the ion energy was 350eV.)



Figure 5b



The effect on contamination related signals of repeated cycles of heating in  $\text{As}_4$  followed by ion sputter cleaning.

Plots: a) oxide on air-exposed MBE GaAs film; b) after heating in  $\text{As}_4$ ; c) after ion-sputter cleaning and re-heating in  $\text{As}_4$ ; d) after further ion-sputter cleaning; e) after final heating in  $\text{As}_4$ .

(The heat treatment consisted of heating to  $580^\circ\text{C}$  for 10 minutes in  $10^{-6}$  Torr of  $\text{As}_4$ . Ion-sputter cleaning consisted of bombardment with  $\text{Ar}^+$  ions. The ion dose was  $10^{16}$  ions- $\text{cm}^{-2}$  and the ion energy was 350eV.)

signals including  $O^-$  disappear leaving only a minimal indication that some oxygen remains on the surface in a small residual  $GaO^+$  signal. The figure shows that the intensity of the  $O^-$  signal is reduced to less than 0.02% of the intensity from the pre-treated surface. Comparing this reduction with reductions in the  $O^-$  signal to 0.6% for the  $As_4$  heat-treatment, and 0.35% for the ion-sputter-anneal treatment, shows that the treatment used here produces a surface which is relatively free of oxygen.

The plots of the contaminant signals in Figure 5b also show that the carbonaceous SIMS signals mostly disappeared. It is possible that those signals which remain, ( $C_2H_n^-$ ) are due to some extent to Al and to the film dopant Si. Mass interferences occurred in the spectra between these species and the dominant peaks in the  $C_2H_n$  group.

The increased SIMS signal intensities for  $As^+$ ,  $Ga_2^+$ ,  $GaAs^+$  and  $As_2^+$  indicate improvements in surface stoichiometry and structure. However, the increased intensities of the  $Ga_4^+$  which indicates conglomerations of Ga atoms, suggest that that it is also possible that the opposite is true.

The ratio of the mean of the negative carbonaceous signals found before the treatment, divided by the mean of these signals after the treatment, will be used as an estimate of the decrease in the surface coverage of carbonaceous contamination produced by the treatment. Although such a crude estimate of relative carbon coverage must be used with caution, it has an advantage in being easily derived from

absolute signal intensities and suffices in that it shows general trends related to carbonaceous signals.

The repeated heating in  $As_4$ , and ion-sputter-cleaning, caused the mean carbonaceous signal intensity to be reduced to 0.2% of the value found before treatment. Equivalent reductions of 12% and 3% for the  $As_4$  heat and ion-sputter-anneal treatments respectively, show the efficacy of the cyclic treatment (heating in  $As_4$  and ion-sputter cleaning) in removing carbon.

One similarity between all the cleaning processes is that there is no obvious correlation in the changes which occur in the alkali, Al and In metal signals. It may be that these species are highly mobile under the influences of heat and/or ion bombardment.

The presence of indium on all the surfaces and at all stages of the proceedings indicates that it initially appears on the GaAs surface through surface diffusion during soldering and 'bake out'. Notice that the  $In^+$ ,  $InO^+$ ,  $InGa^+$  and  $InGaO_2^+$  signals follow a similar behaviour to the equivalent Ga related signals,  $Ga^+$ ,  $GaO^+$ ,  $Ga_2^+$  and  $Ga_2O^+$ . This suggests that In is incorporated at Ga sites in the surface monolayer. If similar secondary ion yields are assumed for the  $In^+$  and  $Ga^+$  signals then, allowing for greater mass discrimination of the In signal, the surface coverage of In may be as much as 10% of an equivalent Ga monolayer.

#### 5.3.4 Comparison of SIMS with AES

The results presented in this chapter show that the response of negative ions in SIMS is qualitatively similar to that seen in AES studies. The results also strongly suggest that surfaces which appear clean to AES analysis often have contaminant levels which are easily detected in SIMS analysis at, or just below, the detection limits of AES apparatus (A.Y. Cho and J.R. Arthur 1975). Such levels ( $>0.001$  monolayer oxygen,  $>0.001$  monolayer carbon) are known to be sufficient to affect electrical properties and MBE growth (G. Lawrence et al. 1979).

In this section the reductions observed in the SIMS signal intensities of the  $O^-$  ion and of the mean signal intensity of the carbonaceous signals ( $CH_n^-$ ,  $C_2H_n^-$  and  $C_3H_n^-$ ) are compared to their Auger counterparts - the ratio of the oxygen signal at 510eV to the Gallium signal at 1070eV - and the ratio of the carbon signal at 272eV to the Ga1070eV signal.

AES spectra show that heating (100) GaAs substrates with a similar oxide to those prepared in this study, in a background of  $As_4$  at  $570^\circ C$ , reduces the ratio of the Auger oxygen to Gallium signal intensities to between  $<0.04\%$  and  $0.3\%$  of their level before heating (below the sensitivity of the Auger apparatus (Ploog and Fisher 1977 and Lawrence et al. 1979)). These decreases compare favourably with the decreases in the  $O^-$  SIMS signal after heating in  $As_4$  to approximately  $0.6\%$ . This indicates that the reduction seen in the  $O^-$  SIMS signal for the substrate prepared by heating in  $As_4$  and ion sputtered cleaning, is indicative of a very clean surface.

A similar exercise can be carried out for carbon. Ploog and Fisher (1977) and Lawrence (1979) report reductions in the ratio of the Auger carbon to gallium signals of greater than 50% and 3% for substrates heated in  $As_4$ . It can be seen that the ones obtained in section 5.3.3 with SIMS are not in disagreement with the AES estimates considering the difference between them.

#### 5.4 Conclusions

The evaluation of the cleaning processes investigated in this study show that SIMS performs well as a tool for monitoring surface treatments. SIMS exhibits very high sensitivity to oxygen. Within this study, oxygen is detected in the  $O^-$  signal at surface coverages, which are probably less than  $2 \times 10^{-4}$  monolayers. (This sensitivity could be easily improved by a factor of 10 or more by selecting only certain signals for analysis i.e. the  $O^-$  and  $C_2H_2^-$  signals).

The sensitivity to surface chemical groupings of SIMS is shown to be a valuable asset capable of determining both the source of contaminants, their form and, the effects of cleaning treatments on these. Most of the results complement the findings of other evaluative work on surface preparation. Namely, that heating etched (100)GaAs substrates in  $As_4$  prevents  $As_4$  depletion and while it is effective at removing oxygen, it is not as effective in removing carbon. Sputtering is also shown as effective in reducing carbon.

SIMS also shows, however, that currently used preparation treatments still leave contamination near or below detection

limits of AES. It is shown that this contamination can be further reduced to near the detection limit of the present SIMS instrument by repeated cycles of heating in  $As_4$  and light ion sputter cleaning. SIMS spectra from surfaces prepared this way show signs that surface stoichiometry is preserved. Estimates of the effects of SIMS on surface coverage of contaminants give estimates which are in approximate agreement with estimates from AES.

SIMS is not considered to be sufficient for monitoring substrate preparation in UHV. Although estimates for the reduction in surface contaminants obtained in this study agree with earlier studies using AES, there must be some lack of confidence in these estimates. This is because of the complexity of the secondary ion emission processes and the fact that their dependency on surface coverage and chemistry are not easily determined. Because of these deficiencies, it is believed that AES (for surface analysis) and LEED (for surface structure) should be used in conjunction with SIMS to monitor surface preparation.

CHAPTER 6

A PRELIMINARY SIMS STUDY OF LOW COVERAGE OXYGEN ADSORPTION  
ON MBE GROWN (100)GaAs

## 6.1 INTRODUCTION

In this chapter 'low dose' SIMS is used in an investigation of low coverage oxygen adsorption on clean(100)GaAs surfaces. This preliminary study utilises the high sensitivity of SIMS and its sensitivity to chemical groupings to determine whether differences exist in oxygen adsorption behaviour of the arsenic rich and gallium stabilised surfaces of the polar, (100)GaAs surface. The effect of excitation of oxygen by an ionisation vacuum gauge head is also investigated to discover if this influences the adsorption behaviour.

Over the past decade chemisorption on the various faces of GaAs has been studied extensively using Auger electron spectroscopy (AES) (Ludeke and Koma 1976, Ranke and Jacobi 1977,1979), ultra-violet photon spectroscopy (UPS) (Ludeke and Koma 1976, Ranke and Jacobi 1977) and electron loss spectroscopy (ELS) (Chye et. al 1979, Spicer et al. 1979).

The main questions which these studies have sought to answer are whether associative or dissociative bonding predominates, and if oxygen is initially bound to Ga or As atoms. Adsorption on the (110) surface has received more attention than the polar surfaces due to its ease of preparation by cleavage in UHV. After extensive research (C.Y. Su et al 1980), there is now some general agreement about adsorption on this surface.

Adsorption of excited oxygen - produced by heated elements (i.e. ionisation vacuum gauges) in the vacuum area - proceeds 500 times faster than with unexcited oxygen and it is initially



composed of  $\text{Ga}_2\text{O}_3$  and  $\text{As}_2\text{O}_3$  with further exposure producing bulk oxide (C.R. Brundle and D Seybold 1979).

With unexcited oxygen there appears to be two low coverage sorption sites (C.Y. Su et al. 1980). Adsorption of the first form occurs at exposures of less than  $10^6$  Langmuirs. This phase saturates at 0.01 monolayers. It probably corresponds to oxygen adsorption of defect sites. The second form of oxygen adsorption has the stoichiometry of  $\text{GaAsO}_3$  but it appears that the surface is passivated by adsorption of 1.0 monolayer coverage of oxygen. This excludes the possibility of direct growth of  $\text{Ga}_2\text{O}_3$  and  $\text{As}_2\text{O}_3$  (C.R. Brundle and D. Seybold, 1979). UPS core level studies on heat treated surfaces suggest the second form of adsorbed oxygen consists of an intermediate chemisorption phase possibly of  $\text{GaAsO}_4$  (C.Y. Su et al. 1980).

On the polar surfaces, oxygen adsorption is not so clear. The main difficulty consists in defining the state of the surface being exposed to oxygen. The polar surfaces exhibit various structures which depend on the ratio of surface Ga and As atoms (P.Drathen et al. 1978). It is very difficult to determine the ratio of Ga to As atoms which the surface preparations produced. The initial state of the surface therefore depends on the details of surface preparation.

Techniques for surface preparation used in most of the relevant studies to date have relied on either cleaning chemically prepared substrates by a combination of heating (to remove oxygen and/or anneal) and ion sputter cleaning (to remove

oxygen or carbon) or, the growth of thin epitaxial films in UHV by molecular beam epitaxy (MBE).

These differences in surface preparation and other prevailing experimental conditions have been unclear. Essential parameters such as the pressure at which oxygen exposures occur, or whether oxygen exposure involves 'excited' oxygen (which dominates oxygen adsorption on the (110)GaAs surface), have often been omitted in the reporting of studies.

A more recent study by Ranke and Jacobi (1979) however, suggests that oxygen sorption on the polar surfaces is similar to adsorption on the(110) surfaces. Again, two distinct forms of low coverage adsorption of unexcited oxygen are observed. Thermal desorption spectrometry shows one form desorbs at  $125^{\circ}\text{C} - 175^{\circ}\text{C}$  mainly as molecular oxygen and the other desorbs at  $450^{\circ}\text{C} - 580^{\circ}\text{C}$  as  $\text{Ga}_2\text{O}$ . The former of these is attributed to associative bonding on As atoms, the latter form is attributed to atomic oxygen bound in an oxide state. Electron irradiation of the first form transforms it into the second. Although explanations of the forms of oxygen adsorption on the (110) and polar surfaces was different (C.Y.Su et al. 1980), the above study shows that a stable intermediate chemisorption phase appears to be present on all surfaces at low coverages before bulk type oxides are observed.

## 6.2 Experimental

### 6.2.1 UHV chamber and SIMS instrumentation

The UHV chamber, SIMS instrument and operating conditions are described in detail in Chapter 3. Chapter 3 also describes provisions for oxygen gas exposure.

### 6.2.2 Substrate preparation

Two air-exposed Si doped  $N_e = 5 \times 10^{18} - 10^{19}$  (100)GaAs MBE thin films of area  $10 \text{cm}^2$ , grown in another UHV chamber in the laboratory (J.D. Grange 19790) were used in the analysis.

Preparation for adsorption studies comprised of two cycles of heating to  $580^\circ\text{C}$  in an arsenic overpressure of  $2 \times 10^6$  Torr for 10 minutes, followed by light ion sputter cleaning with a dose of  $10^{16}$  ions $^{-2}$  of 300eV  $\text{Ar}^+$  ions. This was followed by a further anneal in arsenic as above. To prepare the final surfaces required, the arsenic rich surface was produced by annealing again with an As overpressure of  $10^{-6}$  Torr at  $580^\circ\text{C}$ . The Ga stabilised surface was produced in the same way - but without the As.

The analysis of surface preparation presented in Chapter 5 shows surfaces prepared in this manner give a minimal secondary ion emission of contaminants well below levels observed from surfaces prepared by simply ion sputter cleaning and annealing in UHV.

### Oxygen exposure

An ionisation vacuum gauge was used to excite oxygen when 'excited' oxygen was required for exposure. In such exposures,

steps were taken to ensure that the surface of substrates were not directly exposed ( in line-of-sight) to the ionisation gauge. During unexcited oxygen exposures the vacuum gauge was turned off along with other possible sources of 'excited' oxygen with the exception that it was necessary to use the vacuum gauge at the beginning and end of exposures to check pressure.

### 6.2.3 Experimental procedure

Substrates were prepared in the manner described above. After preparation they were subjected to oxygen exposures in the range  $10^2$  Langmuirs -  $10^6$  Langmuirs at pressures between  $10^{-8}$  Torr and  $2 \times 10^{-5}$  Torr of research grade (99.999%)  $O_2$  (B.O.C. Ltd.). At these low pressures it is assumed that oxygen adsorption is independent of exposure pressure. Before and after the oxygen exposures, the films were analysed with SIMS. Oxygen exposures were accumulative i.e. SIMS spectra were obtained from the 'as prepared' surface and the same film surface after successive, accumulated oxygen exposures.

'low dose' SIMS spectra were obtained in a background pressure of  $5 \times 10^{-8}$  Torr or Argon gas with a residual UHV pressure of typically  $2 \times 10^{-10}$  Torr. The primary ion dose per analysed region was kept to a minimum, ( $2 \times 10^{14}$  ion  $cm^{-2}$  of 1KeV  $Ar^+$  ions) and this produced changes of less than 10% in peak heights during analysis times of 300 sec.

### 6.3 Results

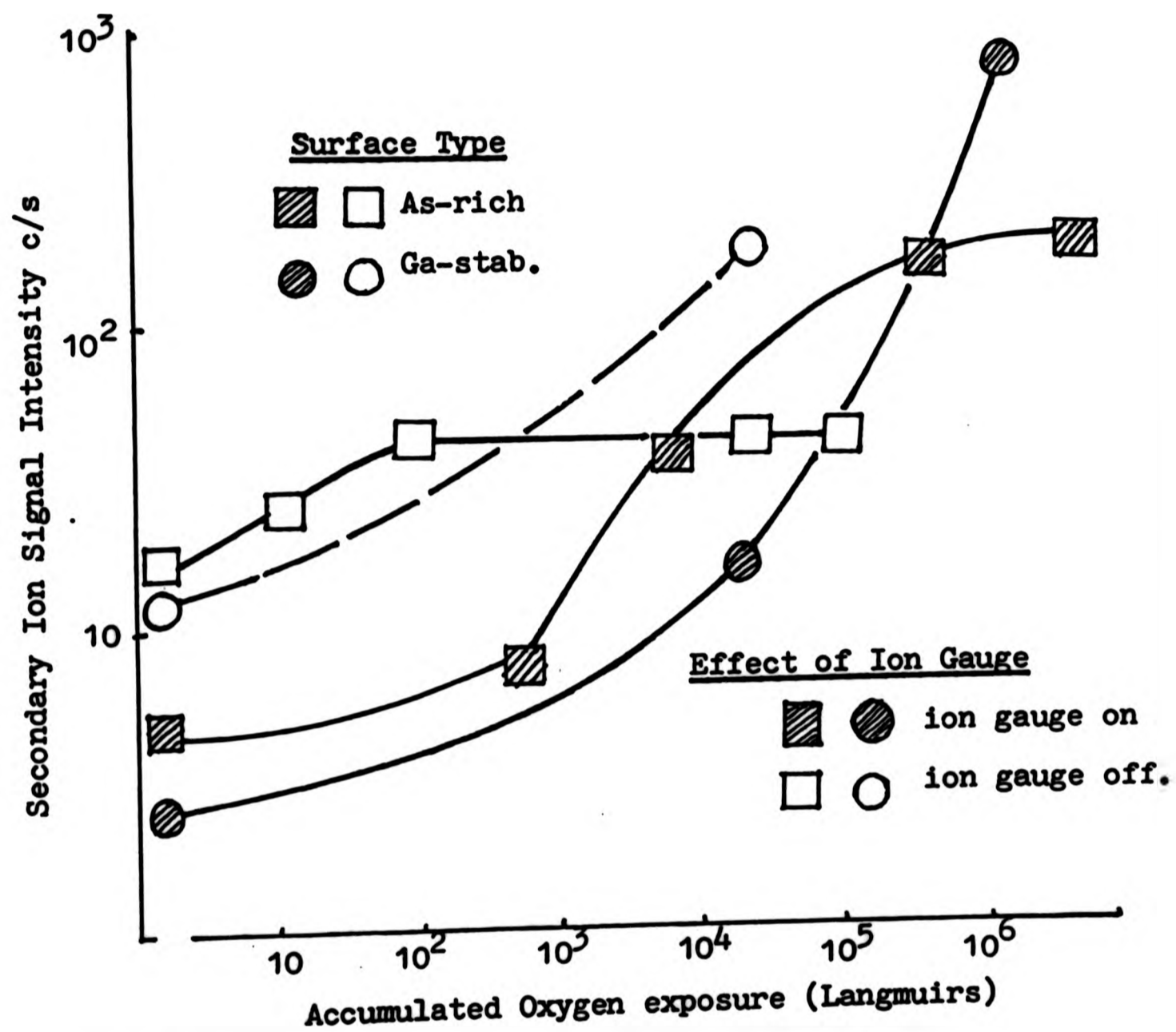
Figures 1 to 6 show plots which compare the response of selected secondary ion signals to oxygen exposure for the different surface types and for the type of exposure gas investigated (excited or unexcited). These particular signals contain most of the information which could be extracted from the study.

Figure 7 shows the response of signals from the As-rich surface to 'excited' oxygen exposure in more detail. The figure also includes data from a large oxygen exposure ( $2 \times 10^{10}$  Langmuirs) at  $10^{-3}$  Torr and from oxide produced by air exposure before film preparation. This data in Figure 7 is used later to obtain an estimate of the sensitivity of SIMS to oxygen.

Figure 8 shows a comparison of how the  $O^-$  SIMS signal from the As-rich and Ga-stabilised surfaces responded to 'excited' oxygen exposure, with the response of ratio of the Auger Oxygen (510eV) to Gallium (1070eV) signal intensities, which have been reported in the literature for oxygen adsorbed on the various polar GaAs surfaces.

Scrutiny of all the figures showing the response of negative ions to oxygen, shows that in all cases except one, the signals respond by increasing monotonically with oxygen exposure. A similar result is reported in Chapter 4 for oxygen adsorption on PbTe. In Chapter 5 it is also reported that negative ion signals of signals containing oxygen atoms decrease monotonically with the removal of oxygen from the

Figure 1



The effect of oxygen on the O<sup>-</sup> SIMS signals

Figure 2

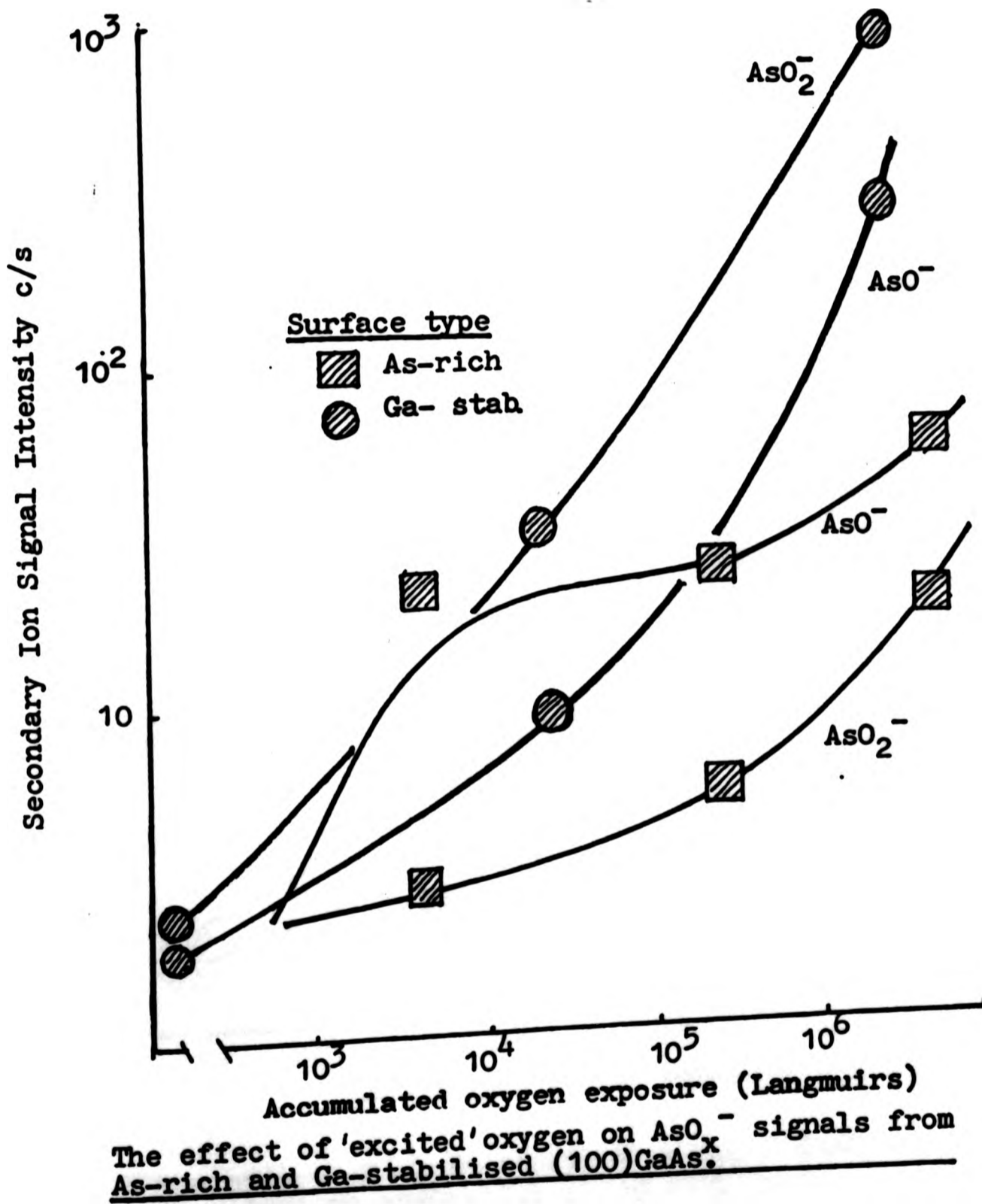
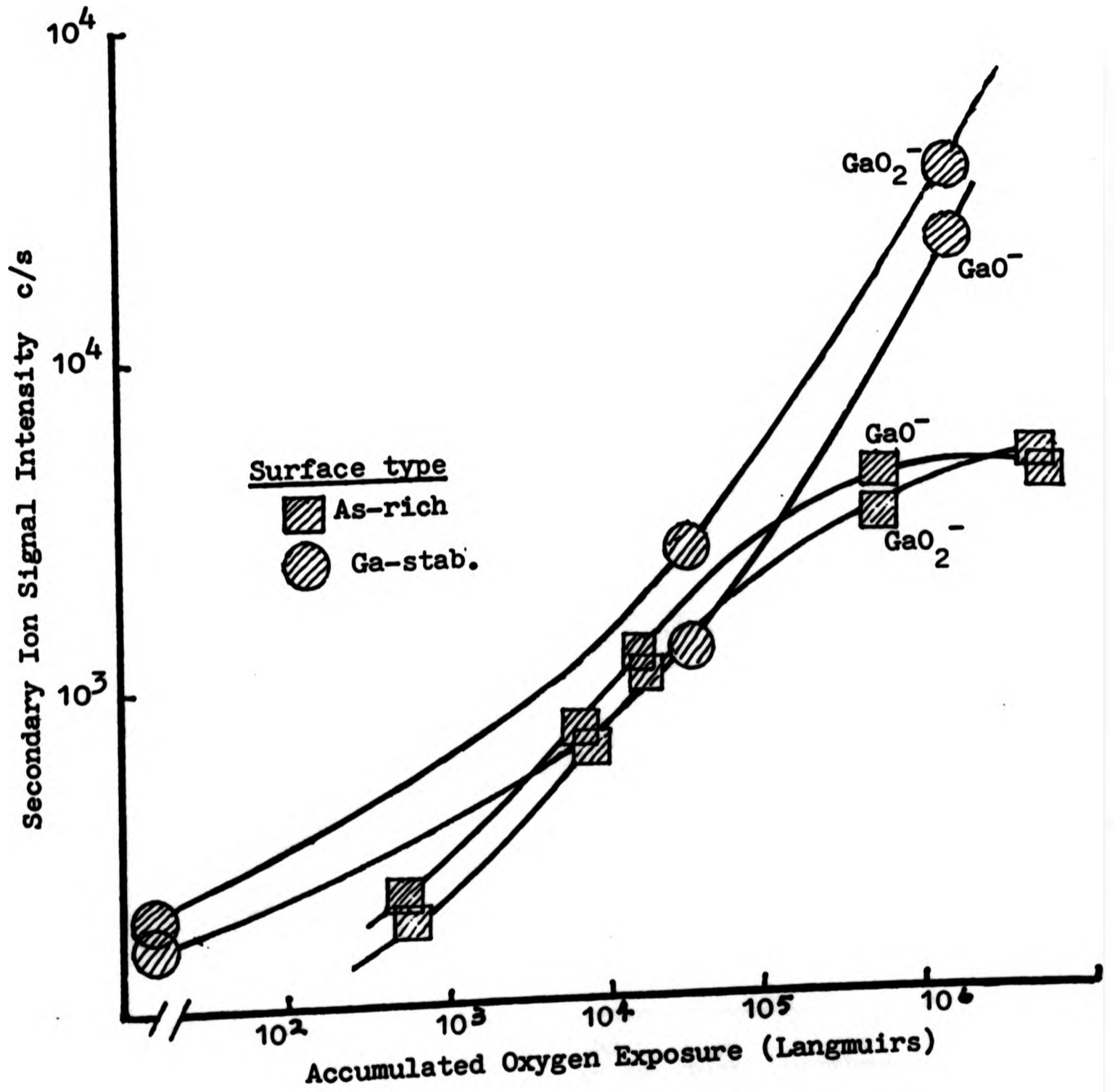


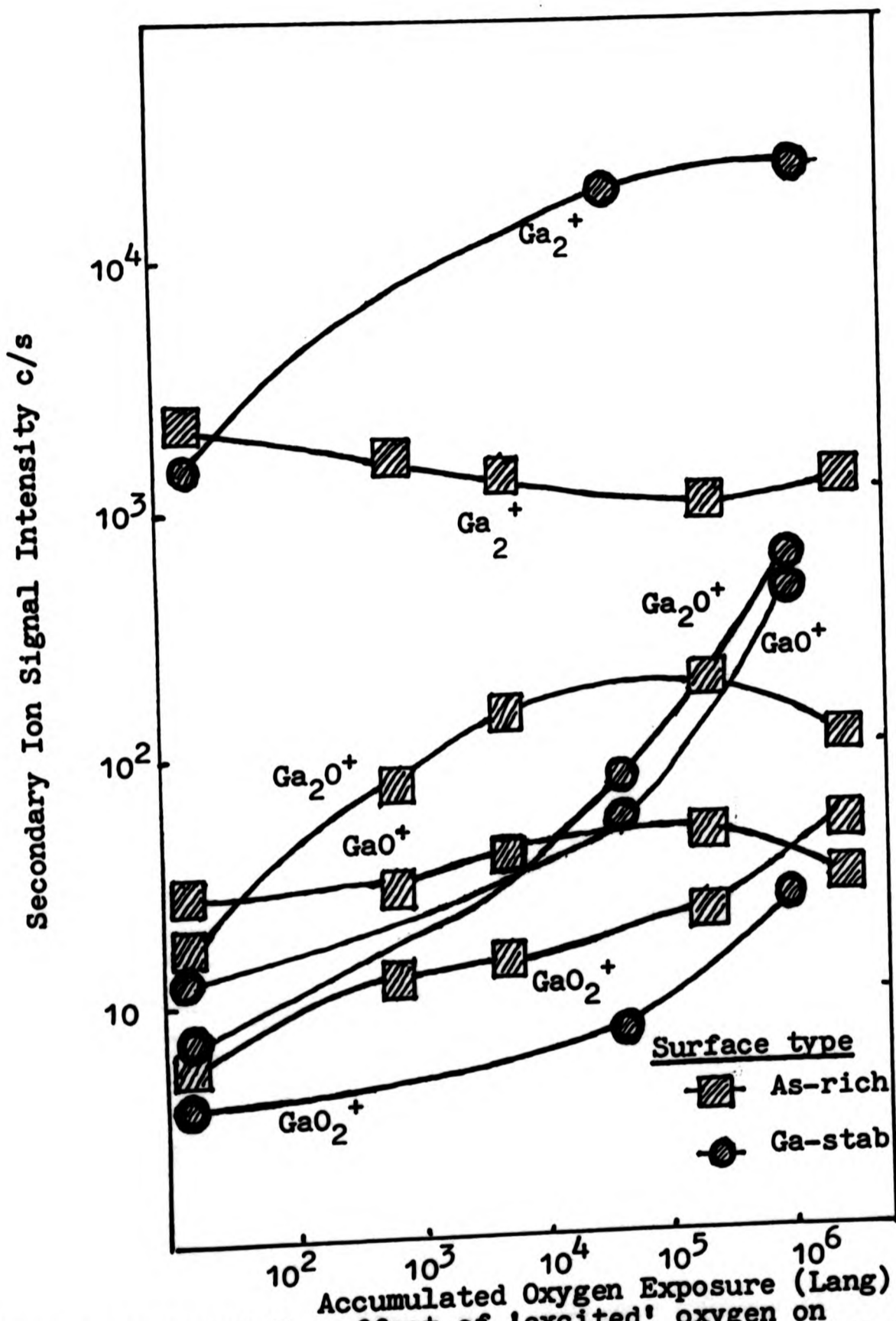
Figure 3



The effect of 'excited' oxygen on GaO<sup>-</sup> SIMS signals from As-rich and Ga-stabilised (100)<sup>x</sup>GaAs.

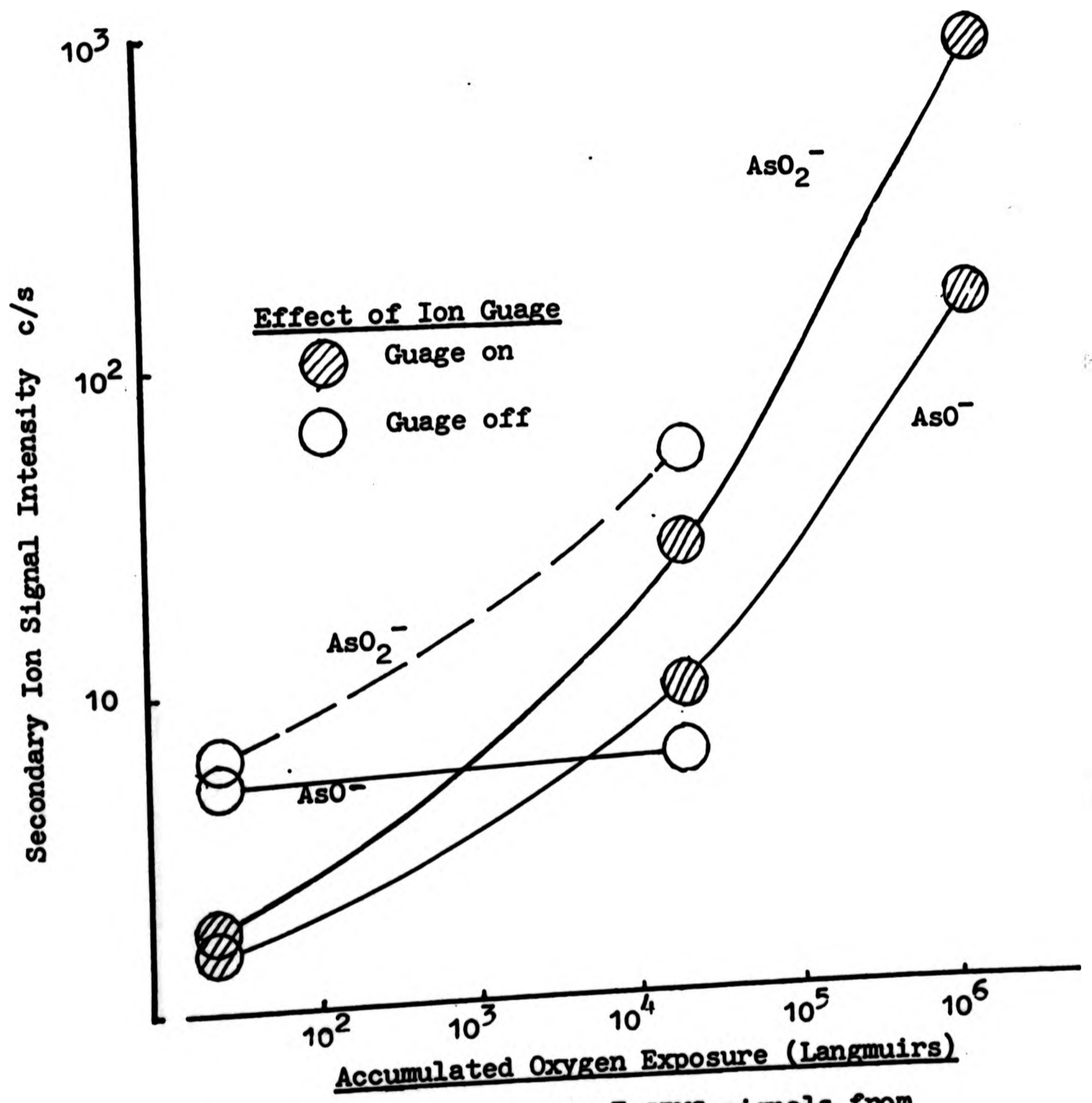


Figure 4



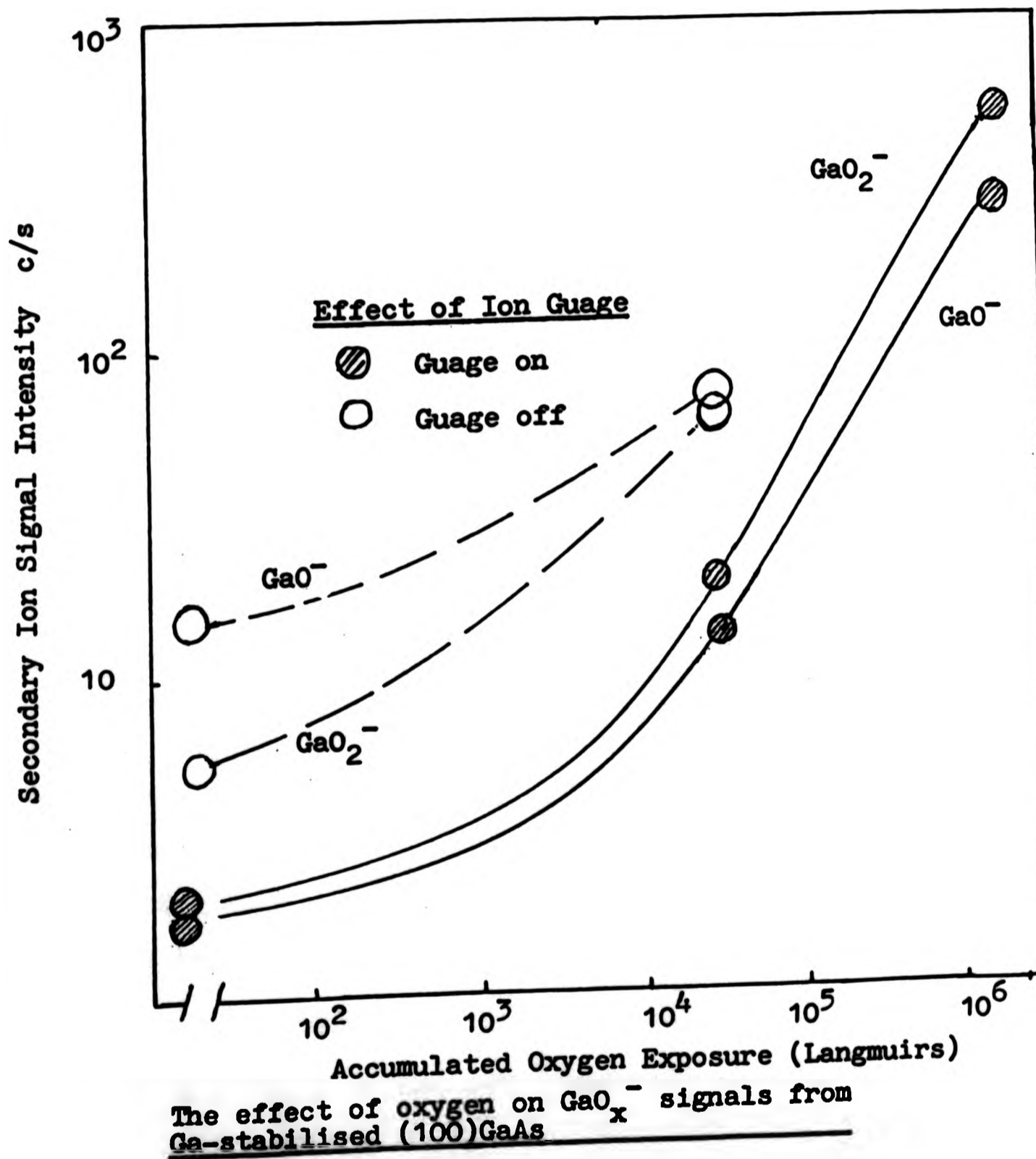
A comparison of the effect of 'excited' oxygen on Ga<sub>x</sub>O<sub>y</sub><sup>+</sup> SIMS signal from As-rich and Ga stabilised (100)GaAs.

Figure 5



The effect of oxygen on  $AsO_x^-$  SIMS signals from Ga-stabilised (100)GaAs

Figure 6



surface. This behaviour suggests that negative ion emission probabilities are not strongly dependent on surface chemistry.

The above suggestion is tentative, but it is also necessary in order to study the significance of changes in SIMS signal intensities produced by oxygen exposure.

### 6.3.1 Exposure to 'excited' oxygen

#### Differences in the response from As-rich and Ga-stabilised GaAs

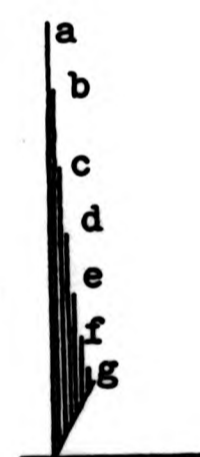
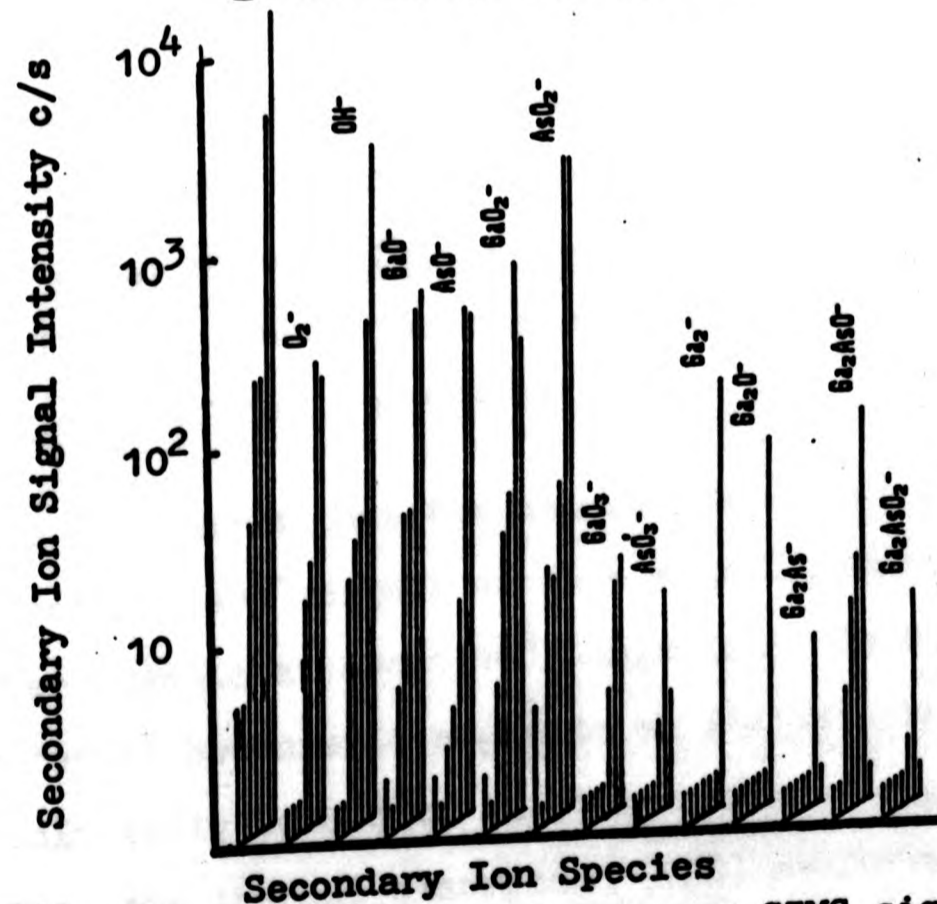
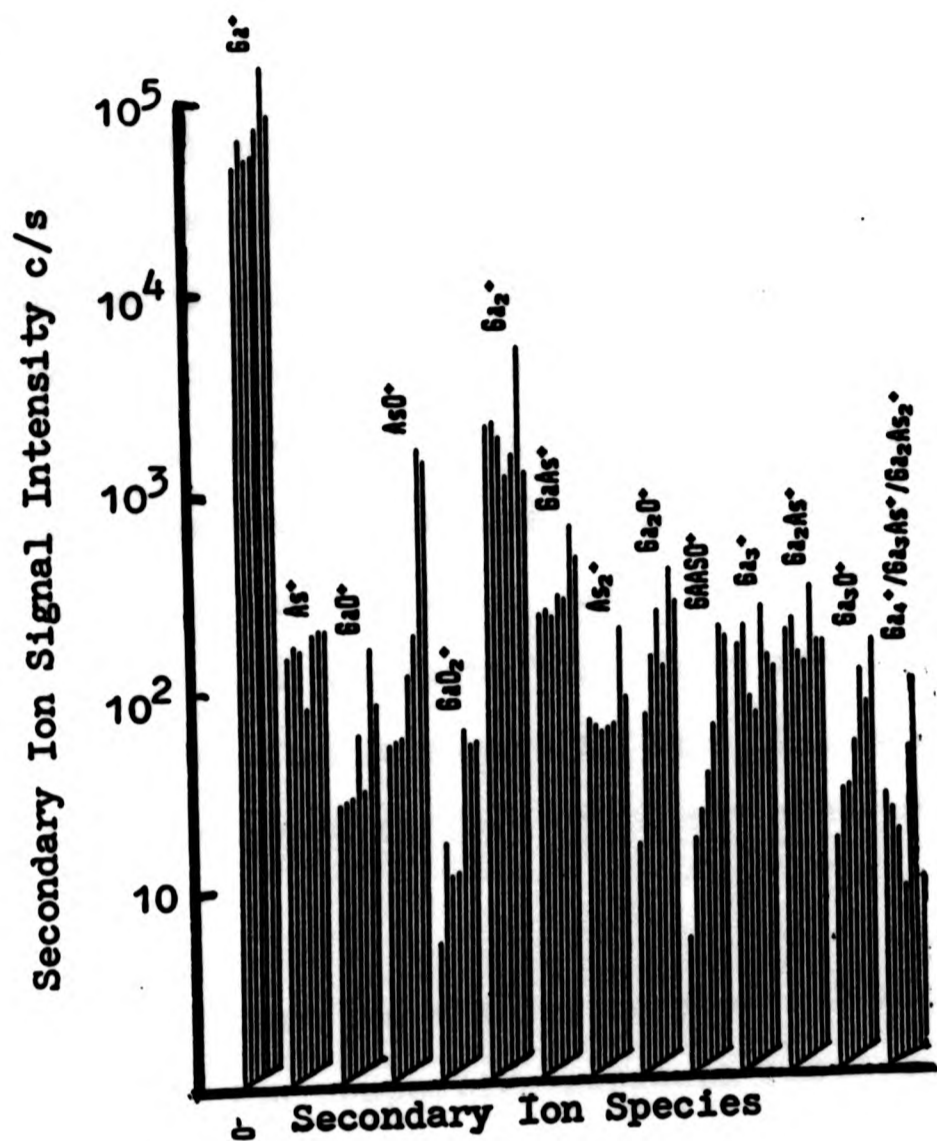
Figures 2 - 4 compare the responses of 'excited' oxygen exposure, of selected SIMS signals from the As-rich and Ga-stabilised surfaces. It can be seen that while the response of signals from the two surfaces is very different, there is a similar response of different signals from the same surface. This difference in the responses from the two surfaces suggests that the mechanisms of oxygen adsorption on these surfaces are different.

#### The As-rich surface

The plots in Figures 1 - 4 show that the  $O^-$ ,  $AsO_2^-$ ,  $GaO^-$  and  $GaO_2^-$  SIMS signals have behaviour that appears to show saturation of oxygen adsorption between  $10^5$  Langmuirs and  $10^7$  Langmuirs exposure.

Figure 7 shows that further changes in these signals occur after further exposure at  $2 \times 10^{10}$  Langmuirs. It can be seen that after this exposure, the intensities of the  $O^-$ ,  $GaO^-$ ,  $GaO_2^-$ ,  $AsO^-$  and  $AsO_2^-$  signals are similar to those found on the air exposed surface. The further change in these signals also indicates that another adsorption phase has become dominant.

Figure 7



The effect of 'excited' oxygen exposure on SIMS signals from As-rich (100)GaAs

Plot (a) is from the clean unexposed (100) GaAs MBE film. The following plots are after oxygen exposures of: b) 600 Lang; c) 6000 Lang; d)  $2 \times 10^5$  Lang; e)  $3.6 \times 10^6$  Lang.; Plot g) is from the air exposed MBE film.

Figure 7 also shows that there is a gradual increase in the signal intensities of the larger secondary ion clusters,  $\text{Ga}_2\text{AsO}^-$  and  $\text{Ga}_2\text{AsO}_2^-$ . It is interesting to note that these signals are not detected on the air-exposed surface. Further, reference to the results in Chapter 5 shows that these signals are not detected at any stage in the preparation of the air-exposed MBE films or etched substrates. This result shows that while SIMS suggests that there are similarities between the oxide after exposure at  $2 \times 10^{10}$  Langmuirs to the oxide on the air-exposed surface, there are some definite differences.

It may be argued that the similar response of most negative ion signals from the respective surfaces shows that they result from recombination of sputtered species with sputtered oxygen atoms (N. Winograd 1978). This appears unlikely, at least for the  $\text{AsO}_2^-$  signal. Figure 2 shows that while the  $\text{AsO}^-$  and  $\text{AsO}_2^-$  signals follow a similar response from the Ga-stabilised surface, the response of these signals from the As-rich surface is different.

Figure 2 also shows that the saturation effect is most definite for the  $\text{AsO}_2^-$  signal as this signal saturates before the other signals at about  $10^4$  Langmuirs. This is an important result because it suggests an initial phase where  $\text{O}_2$  is associatively bonded to As atoms. Such a suggestion corroborates the thermal desorption (TDS) measurements of Ranke and Jacobi (1979) on polar surfaces, where they conclude that  $\text{O}_2$  is associatively bonded at low coverages.

### The Ga-stabilised surface

The behaviour of signals from the Ga-stabilised surface shows no signs of saturation (contrary to those from the As-rich surface). Figures 1-4 show that almost all the signals from the Ga-stabilised surface increase in a similar manner. The  $\text{Ga}_2\text{AsO}^-$  and  $\text{Ga}_2\text{AsO}_2^-$  signals which are not shown in the figures, also exhibit this behaviour. This indicates that oxygen is bonded to both Ga and As atoms. Most SIMS signals from the Ga-stabilised (100)GaAs surface appeared to follow a fairly simple, increasing relationship with oxygen exposure and the spectral content is similar to that from the air-exposed surface.

The above results strongly suggests the following: there is no change of adsorption phase between low and high oxygen coverage on this surface; oxygen is bonded to both Ga and As atoms; and adsorption is dissociative.

Further evidence that this form of oxygen is dissociative and corresponds to a strong chemisorption phase consists of high residual levels in the  $\text{GaO}^-$ ,  $\text{Ga}_2\text{O}^-$  and  $\text{O}^-$  signals. These are found after heating the Ga-stabilised surface, exposed to  $10^6$  Langmuirs of  $\text{O}_2$  at  $580^\circ\text{C}$ . This result also agrees with the thermal desorption results of Ranke and Jacobi (1979) and (Su et al. 1980) discussed in the introduction.

Ranke and Jacobi (1979), however, also observe  $\text{O}_2$  desorption from the Ga-stabilised surface, but they attribute this to associative bonding as opposed to dissociative

bonding. They only observe dissociative bonding characterised by  $\text{GaO}_2$  desorption after electron irradiation.

It is thought that this difference in the type of bonding (associative or dissociative) could be due to surface damage produced by SIMS analysis. Although Ranke and Jacobi show that effects of electron irradiation are local, it is possible that the effects of ion beams used in SIMS are more extensive and produce the dissociative adsorption that is indicated by SIMS analysis. Similar experiments of adsorption on PbTe suggest that the primary ion beam causes extensive damage. However, the associative adsorption seen on the As-rich surface suggests the effect may be less on GaAs.

### 6.3.2 Exposure to un-excited oxygen

#### The As-rich surface

Unexcited oxygen exposure on the As-rich surface produced one of the most striking results of the analysis.

Figure 1 shows that after a small increase in the  $\text{O}^-$  signal, produced by exposure to  $10^2$  Langmuirs of oxygen, no further increase was observed in the measured range of less than  $10^5$  Langmuirs exposure. No other negative ion signals were found to respond to exposure. The positive ion signals did show a response to exposures of  $2 \times 10^4$  Langmuirs and  $10^5$  Langmuirs, however, which was most evident for the  $\text{Ga}_2\text{O}^+$  signal. The response of this signal may indicate the presence of an initial dissociative adsorption at defect sites. A similar effect has been suggested for low coverage adsorption on the (100) cleaved surface (Su et al. 1980).



### The Ga-stabilised surface

Some reservation is put on the SIMS measurements after unexcited adsorption on the Ga-stabilised surface. This is because the measurements are limited to only one oxygen exposure at  $2 \times 10^4$  Langmuirs of oxygen. Also, some residual oxygen contamination was present on the surface before oxygen exposure.

The results in Figures 1, 5, and 6 show that adsorption was faster on this surface than for all in the previous cases. In general, the response is similar to that from the excited oxygen response. It is thought likely that the residual oxide is present in the form of a dissociative oxide and that this is capable of catalysing the dissociation of further adsorbed oxygen.

The differing responses of the  $\text{AsO}^-$  and  $\text{AsO}_2^-$  signals shown in Figure 5 suggest however, that some oxygen may be associatively bonded, but this suggestion is tentative.

#### 6.3.3 Comparison of the SIMS results with results from past AES studies.

The fact that the negative ions increase with oxygen exposure makes it tempting to compare the results of this SIMS, with past studies using Auger. Although such a comparison can be no more than tentative, it is interesting to see whether any obvious similarities or differences can be found.

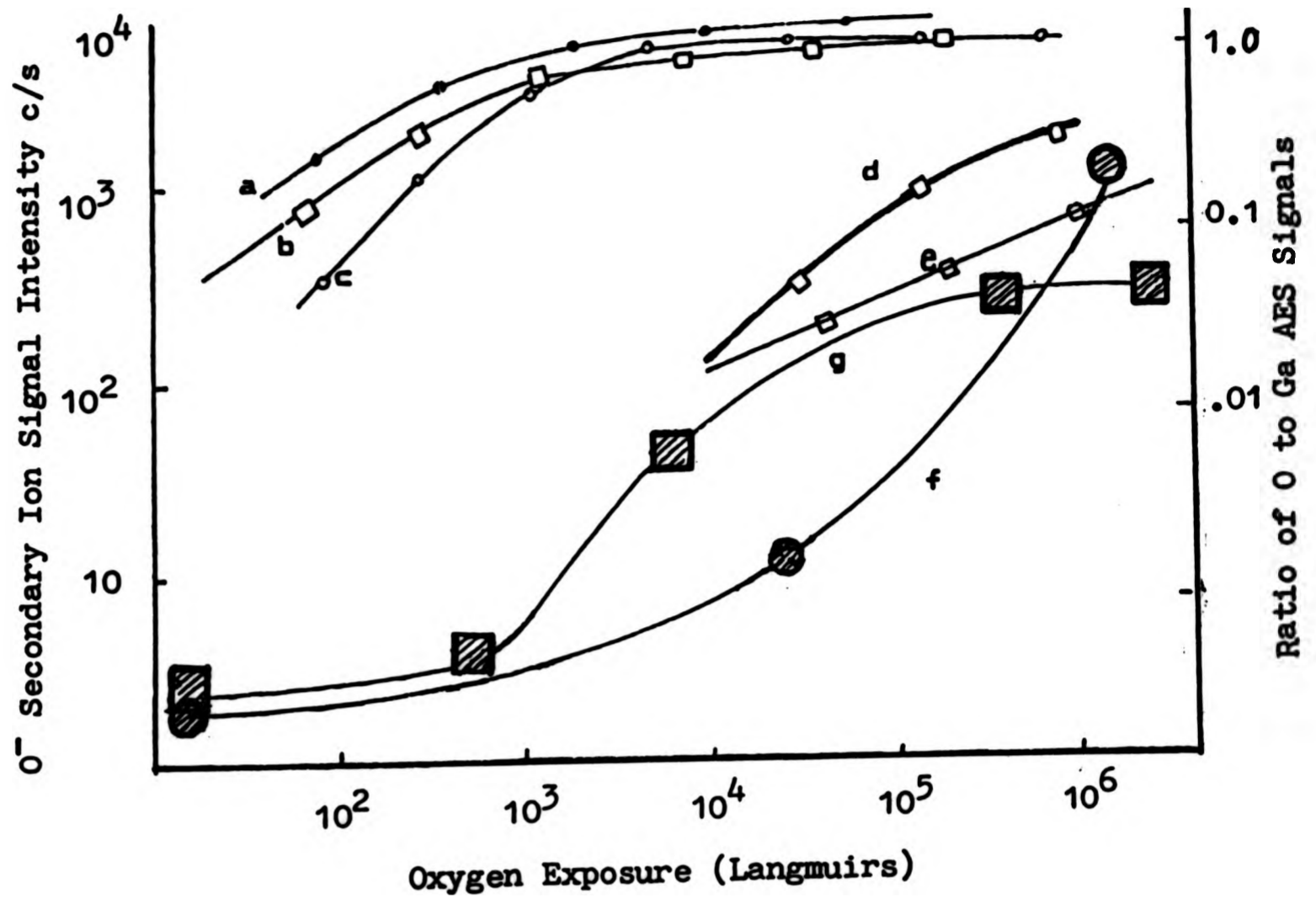
Such a comparison, however, requires at least one reference point for oxygen surface coverage with which the SIMS and the Auger signal intensities can be related. A reference

point is obtained here by assuming the following: 1) that the  $O^-$  intensity from the natural oxide corresponds to an oxygen coverage of 50% - 100%; and 2) that the  $O(510\text{eV})$  and  $Ga(1070\text{eV})$  Auger signals have the same density at the same oxygen coverage.

Figure 8 shows a comparison of the  $O^-$  SIMS signal with the response of the ratio of the Auger  $O(510\text{eV})$  and  $Ga(1070\text{eV})$  signals to oxygen exposure, taken from various Auger studies of oxygen adsorption on polar GaAs surfaces which are reported in the literature. The plots in the figure are from: (a) As-rich and (b) Ga-stabilised (100)GaAs prepared by ion sputter cleaning and annealing at  $400^\circ\text{C}$  (Ludeke and Koma 1976); (c) (111)-As GaAs prepared by sputter cleaning and annealing at  $500^\circ\text{C}$  (Ranke and Jacobi 1977); (d) As-stabilised and (e) Ga-stabilised MBE grown(111)-As GaAs (Ranke and Jacobi 1977). The plots (f) and (g) are for the behaviour of the  $O^-$  SIMS signal intensity for oxygen exposures in this study. Plot (f) is the  $O^-$  signal from the Ga-stabilised (100)GaAs surfaces and plot (g) is the  $O^-$  signal from the As-rich surface, with both surfaces exposed to excited oxygen.

Inspection of the figure suggests that the  $O^-$  SIMS from both the As-rich (plot g) and Ga-stabilised surfaces (plot f) have a response which is more like the response from the MBE grown surfaces (plots d and e), than the response from the surfaces prepared by sputter-cleaning and annealing (plots a, b and c). This suggests that the preparation used in this

Figure 8



A comparison of the effect of oxygen exposure on SIMS and AES signals from polar GaAs surfaces.

Plots: a, b, and c are the AES signal from sputter annealed GaAs; d and e are the AES signal from MBE grown GaAs and g and f are the SIMS O<sup>-</sup> signal from GaAs, sputtered and annealed in As<sub>4</sub>.

(See page 134 for preparation details and references).

study produces surfaces which are more like the surfaces obtained by MBE (plots d and e).

The oxygen surface coverage from sputtered/annealed (111)Ga and (111)As faces after oxygen exposure of  $3 \times 10^5$  Langmuirs is estimated by AES to be approximately 40% (Ranke and Jacobi, 1979). The plots a, b, and c should correspond to a similar coverage at this exposure. SIMS on the other hand, suggests an oxygen coverage of only 0.02 monolayers for such an exposure on both the As-rich and the Ga-stabilised surfaces. This requires a difference of a factor of 50 between the secondary emission probability at this exposure and the  $O^-$  signal from the air-exposed surface.

If, in fact, there is 40% of a monolayer of oxygen on the surface (or thereabouts), then this study actually looks at high coverage adsorption effects rather than the low coverage effects intended. All the indications from previous SIMS studies of oxygen adsorption and surface preparation from substrate with oxide layers, suggest that this is highly unlikely. It is more probable that the truth is somewhere in between, that ion emission probability does vary, but is not a dominant effect.

#### 6.4 Conclusions

The results of this preliminary study of oxygen adsorption on the (100)GaAs surface with SIMS show that 'excited' oxygen adsorption on the As-rich and the Ga-stabilised surfaces is different. Oxygen appears to be associatively bonded to As atoms on the As-rich and the Ga-stabilised

surfaces is different. Oxygen appears to be associatively bonded to the As atoms on the As-rich surface before a bulk type adsorption commences. On the Ga-stabilised surface, no such initial adsorption phase is observed. Adsorption of unexcited oxygen on the As-rich surface appears to be passivated at a low coverage by low exposures of  $10^2$  Langmuirs and no further oxygen uptake is observed below  $10^5$  Langmuirs.

The study shows that SIMS has potential for more exhaustive enquiry into adsorption on the GaAs surface, particularly in regard to differentiating forms of adsorption. Such a study would require several improvements to the SIMS apparatus. These are outlined in Chapter 7. It is believed that most of the difficulties that exist in quantitative analysis with SIMS could be overcome by complementing the technique with AES analysis.

CHAPTER 7

CONCLUSIONS

The main conclusion to be drawn in this thesis is that the surface investigations with the 'low dose' SIMS instrument used were only partially successful. This is particularly true for the studies of oxygen adsorption. Difficulties arise in the interpretation of the SIMS data because the studies relied heavily on comparative analysis with results of other studies, carried out under similar conditions and using different surface analysis techniques. There is little consistency in the experimental conditions (surface preparations and exposure conditions) used in past studies and, actual experimental conditions are rarely reported in sufficient detail. Within these constraints however, interesting results have been obtained from all the experiments.

The study on (100) GaAs in Chapter 5 showed that SIMS does hold promise, especially in detecting and determining possible causes of contamination (etch induced sulphate radicals) at a high sensitivity which cannot be achieved by other means. It is considered that this superior sensitivity and the ability to detect molecular contaminants makes the SIMS technique a desirable addition in any MBE growth study.

Even in this area, however, the qualitative nature of the information that is gained in SIMS needs to be complemented using other techniques (AES etc.) with which surface coverages can be estimated. Comparison with past studies in the literature is not really sufficient because experimental conditions in UHV can rarely be repeated in a precise manner.

There is a clear difference in the quality of information obtained by the two 'low coverage' adsorption studies on (111)PbTe and (100)GaAs (Chapters 4 and 6). This is primarily due to differences in the detail of available background information on these two systems.

### PbTe

The previous information on the sensitivity of the (111)PbTe to both ion and electron irradiation, accurate knowledge of the electrical behaviour and the facility for 'in situ' electrical assessment, provided an extremely useful background to the study of oxygen adsorption. Without this background, it is probable that the effects of primary ion bombardment would not have been studied in such detail. It is also likely that less account would have been taken of oxygen adsorbed on ion damaged PbTe.

Although definite conclusions are not obtained in the PbTe study, the identification of a limited source of  $Pb^+$  ions residing on the surface from the 'as grown' surface is itself significant.

An associated change in the behaviour of the  $Pb^+$  SIMS signal,  $O^-$  SIMS signal and the n-type carrier concentration is found, after low pressure oxygen exposure, during sputter desorption/destruction of the top monolayer. This association provides strong supportive evidence that the 'mobile defect' model, which has been proposed to explain results from earlier electrical analysis, is correct.



There is also evidence that in exposures at higher pressures ( $>10^{-3}$  Torr), oxygen is bound in an oxide of Pb and Te. Ion induced damage, incurred during SIMS analysis, is shown to influence oxygen adsorption and its effects may have a large influence on the oxygen adsorption behaviour observed for higher pressure exposures.

#### GaAs

A background of detailed information like that for PbTe was not available for the study of oxygen adsorption on (100)GaAs. This study suffered most from this lack of relevant information from comparable studies. Studies which were used for this purpose are also marred by ambiguities in the initial preparation of surfaces and in oxygen exposure conditions.

There is also some concern about the effects of ion bombardment which is used in this study for surface preparation and SIMS analysis. It is quite possible that like PbTe, the ion bombardment used causes the surface to change significantly and thus has a consequential effect on oxygen adsorption. Unfortunately it was not possible to study effects of ion induced damage in detail because of time constraints on the project. It is thought however, that ion damage effects are less on GaAs than PbTe because smaller primary ion doses were used to analyse the GaAs surfaces and signals from GaAs varied less than signals in the study on PbTe.

Although the results of the study on GaAs are limited, there is some success in showing that oxygen adsorption is dependent on surface stoichiometry and on whether oxygen is in an 'excited' state or not.

It is considered that the successful use of SIMS in MBE related problems requires that the SIMS instrument be resident in the MBE growth chamber. This would allow the conditions under study to be faithfully reproduced. (Initial findings from very recent SIMS analysis of oxygen adsorption on arsenic-rich 'in situ' grown MBE (100)GaAs, show that adsorption is minimal below  $10^4$  Langmuirs, no negative secondary ion emission being detected below this exposure (W. Croydon 1983 - private communication). This agrees with the present results however, these findings also suggest that an initial adsorption phase reported for the arsenic rich surface is damage related.)

#### Proposed improvements in SIMS

In the concluding sections of both Chapter 4 and Chapter 6, a need is expressed for a system with the following capabilities - to follow adsorption during oxygen exposure (over long periods of time), while ensuring that a minimum of damage is produced by the primary ion beam.

The criteria to follow adsorption kinetics requires that the ion source region of the primary ion optical column is differentially pumped. This enables the ion source to operate in an inert gas environment independent of the presence of any exposure gas used in the main chamber where the target resides.

The requirement for low total ion doses can be achieved by electronically gating the primary ion beam at intervals, and electronically selecting signals of interest.

Secondary ion energy analysis is also mentioned as being useful in helping to differentiate between signals from adsorbates and the underlying substrate. In the study on PbTe this capability would have been helpful in determining the nature of the association between the  $O^-$  and  $Pb^+$  after low pressure exposures.

Any SIMS instrument should be supported by a microcomputer system to control the instrument, supervise the data collection, and to manipulate the data into a final form for presentation. This facility would allow quicker determination of trends that are present in the data and a faster and more accurate response in further experiments.

It is unlikely that work on the PbTe - O system will be continued in the foreseeable future because interests at the City of London Polytechnic are now more concerned with Silicon and GaAs MBE and quantitative aspects of SIMS on silicon (implant and diffusion profiles). Further studies of oxygen adsorption on 'in situ' grown (100)GaAs are however in progress.

### References

- Anderson C.A., 1975, in: Secondary Ion Mass Spectrometry, ed. K.F. Heinrich and D.E. Newbury, NBS spec. Publ. 427, p. 79, Washington.
- Arthur, J.R., 1974, Surf. Sci., 43, 449.
- Benninghoven A., 1975, Surf. Sci., 53, 569.
- Benninghoven A., Ganshow O., and Wiedmann L., 1978, J. Vac. Sci. Technol., 15(2) Mar./Apr..
- Beske H.E., 1967, Z. Naturforsch., 22a, 459.
- Blaise G., 1973, Rad. Eff., 18, 235.
- Blaise G., 1975, Surf. Sci., 60,65.
- Blaise G., 1978, in: Material Characterisation Using Ion Beams. Ed. J.P. Thomas and A. Carhard, Plenum Press, New York, 143.
- Brundle C.R. and Seybold D., 1979, J.Vac.Sci.Technol., 16(5), Sept/Oct.
- Buhl R. and Preisinger A., 1975, Surf. Sci., 47,344.
- Chang C.C., Shartz B. and Murarka S.P., 1977, J. Electrochem. Soc., 124(6), 922.
- Chang C.C., 1974, in: Characterisation of Solid Surfaces, ed. by P.E. Kane and G.B. Larrabee. (Plenum Press, New York 1974), p. 509.
- Cho A.Y., and Arther J.R., 1975, in: Progress in Solid State Chemistry. ed. by G. Somorjai and J. McCaldin (Paragamon Press) New York. 157.
- Cho A.Y., and Arther J.R. 1975,Prog. Solid State Chem., 10(3), 157.
- Chye P.W., Su C.Y., Lindau L., Skeath P.R. and Spicer W.E.: J. Vac Sci. Technol., 16(5) Sept/Oct. 1979
- Cini M., 1976, Surf. Sci., 54,71.
- Dawson P.H., 1974, Inter. J. of Mass Spect. and Ion Phys., 14,371.
- Dawson, P.H., 1975, Inter. J. of Mass Spect. and Ion Phys., 17, 447.
- Dawson P.H., 1976, Surf. Sci., 57 24.

- Dawson P.H., 1977, Phys. Rev. b, 15(12).
- Dawson P.H., and Wing C.T., 1979, Surf. Sci., 81, 464.1
- Dell'Oca C.T., Yan G., and Young L., 1971, J. Electrochem. Soc., 118(1), 89.
- Dowsett M.G., King R.M. and Parker E.H.C., 1977, Applied Physics Letters, 31(8).
- Dowsett M.G., King R.M. and Parker E.H.C., 1978, Surf. Sci., 71, 541.
- Dowsett M.G. and Parker E.H.C., 1979, J. Vac. Sci. Technol. 16(5), Sept./Oct.
- Dowsett M.G., 1979, PhD Thesis CNAA City of London Polytechnic.
- Drathen P., Ranke W., Jacobi K., 1978, Surf. Sci. 77L, 162.
- Egerton R.F. and Juhasz C., 1969, Thin Solid Films, 4, 239.
- Estel J., Hoinkes H., Kaarmaan H., Nahr H. and Wilch H., 1976, 54, 393.
- Foxton, C.T. and Joyce B., 1973, Surf. Sci., 50, 434.
- Gaworski P., Kees K.H., and Mai M., Int. J. of Mass Spect. and Ion Phys., 1974, 13, 99.
- Grange J.D., 1979 PhD Thesis, CNAA City of London Polytechnic.
- Grange J.D., 1979, Parker E.H.C. and King R.M., J. Phys. D 12, 6948.
- Green M. and Lee M., 1966, J. Phys. of Chem Solids, 27, 797.
- Hagstrum H.D., 1975, J. Vac. Sci. and Technol., 12(7).
- Hewitt R.W. and Winograd N., 1978, Surf. Sci. 78.
- Honda E., Lancaster G.M. and Rabalais J.W., 1978, Surf. Sci. 76, 1613.
- Joyes P., 1973, Rad. Eff. 18, 235.
- Jurela Z., 1973 Int. J. of Mass Spect. and Ion Phys. 12,1421.
- Kazmerski L.L. and Ireland P.J., 1980, J. Vac. Sci. Technol. 17(1), Jan/Feb.
- Kubiak R.A., Parker E.H.C., King R.M. and Wittmaack K., 1983, J. Vac. Sci. Technol. A 1(1), 34.
- Kubiak R.A., 1983 CNAA PhD. City of London Polytechnic.

- Lawrence G., Simondet F. and Saget P., 1979, Applied Physics 19,63.
- Lawson G. and Todd J.F., 1972, Chem. in Brit. 8(9) 373.
- Lida S and Ito K., 1971, J. Electrochem. Soc. 118(5), 768.
- Ludeke R. and Koma A., 1976, J. Vac. Sci. Technol., 13(1), Jan/Feb.
- Malane G. and Zemal J.N., 1969, Thin Solid Films 7, 229.
- McLashan S.R.L., Parker E.H.C. and King R.M., 1979, J. Vac. Sci. Technol., 16(4), Jul/Aug.
- McGlashan S.R.L., 1981, PhD Thesis, CNAA, City of London Polytechnic.
- Meggitt B.T. 1979, PhD. Thesis, CNAA, City of London Polytechnic.
- Parker E.H.C. and Williams D., 1976, Thin Solid Films 35, 373.
- Parker E.H.C. and Williams D. 1977, Solid State Electronics 20,567.
- van der Pauw, L.J., 1958, Philips Res. Rep. 13,1.
- Ploog K. and Fisher A., 1977, Applied Physics 13, 111.
- Prutton M., 1978. 'Surface Physics', Clarendon Press.
- Ranke W. and Jacobi K., 1975, Surf. Sci. 47, 525.
- Ranke W. and Jacobi K., 1976, Surf. Sci. 64, 33.
- Ranke W. and Jacobi K., 1977, Surf. Sci. 63, 33.
- Ranke W. and Jacobi K., 1979, Surf. Sci. 81, 504.
- Rudenauer F.G. and Steiger W., 1976, Vacuum 26(12), 537.
- Schoer J.M., Rhodin T.N. and Bradley R.C. 1973, Surf. Sci. 34, 571.
- Scroubek Z., 1974, Surf. Sci. 44,47.
- Sigmund P., 1969, Phys. Rev. 184, 383.
- Smith D.A., Christie W.H., and Ohashi Y., 1978, Jap. J. Appl. Phys. 26, 61.
- Spicer W.E., Chye P.W., Garner C.M., Lindau L., and Pianetta P., 1979, Surf. Sci. 86, 763.
- Su C.Y., Chye P.W., Skeath P.R. and Spicer W.E., 1980, J. Vac. Sci. Technol. 17(5) Sept/Oct.

- Sun T.S., Byer N.E. and Chen J.M., 1978, J. Vac. Sci. Technol. 15(2), Mar/Apr.
- Thomson M.W., 1968, Phil. Mag. 18, 377.
- Uebbing J.J., 1970, J. Appl. Phys. 41, 802.
- Wilmsen C.W. and Kee R.W., 1978, J. Vac. Sci. Technol. 15(4) Jul/Aug.
- Whittmaack K., 1977, in: 'Inelastic Ion-Surface Collisions', Ed. N.H. Tolk, J.C. Tully, W. Heiland and C.W. White, Academic Press, New York, 153.
- Whittmaack, K., 1979, Surf. Sci., 89, 668.
- Winograd N., Harrison D.E. and Garrison B.J., 1978, Surf. Sci. 76, 1613.
- Winograd N., Harrison D.E. and Garrison B.J., 1978, Surf. Sci. 78, 467.
- Winters and Sigmund P., 1974, J. Appl. Phys. 45, 4760.
- Yu M.L., 1977 Surf. Sci. 71, 121.
- Yu M.L., 1978, J.Vac. Sci Technol. 15(2), 668.

Attention is drawn to the fact that the copyright of this thesis rests with its author.

This copy of the thesis has been supplied on condition that anyone who consults it is understood to recognise that its copyright rests with its author and that no quotation from the thesis and no information derived from it may be published without the author's prior written consent.

III



D53686 '85